

**International Symposium  
on  
Ligaments and Tendons-XIV**

**MGM Grand Hotel**

**Las Vegas, NV**

**March 27, 2015**

**Edited by:**

**Savio L-Y. Woo, PhD, DSc, DEng – Co-Chair**

**Stavros Thomopoulos, PhD – Co-Chair**

**Helen H. Lu, Program Chair**

**Diann DeCenzo, MS**

**Jonquil Flowers, MS**

**Megan L. Killian, PhD**

**Andrea Schwartz, PhD**

**Dovina Qu, MS**

**Nancy Lee, MS**

**Danielle Bogdanowicz, MS**

**Volume 14**

## ISL&T-XIV Sponsors

---

We gratefully acknowledge our kind sponsors. They contribute to the greatness of the meeting.



Orthopaedic Research Society



Musculoskeletal  
Research Center



Asian American Institute  
for Research & Education



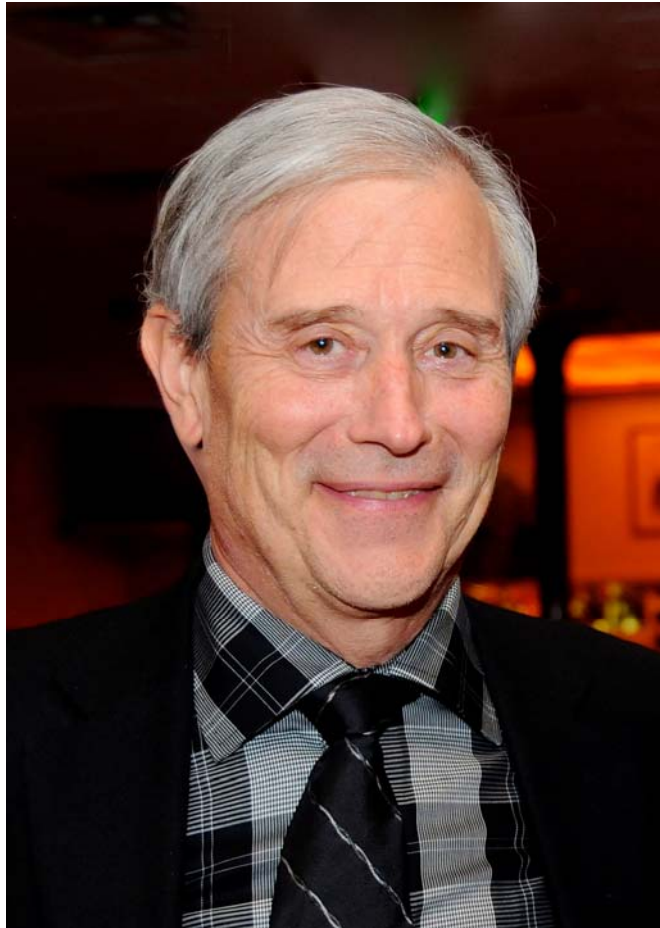
Flexcell International  
Corporation



Steadman Philippon  
Research Institute



# *In Memoriam*



**Cyril B. Frank, M.D.**

*August 3, 1949 – March 5, 2015*

**A Pioneer and a Brilliant Leader in Ligament Research and Education.  
A Kind Care Giver and a Visionary in Health Services.  
And above all,  
A Revered Teacher,  
An Admired Colleague,  
A Trusted Friend,  
and a Loving Family Man.**



# Volume 14

## Table of Contents

	<u>Page</u>
Welcome by Professors Savio L-Y. Woo and Stavros Thomopoulos	2
ISL&T-XIV Committees	3
ISL&T-XIV Awards	4-6
Instructions to Presenters	7
Program	
● Podium Sessions	8-13
● Poster Sessions	14
Savio L-Y. Woo Young Researcher Award	15-18
ISL&T-XIV Abstracts	
● Session 1: Tissue Engineering	19-26
● Session 2: Enthesis	27-34
● Session 3: Biology and Biomechanics	35-41
● Session 4: Tendinopathy	42-52
● Session 5: Rotator Cuff	53-60
● Session 6: Tissue Engineering and Stem Cells	61-64
● Poster Sessions	65-77

## **Welcome by Professors Savio L-Y. Woo and Stavros Thomopoulos**

It is our pleasure and honor to welcome you to the Fourteenth International Symposium on Ligaments and Tendons (ISL&T-XIV).

The first ISL&T was held in Orlando, FL in 2000 with the goals of promoting ligament and tendon research and providing a forum for presenting the very best research in our field. Over the past fifteen years, the symposium has placed an emphasis on mixing bioengineers, biologists, and clinician scientists to stimulate discussions on current research and future collaborations. This year's program committee, led by Dr. Helen H. Lu, has put together an outstanding scientific program for ISL&T-XIV. We look forward to active discussions throughout the day and encourage junior investigators in particular to participate.



We wish to congratulate all of our younger colleagues who are finalists for this year's awards. The quality of the abstract submissions was excellent, and the judges will be hard-pressed to pick winners! We also wish to congratulate Ms. Sarah Rooney for winning the Savio L-Y. Woo Young Researcher Award. A special acknowledgement must also be given to Dr. and Mrs. Albert Banes of Flexcell International for their generous support of the Woo Award as well as a number of ISL&T awards over the years!

We look forward to discussions with the International Advisory Committee (IAC), which was formed in 2009 to guide the direction of the ISL&T. Due in part to the efforts of the IAC and the ISL&T, the ligament and tendon community was able to expand over the years, including strong representation of ligament/tendon science at the Orthopaedic Research Society Annual Meeting and ligament/tendon scientists on National Institutes of Health study sections. The IAC is now well positioned to define future goals and strategies to move our community forward. If you have any suggestion or comments, please let us know.

Finally, the organizing committee thanks all the sponsors for their generous support. In addition, we are particularly pleased to thank a number of laboratory directors for helping to fund the banquet and award ceremony this evening.

Enjoy the symposium!

Savio L-Y. Woo, PhD, DSc, DEng  
Stavros Thomopoulos, PhD  
Co-Chairs, ISL&T-XIV

## **ISL&T-XIV Committees**

---

### **PLANNING COMMITTEE**

#### **CHAIRS**

Savio L-Y. Woo, PhD, DSc, DEng (Co-Chair)

Stavros Thomopoulos, PhD (Co-Chair)

#### **COMMITTEE**

Diann DeCenzo, MS

Andrea Schwartz, PhD

Nancy Lee, MS

Jonquil Flowers, MS

Dovina Qu, MS

Danielle Bogdanowicz, MS

Megan L. Killian, PhD

### **INTERNATIONAL PROGRAM COMMITTEE**

#### **CHAIR**

Helen H. Lu, PhD

#### **COMMITTEE**

Chih-Hwa Chen, MD, PhD

Mahmut Nedim Doral, MD

Michael Lavagnino, PhD

Paul Ackermann, MD, PhD

Fabio Vercillio, MD

Sai-Chuen Fu, PhD

Braden Fleming, PhD

Milan Handl, MD

David Corr, PhD

Catherine Kuo, PhD

Thay Lee, PhD

Joo Han Oh, MD

Roger Smith, PhD

Maurilio Marcacci, MD

Hazel Screen, PhD

Guoan Li, PhD

Giovanni Zamarrà, MD

Scott Rodeo, MD

Louis Soslowsky, PhD

Matthew Fisher, PhD

Alice Huang, PhD

Zong-Ming Li, PhD

James Wang, PhD

Jason Shearn, PhD

Philippe Neyret, MD

Alex Almarza, PhD

Spencer Lake, PhD

### **INTERNATIONAL ADVISORY COMMITTEE**

#### **CHAIR**

Savio L-Y. Woo, PhD, DSc, DEng

#### **COMMITTEE**

Tom Andriacchi, PhD

Mahmut Nedim Doral, MD

Christos Papageorgiou, MD

Steven Arnoczky, DVM

James Goh, PhD

Per Renstrom, MD

Albert Banes, PhD

Catherine Kuo, PhD

Richard Steadman, MD

David Butler, PhD

Thay Q. Lee, PhD

Louis Soslowsky, PhD

Giuliano Cerulli, MD

Guoan Li, PhD

Stavros Thomopoulos, PhD

Kai-Ming Chan, MD, PhD

Zong-Ming Li, PhD

Ray Vanderby, PhD

Chih-Hwa Chen, MD, PhD

Helen H. Lu, PhD

James Wang, PhD

David Corr, PhD

Nicola Maffulli, MD

Jennifer Wayne, PhD

## **ISL&T-XIV Awards**

---

We established awards to stimulate high quality scientific research by investigators in the study of ligaments and tendons. The awardees are selected by members of the program committee based on the quality of the abstract and presentation as well as the overall merit of the study.

### **Savio L-Y. Woo Young Researcher Award**

**Award: up to USD\$1,000 and Certificate (up to 4)**

**Purpose:** Professor Savio L-Y. Woo founded the International Symposium on Ligaments and Tendons (ISL&T) to promote awareness of the field, the exchange of information, and collaboration both nationally and internationally. The ISL&T has been a venue for lively discussion of current topics in connective tissue research and clinical applications. In addition to his leadership and significant scientific contributions to our field, Professor Woo has been an internationally recognized intellectual ambassador for training, mentoring, and for inspiring students in the field of biomedical engineering and orthopaedic surgery. We are honored to present the Savio L-Y. Woo Young Researcher Award to individuals who perform the best research in three major areas: biomechanical, biological and translational/clinical, and have submitted their work to the ISL&T meeting.

The Award is intended to provide partial support (up to \$1,000) towards the applicant's research or for travel expenses to attend the ISL&T-XIV meeting. Up to four awards will be given.

**Eligibility:** Open to graduate students and post-doctoral fellows. Applicant must be the first and presenting author of the abstract and be present at the ISL&T meeting and banquet to accept the award. Advisor's verification of eligibility with a letter is required.

### **Award Committee**

Albert Banes, PhD – Chair, Award Committee

Per Renstrom, MD

Thay Lee, PhD

Guoan Li, PhD

Catherine Kuo, PhD

Hazel Screen, PhD

Jonquil Flowers, MS (Assistant)

**Acknowledgements:** Sponsored by Flexcell International Corporation

## Past Recipients of the Savio L-Y. Woo Young Researcher Award

### ISL&T-X, Hong Kong, China (2010 Inaugural Year)



Biological Research –  
**Xiao Chen**  
Advisor: H-W. Ouyang  
Zhejiang University  
Zhejiang, China



Clinical Research –  
**Saira Chaudhry**  
Advisor: D. Morrissey  
Queen Mary University of London  
London, United Kingdom

### ISL&T-XI, Irvine, CA



Biomechanical Research –  
**Joo H. Oh**  
Advisor: T.Q. Lee  
VA Long Beach Healthcare System  
University of California  
Irvine, CA



Biological Research –  
**Jeffrey P. Brown**  
Advisor: C.K. Kuo  
Tufts University  
Medford, MA

### ISL&T-XII, San Francisco, CA



Biological Research –  
**Jonathan P. Gumucio**  
Advisor: C.L. Mendias  
University of Michigan  
Ann Arbor, MI

### ISL&T-XIII, Arezzo, Italy



Biomechanical Research –  
**Chauvanne T. Thorpe**  
Advisor: H.R. Screen  
Queen Mary University of London  
London, United Kingdom

### ISL&T-XIV Award Recipient

Biological Research – **Sarah Rooney**

Advisor: L.J. Soslowsky

University of Pennsylvania

Philadelphia, PA

Abstract Title: Genetic Response of Rat Supraspinatus Tendon and Muscle to Exercise

To acknowledge the work by students, fellows, and residents, we will provide the following two awards:

### **Best Student Paper Award**

### **Best Research Fellow Paper Award**

To be eligible, the presenters must be the first author of the abstract and be present at the meeting and banquet. Each award consists of a certificate and a check for \$200 (donated by Flexcell International Corporation).

### **Best Poster Award**

To be eligible, the presenters must be the first author of the abstract and be present at the ISL&T meeting and banquet. This award consists of a certificate as well as a check for \$200 (donated by Flexcell International Corporation).

## **Instructions to Presenters**

---

### **Podium Presenters**

The time for presentations has been limited, in favor of discussion. Please see the presentation formats listed below. Your moderators have been asked to adhere to the time allotted for your presentation as well as the number of slides.

### **An Important Note on Slides**

All speakers must be prepared to present their research using PowerPoint format.

### **Podium Presentation Requirements**

#### Keynote Presentations

- 10 min. presentations each immediately followed by a 5 min. discussion.
- Maximum 10 PowerPoint slides for computer presentation.

#### Regular Presentations

- 5 min. presentations followed by a 15 min. group discussion of 4-5 abstracts.
- Maximum 5 PowerPoint slides for computer presentation.

**Important: All speakers are asked to check-in with the session moderators 15 minutes before the session in which they will present to meet the projectionist and the moderator.**

### **Poster Presenters**

Poster should be limited to 45 inches by 45 inches (114 cm x 114 cm).

Poster boards will be available in the meeting room. Please set up your poster between 7:30 am - 8:00 am and leave the posters up throughout the day. Posters are to be taken down by 6:00 pm.

**Note: An opportunity has been provided for you to present your posters during different breaks. Please be sure to attend to your poster at the assigned time.**

# PROGRAM

## Podium Sessions

<u>Time</u>	<u>Topics</u>	<u>Speakers</u>
7:00	<b>Registration and Light Breakfast</b>	
8:00	<b>Welcome</b>	<b>Savio L-Y. Woo, Ph.D.</b> <b>Helen H. Lu, Ph.D.</b>
8:15	<i>Clinical Lecture: ACL Surgery – Where Are the Missing Gaps?</i>	<b>Kai-Ming Chan, M.D., Ph.D.</b>
	<b>Podium Session 1: Tissue Engineering (pg. 19-26)</b>	<b>Session Chairs:</b> <b>James Goh, Ph.D.</b> <b>Chunfeng Zhao, Ph.D.</b>
8:30	<i>Keynote Lecture: Endoscopy and Percutaneous Suturing in the Achilles Tendon Ruptures and the Importance of Paratenon</i>	<b>Mahmut Nedim Doral, M.D.</b>
8:40	<i>Discussion</i>	
8:45	A Novel Magnesium Ring for Regeneration of an Injured Anterior Cruciate Ligament – <i>In Vitro</i> and <i>In Vivo</i> Studies in Goats	Kathryn Farraro
8:50	Fabrication of Multi-Layered Tendon Tissue Engineering Scaffold Consisting of Electrospun Nanofibers and Photocrosslinked Hydrogel	Guang Yang
8:55	<i>In Vivo</i> Evaluation of a Bioresorbable PLLA Device for Regeneration of the ACL	William Walsh, Ph.D.
9:00	<i>Discussion</i>	
9:10	Platelet Based Blood Products for Stimulation of Tendon Healing – An <i>In Vitro</i> Cell Culture Study	Tanja Schmidt, DVM
9:15	Biaxially Aligned Tendon-Derived Matrix-Poly( $\epsilon$ -Caprolactone) (PCL) Electrospun Scaffolds for Rotator Cuff Tendon Tissue Engineering	Dianne Little, DVM, Ph.D.

9:20	A Novel Murine Model of Autograft Anterior Cruciate Ligament Reconstruction	Camilla Carballo
9:25	<i>Discussion</i>	
	<b>Podium Session 2: Enthesis (pg. 27-34)</b>	<b>Session Chairs: William Walsh, Ph.D. Johnna Temenoff, Ph.D.</b>
9:40	<i>Keynote Lecture: Engineering the Interface Between Tendon and Bone</i>	<b>William Levine, M.D.</b>
9:50	<i>Discussion</i>	
9:55	Indian Hedgehog Signaling in Tendon-Bone Healing: A Potential Regulator of Enthesis Repair	Andrew Carbone
10:00	Enthesis Mineral Apposition During Postnatal Growth and Following Joint Destabilization in the Adult	Nathaniel Dymont, Ph.D.
10:05	Insertion Fibrochondrocyte Growth and Biosynthesis on Nanofiber Scaffolds	Dovina Qu
10:10	Engineering and Characterizing Nanofibrous Composite Scaffolds with Spatially-Varying Architecture	David Corr, Ph.D.
10:15	<i>Discussion</i>	
10:30	Multiple-Techniques to Evaluate the Fibrous Interzone During the Bone-Tendon Junction Healing for Anterior Cruciate Ligament Reconstruction (ACLR) Model in Rabbits	Jiali Wang, Ph.D.
10:35	Gradient Polyurethane Scaffolds for Improved Regeneration of the Tendon Enthesis	Tyler Touchet
10:40	Ageing, Deep Venous Thrombosis and Male Gender Impair Outcome After Achilles Tendon Rupture	Paul Ackermann, M.D., Ph.D.
10:45	Silk Scaffold with Osteoconductive and Osteoinductive Cues for Enthesis Regeneration in Anterior Cruciate Ligament Reconstruction	Thomas Teh, Ph.D.

10:50	<i>Discussion</i>	
11:00	<b>Break/ Poster Session I (even numbers)</b>	
	<b>Podium Session 3: Biology &amp; Biomechanics (pg. 35-41)</b>	<b>Session Chairs: Albert Banes, Ph.D. Alice Huang, Ph.D.</b>
11:30	<i>Keynote Lecture: Biomechanics of the Transverse Carpal Ligament</i>	<b>Zong-Ming Li, Ph.D.</b>
11:40	<i>Discussion</i>	
11:45	The Interfascicular Matrix Enables Fascicle Sliding and Recoil in Tendon, and Behaves More Elastically in Energy Storing Tendons	Chavaunne Thorpe, Ph.D.
11:50	3-D Reconstruction of Intact and Stress Deprived Rat Tail Tendon Cells	Monika Egerbacher, DVM, Ph.D.
11:55	The Role of p38 MAPK in Tendon Growth and Remodeling	Kristoffer Sugg, M.D.
12:00	<i>Discussion</i>	
12:15	Early Embryonic Tendon Possesses an Actin Cytoskeleton Network with Crimp	Nathan Schiele, Ph.D.
12:20	Full-Field Methods for Anterior Cruciate and Other Ligament Biomechanical Characterization	Ellen Arruda, Ph.D.
12:25	New Biomechanical Testing Standards for Evaluating Adjustable Femoral Cortical Suspension Devices	Alexander Peterson
12:30	<i>Discussion</i>	
12:45	<b>Group Photo and Lunch (Flash Presentations by Poster Presenters)</b>	
	<b>Podium Session 4: Tendinopathy (pg. 42-52)</b>	<b>Session Chairs: Louis Soslowsky, Ph.D. David Corr, Ph.D.</b>
13:45	<i>Keynote Lecture: Aberrant Differentiation of Tendon Stem Cells Causes Tendinopathy</i>	<b>James Wang, Ph.D.</b>

13:55	<i>Discussion</i>	
14:00	The Role of NF- $\kappa$ B Signaling in Rotator Cuff Tendinopathy	Shivam A. Shah
14:05	Cathepsin Activity in Human and Rat Supraspinatus Tendinopathy	Akia Parks
14:10	Disruption of TGF $\beta$ Signaling in the Scleraxis Cell Lineage Leads to Tenocyte Dedifferentiation and Tendon Degeneration	Guak-Kim Tan, Ph.D.
14:15	<i>Discussion</i>	
14:25	Inhibition of HIF-2A Signaling with Digoxin Decreases Calcification in Tendinopathy	Jiajie Hu
14:30	Is NOD1 Activation Involved in Tendinopathy? Characterization on Clinical Samples and <i>In Vitro</i> Studies of NOD1 Activation on Cultured Tendon Cells	Chelsea Hopkins
14:35	MicroRNA in Tendinopathy: A Translational Target	Neal L. Millar, M.D. Ph.D.
14:40	<i>Discussion</i>	
14:50	Does Hypoxia Contribute to Tendinopathy? Evidence From an <i>In Vivo</i> Murine Model	Katie J. Trella
14:55	Low-Dose Hydrogen Peroxide Impaired Tendon Healing And Induced Tendinopathic Changes	Man-Yi Yeung
15:00	Shear-Tension Ratio Effect on Healthy and Tendinopathic Human Tenocyte Metabolism	Dharmesh Patel
15:05	Pathological Tendon Properties: Stiffness, Strength and Proteoglycans	Rachel K. Choi
15:10	<i>Discussion</i>	
15:25	<b>Break/Poster Session II (odd numbers)</b>	

15:55	<b>Clinical Panel: Soft Tissue Fixation Strategies</b>	<b>Panel Chairs:</b> <b>Scott Rodeo, M.D.</b> <b>Leesa Galatz, M.D.</b>
	<b>Podium Session 5: Rotator Cuff (pg. 53-60)</b>	<b>Session Chairs:</b> <b>Hazel Screen, Ph.D.</b> <b>Jason Shearn, Ph.D.</b>
16:15	<i>Keynote Lecture: Does My Shoulder Look Fat to You? Muscle Phenotypic Changes and Rotator Cuff Pathology</i>	<b>Ranjan Gupta, M.D.</b>
16:25	<i>Discussion</i>	
16:30	<b>Savio L-Y. Woo Young Researcher Award Winner:</b> Genetic Response of Rat Supraspinatus Tendon and Muscle to Exercise	Sarah I. Rooney
16:40	<i>Discussion</i>	
16:45	Matrix Metalloproteases and Tissue Inhibitors of Metalloproteases in Tenocytes of the Rotator Cuff Differ with Varying Donor Characteristics	Franka Klatte-Schulz, Ph.D.
16:50	Effect of Bone Mineral Density on Rotator Cuff Tear: An Osteoporotic Rabbit Model	Hugo Giambini, Ph.D.
16:55	Biomechanical Role of Capsular Continuity in Superior Capsule Reconstruction for Irreparable Rotator Cuff Tears	Teruhisa Mihata, M.D., Ph.D.
17:00	<i>Discussion</i>	
17:10	Optimum Tension for the Bridging Sutures in Trans-Osseous Equivalent Rotator Cuff Repair	Joo Han Oh, M.D., Ph.D.
17:15	Non-Genetic Fabrication of a Novel Tendon-Derived Stem Cell (TDSC) Sheet for the Biological Repair of Rotator Cuff Tear	Jian-kun Xu, Ph.D.
17:20	Ultrasound-Guided Dry Needling on Healthy Rat Supraspinatus Tendon	Corinne N. Riggin
17:25	<i>Discussion</i>	

	<b>Podium Session 6: Tissue Engineering and Stem Cells (pg. 61-64)</b>	<b>Session Chairs: Ronen Schweitzer, Ph.D. Matthew Fisher, Ph.D.</b>
17:35	Stepwise Differentiation of Human Induced Pluripotent Stem Cells for Achilles Tendon Regeneration by Change of Physical Substrate	Can Zhang
17:40	Multiple Omics Analysis Reveals Age-Related Changes in Tendon Differentiation from Mesenchymal Stem Cells	Mandy J. Peffers, Ph.D.
17:45	An Irradiation-and-Injection Approach to Study TSC Differentiation in Mice	Jianying Zhang, Ph.D.
17:50	Autologous Tenocyte Injection for Tendinopathy: Current Pilot Trials	Ming-Hao Zheng, D.M., Ph.D.
17:55	<i>Discussion</i>	
18:05	<b>Updates from Tendon/Ligament Meetings</b>	<b>Louis Soslowky, Ph.D. Hazel Screen, Ph.D.</b>
18:10	<b>Closing Remarks for ISL&amp;T - XV</b>	<b>Stavros Thomopoulos, Ph.D.</b>
18:15	<i>Proceed to Dinner Venue</i>	
18:45	<b>Reception/Dinner and Award Ceremony</b> <i>Joyful House Cuisine</i>	

## Poster Presentations

**Moderators: Nelly Andarawis-Puri, Ph.D.; Thay Lee, Ph.D.;  
Kevin Hildebrand, M.D.; Alex Almarza, Ph.D. (pg. 65-77)**

<u>Poster Number</u>	<u>Title</u>	<u>Presenter</u>
<b>1</b>	A New Approach to Enhance Tendon-Bone Junction Healing by Regenerating Fibrocartilage Zone	Jianying Zhang, Ph.D.
<b>2</b>	Investigating a Mouse Model of Collagenase-Induced Tendinopathy	Jason Shearn, Ph.D.
<b>3</b>	Histological Evaluation of the Equine Superficial Digital Flexor Tendon (SDFT) During Ageing	Othman Ali
<b>4</b>	A Hyperelastic Fiber-Reinforced Continuum Model of Healing Tendon with Distributed Collagen Fiber Orientations	Mohd Nazri Bajuri
<b>5</b>	Direct Functional Mobilization After Achilles Tendon Rupture Promotes Early Healing Response	Paul Ackermann, M.D., Ph.D.
<b>6</b>	A Novel Magnesium Based Suture Anchor for Soft Tissue Fixation	Jonquil Flowers
<b>7</b>	Differential Matrix Turnover of the Interfascicular Matrix of Tendons at Different Risk of Injury	Karen Sanders
<b>8</b>	Development of a Novel Murine Achilles Tendon Explant System	Katie J. Trella
<b>9</b>	Outcomes Following Revision Rotator Cuff Repair With Concentrated Bone Marrow Aspirate Obtained from the Proximal Humerus	Andreas Voss, M.D.
<b>10</b>	Transplantation of Fetal Instead of Adult Fibroblasts Display Intrinsic Differences in Tendon Regeneration and Reduce the Probability of Ectopic Ossification	Xiao Chen, Ph.D.
<b>11</b>	Morphologic Change of Gluteus Maximus and Medius After Harvesting Fascia Lata: Quantitative Evaluation by Magnetic Resonance Imaging	Yasuo Itami, M.D.
<b>12</b>	Manufacture of Scaffold-Free Tendon in an <i>Ex Vivo</i> Tissue-Engineered System	Ming-Hao Zheng, D.M., Ph.D.

SAVIO L-Y. WOO YOUNG RESEARCHER AWARD

## GENETIC RESPONSE OF RAT SUPRASPINATUS TENDON AND MUSCLE TO EXERCISE

<sup>1</sup>S.I. Rooney, <sup>2</sup>J.W. Tobias, <sup>1</sup>P.R. Bhatt, <sup>1</sup>A.F. Kuntz, <sup>1</sup>L.J. Soslowsky

<sup>1</sup>McKay Orthopaedic Research Lab, <sup>2</sup>Penn Molecular Profiling Core, University of Pennsylvania, Philadelphia, PA

### INTRODUCTION

Muscle and tendon beneficially adapt to non-injurious exercise. This adaptation may present as protein or organizational changes that improve the mechanics of the tissue in the desired loading condition. Acute inflammation is a complex biologic event that aims to protect and repair tissue. Two important processes related to inflammation are activation of the arachidonic acid (AA) cascade and degradation of extracellular matrix (ECM) proteins by matrix metalloproteinases (MMPs). In the AA cascade, AA is converted by cyclooxygenase (COX) to prostaglandins, prostacyclins, or thromboxane or by 5-lipoxygenase to leukotrienes. Prostaglandins can mediate blood flow to tissue<sup>1</sup> and upregulate MMP expression.<sup>2</sup> MMPs and their inhibitors (TIMPs) are responsible for matrix turnover and if not carefully balanced, can result in excess fibrosis or degeneration. Previous studies suggest that inflammation plays an important role in the regeneration of muscle and tendon following acute injury;<sup>6,g.3</sup> however, the mechanisms governing the roles of inflammation in the adaptation of muscle and tendon to beneficial loading have not been identified. If the appropriate balance in acute inflammation is not achieved, the tissue may not be able to adapt, resulting in injury. Identifying the response of healthy tissue to known non-injurious loading conditions would help distinguish detrimental and beneficial inflammation. The **objective** of this study was to screen for acute and chronic inflammatory and ECM genes involved in the beneficial adaptation of rat supraspinatus (supra) tendon and muscle to non-injurious loading. Our global **hypothesis** was that a mild inflammatory response is a normal, physiologic requirement for muscle and tendon to adapt to load. Specifically, 1) a mild inflammatory response (changes in AA cascade) would present in the tendon and muscle after a single bout of loading, and 2) the tissue will show adaptive matrix changes (increased collagen expression and MMP/TIMP changes indicating turnover) with chronic loading.

### METHODS

20 male, Sprague-Dawley rats (400-450g) were divided into cage activity (CA) or acute or chronic exercise (EX) groups (IACUC approved). Acute groups were divided into 12 or 24 hour euthanasia time points following a single exercise bout, and chronic groups were divided into 1 or 8 weeks of repeated exercise (n=4 each group). Acute EX animals underwent 2 weeks of progressive, downhill training to acclimate to the treadmill. After 72 hours of rest, animals underwent a single treadmill exercise session at a constant speed of 10m/min for 1 hour on a flat treadmill. After 2 weeks of flat treadmill acclimation, chronic EX animals walked on a flat treadmill at 10 m/min, 1 hour per day, 5 days/wk as previously described.<sup>4</sup> This protocol has been shown to produce beneficial gross adaptations in the rat supraspinatus without inducing tendon mechanical injury. Chronic EX rats were euthanized 72 hours after their final treadmill session to avoid any confounding acute effects. Control CA animals maintained cage activity for 5 weeks total to reach a final weight within 10% of the groups investigated for comparison. Supra tendon and muscle were harvested, RNA was extracted, and a custom Panomics QuantiGene 2.0 Multiplex array was used to detect 48 target genes for inflammation (*Ptgs1*, *Ptgs2*, *Alox5ap*, *Ptges*, *Ptger4*, *Ptgfr*, *Il1a*, *Il1b*, *Il6*, *Il10*, *Cxcl1*, *Tnf*, *Nfkb1*, *Tac1*), ECM components (*Coll1a1*, *Col2a1*, *Col3a1*, *Dcn*, *Bgn*, *Acan*, *Fmod*, *Vcan*), matrix turnover (*Mmp2*, *Mmp3*, *Mmp9*, *Mmp13*, *Mmp14*, *Timp1*, *Timp2*, *Timp3*, *Timp4*), and factors associated with tissue adaptation or degeneration (*Tgfb1*, *Tgfb3*, *Ctgf*, *Igfl*, *Fnl*, *Tnc*, *Sox9*, *Bmp2*, *Bmp7*, *Ppargc1a*, *Casp3*, *Casp8*, *Hspb1*, *Hspa2*, *Vegfa*, *Nos2*, *Nos3*). Target gene signal was normalized by the geometric mean of 3 housekeeping genes (*Gapdh*, *Actb*, *Rplp0*) and log<sub>2</sub> transformed. Principal components analysis (PCA) was used to visualize global similarities among the 40 samples and for the 4 separate categories of interest: chronic tendon, chronic muscle, acute tendon, and acute muscle. For each category, a 1-way ANOVA with 3 levels (i.e., CA vs. EX 12 hr vs. EX 24 hr for acute; CA vs. EX 1 wk vs. EX 8 wk for chronic) with pairwise contrasts was used to compare CA and EX genes. Because this was primarily a screening experiment, an inclusive analysis was conducted. Significance was set at  $p \leq 0.05$  and genes with a positive or negative fold change  $\geq 1.25$  were included.

### RESULTS

PCA of the entire sample pool revealed the greatest variance between muscle and tendon specimens, confirming that these tissues were isolated from each other during dissection. Additionally, a clear distinction could be seen between acute and chronic groups, suggesting that 72 hours provided enough time to avoid acute effects in the chronic time points. Finally, and importantly, individual PCA of each of the four categories revealed distinct clusters corresponding to each of the 3 groups (levels) within the category, supporting our study design (not shown).

Quantitative conclusions about gene expression could not be made for the following targets that were below the limit of detection: *Ptgs2* (tendon and muscle), *Il1a* (tendon and muscle), *Il1b* (tendon and muscle), *Il6* (tendon and

muscle), *Il10* (tendon and muscle), *Tac1* (tendon and muscle), *Mmp3* (muscle), *Mmp9* (tendon and muscle), *Mmp13* (tendon and muscle), *Col2a1* (muscle), and *Acan* (muscle).

Supporting our hypotheses, acute exercise caused an altered inflammatory response in muscle and tendon, indicated by changes in AA cascade components and MMP/TIMPs (summarized in **Table 1**). As expected, inflammatory genes were more changed acutely than chronically. Chronic tissue had more matrix-related gene changes, suggesting tissue adaptation (summarized in **Table 2**).

For the **acute tendon** category, 10 target genes were identified as having a significant ANOVA effect: *Tnf*, *Timp3*, *Ptges*, *Sox9*, *Bmp7*, *Mmp14*, *Tnc*, *Igf1*, *Ptger4*, and *Ctgf*. Pairwise comparisons indicated downregulation of *Ptger4*, *Tnf*, and *Bmp7* and upregulation of *Ctgf*, *Sox9*, and *Tnc* 12 hours after an acute bout of exercise. 24 hours following an acute bout of exercise, pairwise comparisons revealed downregulation of *Tnf*, *Timp3*, *Sox9*, and *Bmp7* and upregulation of *Ptges*, *Mmp14*, and *Igf1*.

For the **acute muscle** category, 13 target genes were identified as having a significant ANOVA effect:

*Timp3*, *Hspa2*, *Bmp7*, *Ptges*, *Tgfb3*, *Colla1*, *Ctgf*, *Timp4*, *Ppargc1a*, *Hsp27*, *Tgfb1*, *Ptgfr*, and *Ptger4*. Pairwise comparisons indicated downregulation of *Ptges* and *Bmp7* and upregulation of *Colla1*, *Timp4*, *Tgfb1*, *Ctgf*, and *Hsp27* 12 hours after an acute bout of exercise. 24 hours following an acute bout of exercise, pairwise comparisons revealed downregulation of *Ptgfr*, *Ptger4*, *Timp3*, *Tgfb3*, *Hspa2*, *Ppargc1a*, and *Bmp7* and upregulation of *Colla1*.

For the **chronic tendon** category, 12 target genes were identified as having a significant ANOVA effect: *Timp1*, *Mmp14*, *Colla1*, *Timp3*, *Col3a1*, *Alox5ap*, *Igf1*, *Casp3*, *Vegfa*, *Fnl*, *Dcn*, and *Tgfb3*. Pairwise comparisons indicated downregulation of *Alox5ap*, *Timp1*, *Timp3*, *Dcn*, and *Casp3* and upregulation of *Mmp14*, *Colla1*, *Col3a1*, *Igf1*, and *Vegfa* after 1 week of exercise. After 8 weeks of exercise, pairwise comparisons revealed downregulation of *Alox5ap*, *Timp1*, and *Fnl* and upregulation of *Mmp14*, *Colla1*, and *Igf1*.

For the **chronic muscle** category, 8 target genes were identified as having a significant ANOVA effect: *Ctgf*, *Tnc*, *Ptgfr*, *Tgfb3*, *Col3a1*, *Mmp14*, *Colla1*, and *Fmod*. Pairwise comparisons indicated downregulation of *Ptgfr* and *Tgfb3* and upregulation of *Mmp14*, *Colla1*, *Col3a1*, *Ctgf*, and *Tnc* after 1 week of exercise. After 8 weeks of exercise, pairwise comparisons revealed downregulation of *Ptgfr* and *Tgfb3* and upregulation of *Mmp14*.

## DISCUSSION

This study investigated the acute and chronic gene changes in rat supraspinatus tendon and muscle following a non-injurious exercise protocol. PCA confirmed clear distinctions between tissues and between time points supporting the study design and groups for evaluation. Undetectable levels of *Acan* and *Col2a1* in muscle, but not tendon samples, further confirmed complete isolation of these two tissues during dissection. Tendon and muscle samples showed differential, time-dependent responses to exercise. Similar to other studies, there was a load-induced alteration of growth factors (*Igf1*, *Ctgf*, *Tgfb1*, *Tgfb3*, *Vegfa*) in muscle and tendon.<sup>5</sup> Chronic, compared to acute, tendon and muscle samples were characterized as having more matrix-related gene changes, suggesting tissue adaptation to chronic loading. Specifically, both muscle and tendon demonstrated increases in collagen type I gene expression and alterations in *Mmp14* and TIMPs, implying that matrix turnover is an important component of tissue adaptation to load. More gene changes were found at the 1 week time point than the 8 week time point, indicating that this adaptive process begins soon upon initiation of an exercise routine. Then, as the tissue adapts, it may require a greater loading stimulus to achieve the same gene expression and matrix turnover response. Acutely, genes associated with the arachidonic acid cascade (*Ptges*, *Ptger4*, and *Ptgfr*) were altered in muscle and tendon 12 and 24 hours following a single bout of exercise. Furthermore, changes in *Mmp14* and TIMPs suggest an acute matrix turnover response to exercise in addition to the chronic, adaptive matrix turnover response. Acute and chronic

**Table 1.** Inflammatory and matrix turnover genes changed with acute exercise.

		Acute Tendon	Acute Muscle
Arachidonic Acid Cascade	CA-EX12	<i>Ptger4</i>	<i>Ptges</i>
	CA-EX24	<i>Ptges</i>	<i>Ptger4</i> , <i>Ptgfr</i>
	EX12-EX24	<i>Ptges</i> , <i>Ptger4</i>	<i>Ptges</i> , <i>Ptgfr</i>
Matrix Turnover	CA-EX12	---	<i>Timp4</i> , <i>Colla1</i>
	CA-EX24	<i>Mmp14</i> , <i>Timp3</i>	<i>Timp3</i> , <i>Colla1</i>
	EX12-EX24	<i>Mmp14</i> , <i>Timp3</i>	<i>Timp3</i> , <i>Timp4</i>

**Table 2.** Inflammatory and matrix turnover genes changed with chronic exercise.

		Chronic Tendon	Chronic Muscle
Arachidonic Acid Cascade	CA-EX12	<i>Alox5ap</i>	<i>Ptgfr</i>
	CA-EX24	<i>Alox5ap</i>	<i>Ptgfr</i>
	EX12-EX24	---	---
Matrix Turnover	CA-EX01	<i>Mmp14</i> , <i>Timp1</i> , <i>Timp3</i> , <i>Colla1</i> , <i>Col3a1</i>	<i>Mmp14</i> , <i>Colla1</i> , <i>Col3a1</i>
	CA-EX08	<i>Mmp14</i> , <i>Timp1</i> , <i>Colla1</i>	<i>Mmp14</i>
	EX01-EX08	<i>Mmp14</i> , <i>Timp3</i> , <i>Colla1</i> , <i>Col3a1</i>	<i>Col3a1</i>

responses of MMPs/TIMPs to exercise have been seen in other studies as well.<sup>e.g., 5,6</sup> Similar to the present study, MMP-14 mRNA in skeletal muscle increased with 10 days of training.<sup>6</sup> Acute changes may play an important role in initiating the downstream processes that lead to beneficial adaptation to exercise. Results of this study support our hypothesis that a mild, acute inflammatory response occurs in tendon and muscle following a single bout of exercise; however, the precise timing of this response and when levels return to baseline has not been determined. As expected, inflammatory genes were more changed at acute time points than chronic, and results support the hypothesized adaptive matrix changes following chronic loading.

The Panomics QuantiGene 2.0 multiplex assay used in this study has the benefit of detecting original RNA quantities with high precision and accuracy by using branched DNA signal amplification without reverse transcription. Genes can be simultaneously detected within a sample. However, due to limitations on the size of the plate, only one RNA sample was run per specimen rather than averaging replicates. Furthermore, the sample size was restricted to 4 specimens per group to allow investigation of multiple time points. A single, untrained cage activity group within 10% of the weight of the other groups was used for all comparisons. Several genes did not meet the limit of detection, despite our best efforts in optimizing the quantity of RNA. Despite these limitations, we detected several gene changes in supraspinatus muscle and tendon suggesting a role for the AA cascade and MMPs and TIMPs in the adaptation of tissue to beneficial exercise. As with any RNA screening study, future work should seek to confirm protein changes in muscle and tendon associated with acute and chronic responses to exercise.

*In vitro* experiments have shown that cultured human tenocytes respond to strain by modulating production of prostaglandin E2 (PGE<sub>2</sub>), COX-1, COX-2,<sup>8</sup> and leukotriene B(4),<sup>9</sup> implying load-induced activation of the AA cascade in tendon. Despite implications that prostaglandins may contribute to early tendon degeneration,<sup>10-12</sup> their presence may indicate tendon remodeling,<sup>13</sup> which is supported by increased PGE<sub>2</sub> levels in humans following a bout of exercise.<sup>14,15</sup> The present study adds further evidence of a physiologic (not pathologic), acute prostaglandin response to beneficial exercise in tendon and muscle. Whether these up and downregulations correspond with increased and decreased protein expression will need to be verified in future studies. Importantly, gene changes occurred as a result of an acute bout of exercise, implying that this pathway plays a role in the tissue response to exercise and could lead to activation of downstream processes. PGE<sub>2</sub> may be involved in converting mechanical load to type I collagen synthesis, the primary component of tendon,<sup>1</sup> further supported by the increased tendon and muscle *Colla1* expression in this study.

The results of this screening assay suggest that tendon response to chronic beneficial exercise is distinct from chronic overuse loading. Specifically, following chronic overuse, tendon exhibits a more cartilaginous phenotype<sup>16</sup> with increased type III:I collagen ratio (fibrosis), heat shock proteins,<sup>17</sup> and nitric oxide synthases.<sup>18</sup> Following chronic exercise in this study, we did not find increased expression of the cartilage markers *Sox9*, *Acan*, or *Col2a1*, the heat shock proteins *Hspa2* and *Hspb1*, or the nitric oxide synthases *Nos2* and *Nos3* in tendon. After 1 week of exercise, both *Colla1* and *Col3a1* expression increased; however, by 8 weeks *Col3a1* returned to baseline expression levels, while *Colla1*, the main structural component of tendon, remained elevated. Increased type I collagen may lead to improved tendon mechanical properties. Finally, chronic overuse tendons demonstrate increased COX-2 and 5-lipoxygenase activating protein gene expression;<sup>19</sup> however, in this non-injurious exercise animal model, 5-lipoxygenase activating protein (*Alox5ap*) gene expression decreased in tendon with chronic exercise, and COX-2 synthase (*Ptgs2*) was below the limit of detection. These results indicate differential responses of the inflammatory cascade in tendon following chronic overuse compared to non-injurious exercise.

In conclusion, this study demonstrates a role of inflammatory processes and matrix turnover in the beneficial adaptation and response of supraspinatus muscle and tendon to acute and chronic load. Future studies can use these results to distinguish beneficial and detrimental loading effects on tissue, identify tissue recovery, and develop new treatment options.

## REFERENCES

1. Kjaer+: *J Appl Physiol*, 115:879-83, 2013.
2. Thampatty+: *Gene*, 372:103-9, 2006.
3. Connizzo+: *Clin Orthop Relat Res*, 472:2433-9, 2014.
4. Rooney+: *Muscles Ligaments Tendons J*, 4:413-9, 2014.
5. Kjaer+ *Physiol Rev*, 84:649-98, 2004.
6. Rullman+: *J Appl Physiol*, 106:804-12, 2009.
7. Rullman+: *J Appl Physiol*, 102:2346-51, 2007.
8. Wang+: *Connect Tissue Res*, 44:128-33, 2003.
9. Li+: *Am J Sports Med*, 32:435-40, 2004.
10. Khan+: *Clin J Sport Med*, 15:27-33, 2005.
11. Devkota+: *Connect Tissue Res*, 51:306-13, 2010.
12. Zhang+: *J Orthop Res*, 28:198-203, 2010.
13. Ferry+: *Sports Med Arthrosc Rehabil Ther Technol*, 4:2-10, 2012.
14. Langberg+: *J Physiol*, 515:919-27, 1999.
15. Langberg+: *J Physiol*, 521:299-306, 1999.
16. Archambault+: *J Orthop Res*, 25:617-24, 2007.
17. Millar+: *Clin Orthop Relat Res*, 466:1569-76, 2008.
18. Szomor+: *J Orthop Res*, 24:80-6, 2006.
19. Perry+: *J Shoulder Elbow Surg*, 14:79S-83S, 2005.

## ACKNOWLEDGEMENTS

The authors thank H. Rodriguez and J. Tucker. Funding: PCMD (NIH/NIAMS P30 AR050950) and a VA grant

# PODIUM PRESENTATIONS

## ENDOSCOPY AND PERCUTANEOUS SUTURING IN THE ACHILLES TENDON RUPTURES AND THE IMPORTANCE OF PARATENON

Mahmut Nedim DORAL<sup>1</sup>, Gazi Huri<sup>1</sup>, Pınar Huri<sup>2</sup>, Gürhan Dönmez<sup>3</sup>, Defne Kaya<sup>4</sup>, Mustafa Fevzi Sargon<sup>5</sup>, Egemen Turhan<sup>1</sup>,

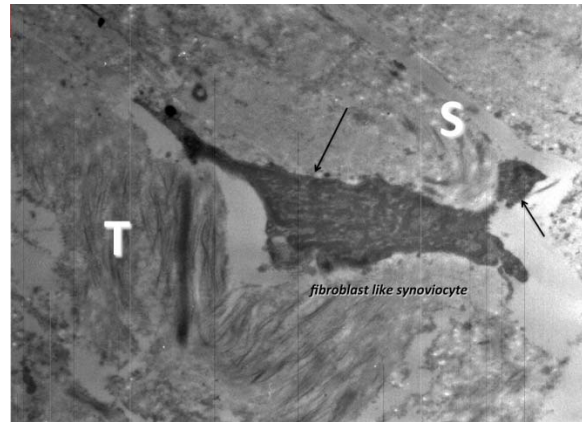
<sup>1</sup>*Dept. of Orthopaedics&Traumatology, Hacettepe University*<sup>2</sup>

<sup>3</sup>*Dept. of Sports Medicine, Hacettepe University*

<sup>4</sup>*School of Physiotherapy, Biruni University*

<sup>5</sup>*Dept. of Anatomy, Hacettepe University*

Although the Achilles tendon (AT) is the strongest tendon in the human body, rupture of this tendon is one of the most common sports injuries in the athletic population. The management of AT ruptures should aim to minimize the morbidity of the injury, optimize rapid return to full function, and prevent complications. Since endoscopy-assisted percutaneous AT repair allows direct visualization of the synovia and protects the paratenon that is important in biological healing of the AT, this technique becomes a reasonable treatment option in AT ruptures. Thirty-four male patients with a mean age of 37.8 years were treated by percutaneous suturing with a modified Bunnel technique under endoscopic control within 10 days after acute total rupture. During the endoscopic visualization of the synovia paratenon of the fifteen patient's Achilles tendons were noted as intact whether the nineteen was torn. Platelet-rich plasma was injected to stimulate the biologic repair process at the end of suturing. Patients were immediately encouraged to weight-bearing as tolerated after early functional physiotherapy. The procedure was tolerated in all patients and they were all achieved full weight-bearing without a brace at a minimum of 3 weeks of post-operative period. Eighty-two percent of patients, including professional athletes, returned to their previous sports activities that was significantly better in paratenon intact patients (93% vs 73% respectively). The interval from injury to return to regular work and rehabilitation training was 12.3 weeks (range 10-14 weeks) in all patients similarly shorter in paratenon intact group. At the latest follow-up (mean 22,7 months; range 12-31 months), all patients had satisfactory results with a mean American Orthopaedic Foot and Ankle Society's ankle-hind foot score of 97.2 vs 92.3 better in paratenon intact group. No re-ruptures, deep venous thrombosis or wound problems was observed in follow-up.



Electron microscopic evaluation of the paratendons revealed fibroblast-like synoviocytes in paratenon intact injuries. It should be note that compact paratenon improves the results of Achilles tendon repair.

A NOVEL MAGNESIUM RING FOR REGENERATION OF  
AN INJURED ANTERIOR CRUCIATE LIGAMENT – *In Vitro* and *In Vivo* Studies in Goats

K. F. Farraro, A. Pastrone, M. M. Tei, K. E. Kim, J. R. Flowers, S. L-Y. Woo  
*Musculoskeletal Research Center, University of Pittsburgh, Pittsburgh, PA, USA*

**INTRODUCTION:** Recent advances in functional tissue engineering have renewed interest in healing an injured anterior cruciate ligament (ACL) <sup>1,2</sup>. In our research center, we used biological augmentation via an extracellular matrix (ECM) sheet and hydrogel to successfully heal a fully transected ACL in a goat model <sup>3</sup>. However, during the process of ACL healing, there was disuse atrophy of its insertion sites. Thus, mechanical augmentation of the healing ACL is also necessary to restore initial joint stability and load the ACL throughout the healing process <sup>4,5</sup>. To this end, we have designed a bioresorbable magnesium (Mg) ring to connect the two ends of an injured ACL and facilitate healing <sup>6</sup>. We hypothesized that the ring could keep the repaired ACL (and its insertions) loaded and restore joint stability immediately after surgery. When used alongside *in vivo* with an ECM bioscaffold, it would aid in the healing of the entire femur-ACL-tibia complex (FATC).

**METHODS:** 8 eight cadaveric goat stifle joints were first used. The function of the intact and ACL-deficient joint was measured using a robotic/universal force-moment sensor (UFS) testing system <sup>7</sup>. The stifle joint kinematics and in-situ forces in the intact ACL were obtained at 3 flexion angles (30°, 60°, and 90°) under an externally-applied 67-N anterior tibial load (ATL). Then, the ACL was repaired using the Mg ring, and the entire test sequence was repeated. The anterior tibial translation (ATT) and in-situ forces in the repaired ACL were compared to those in the intact and ACL-deficient stifle joint <sup>5</sup>.

In the second study, the Mg ring was applied *in vivo* to 4 goats with a surgically transected ACL. It was used in combination with an ECM sheet and hydrogel composed of porcine urinary bladder matrix (UBM). Two animals each were sacrificed at 6 and 12 weeks and gross morphology, histological appearance, and degradation of the Mg ring via micro-computed tomography (micro CT) of the healing ACL were assessed.

**RESULTS:** In the *in vitro* study, the ATT of the intact joint was measured to be  $2.5 \pm 0.6$ ,  $2.7 \pm 0.9$ , and  $1.8 \pm 1.0$  mm at 30°, 60°, and 90° of knee flexion, respectively. After the ACL was cut, it increased to  $15.2 \pm 2.3$ ,  $15.8 \pm 1.7$ , and  $12.4 \pm 1.6$  mm, respectively. After the application of the Mg ring, the ATT was reduced by 60 – 70% from the ACL-deficient state, and was  $5.0 \pm 1.0$ ,  $5.8 \pm 1.0$ , and  $4.3 \pm 1.3$  mm, respectively ( $P < 0.05$ ). Mg-based ring repair was able to restore in-situ forces in the ACL to those of the intact ACL at all tested knee flexion angles ( $60 \pm 8$ ,  $57 \pm 4$ , and  $49 \pm 9$  N versus  $61 \pm 7$ ,  $62 \pm 7$ , and  $54 \pm 7$  N;  $P > 0.05$ ).

In the *in vivo* study, all animals had returned to their pre-injury activity levels by 6 weeks, with minimal lameness and joint swelling. Also, healing of the treated ACL had taken place, with continuous neo-tissue formation between the two ends of the ACL as well as surrounding the Mg ring. H&E staining of the FATC also revealed a normal immune response with no cytotoxic effect of the Mg ring on surrounding tissue. The ECM was no longer visible. A volumetric analysis via micro CT revealed 40% corrosion of the ring, with the majority of corrosion products (~98%) remaining adhered to the surface of the ring. By 12 weeks, the healing ACL was more robust with continuous, opaque, collagen bundles aligned in the longitudinal direction. It had become similar in size and shape to the normal ACL (see Figure 2). Both the Mg ring and ECM bioscaffold appeared to be fully resorbed.

**DISCUSSION:** The Mg ring was able to successfully load the ACL and restore joint stability in a goat model, confirming our hypothesis. When used in combination with an ECM bioscaffold, it was able to successfully heal a fully transected ACL by 12 weeks. With these positive results, we are confident of its use and have designed a 12-week study with morphological and biomechanical evaluation, followed by a 26-week study to examine if these positive effects persist and moreover, if the Mg ring would protect the insertion sites from disuse atrophy.

**ACKNOWLEDGEMENTS:** Support from an NSF Engineering Research Center Grant (#0812348), the Commonwealth of Pennsylvania, and Biomechanics in Regenerative Medicine training grant (NIH T32), is gratefully acknowledged.

**REFERENCES:** 1. Murray, et al. 2013. *Am J Sports Med.* 2. Steadman, et al. 2006. *J Knee Surg.* 3. Fisher, et al. 2012, *KSSTA.* 4. Fleming, et al., 2008. *JOR.* 5. Fisher, et al. 2011. *J Biomech.* 6. Farraro, et al. 2014. *J Biomech.*, 7. Sakane, et al. 1999, *KSSTA.* \* PCT patent application has been filed

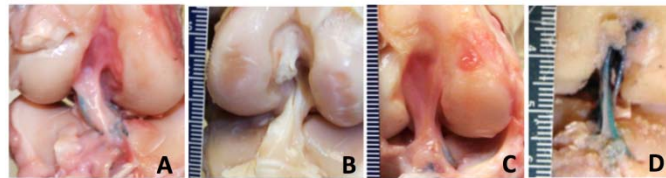


**Figure 1:** Gross morphology at 12 weeks of healing of the Mg ring-repaired ACL (A), sham-operated control (B), ECM-treated ACL (C), and suture-repaired ACL (D) <sup>3</sup>

# FABRICATION OF MULTI-LAYERED TENDON TISSUE ENGINEERING SCAFFOLD CONSISTING OF ELECTROSPUN NANOFIBERS AND PHOTOCROSSLINKED HYDROGEL

Guang Yang, Hang Lin, Benjamin B. Rothrauff, Rocky S. Tuan

*Center for Cellular and Molecular Engineering, University of Pittsburgh, Pittsburgh, PA, USA*

## INTRODUCTION:

Tendon and ligament (T&L) tissue regeneration after injuries continues to present clinical challenge due to poor intrinsic healing capacity. Tissue engineering provides a promising alternative treatment approach to autograft/allograft transplantation. Functional tendon tissue engineering requires the use of biomimetic scaffolds that create a three-dimensional (3D) environment similar to that in the native tendon tissue. We describe here the development and characterization of a novel stem cell-loaded composite scaffold, consisting of electrospun nanofibers impregnated with photocrosslinked hydrogel, as a tendon graft.

## MATERIALS AND METHODS:

The scaffold was fabricated by co-electrospinning of polycaprolactone (PCL) and methacrylated gelatin (mGLT). The scaffold was wetted in photo-initiator to increase porosity and then UV photocrosslinked to retain gelatin after soaking. Simultaneous cell seeding and photocrosslinking of multiple scaffold layers were performed to create cell-impregnated multilayer construct.

## RESULTS:

While both PCL and mGLT appeared fibrous in the dry electrospun scaffold, mGLT lost fibrous architecture upon scaffold wetting (Fig. 1A; red, PCL; green, mGLT). Photocrosslinking retained mGLT within the scaffold and resulted in a uniform distribution of GLT throughout the scaffold, compared to conventional surface coating of GLT on the scaffold (Fig. 1B, picosirius red staining). mGLT photocrosslinking also retained scaffold mechanical strength after incubation in PBS for up to 7 days (Fig. 1 C).

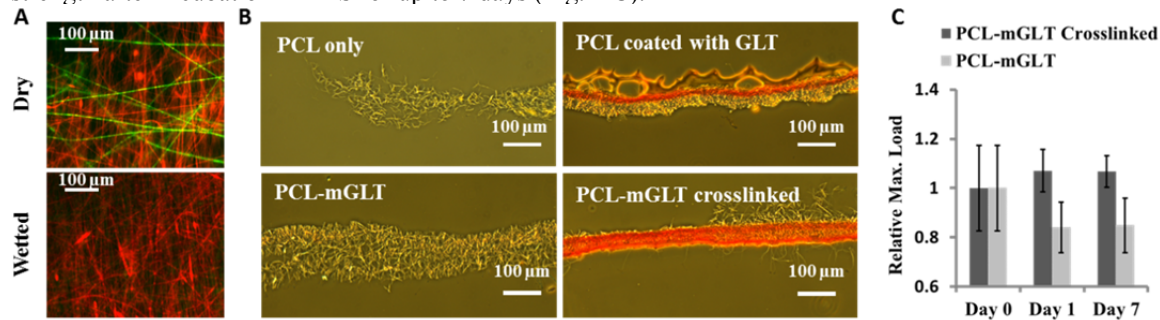


**Fig. 1.** Characterization of composite scaffold

To create a complex multi-layered structure, 5 layers of aligned scaffold were stacked, with or without photocrosslinking, and incubated for 7 days in PBS. A significant difference in scaffold integrity was seen in cross-sectional views. As shown in Fig. 2B (picrosirius red staining), without crosslinking (left), the scaffold layers did not adhere to each other, most likely due to mGLT loss, with reduced elastic modulus, PCL-mGLT sandwich construct showed partial failure (center), while photocrosslinked composite scaffold remained fully integrated (right).

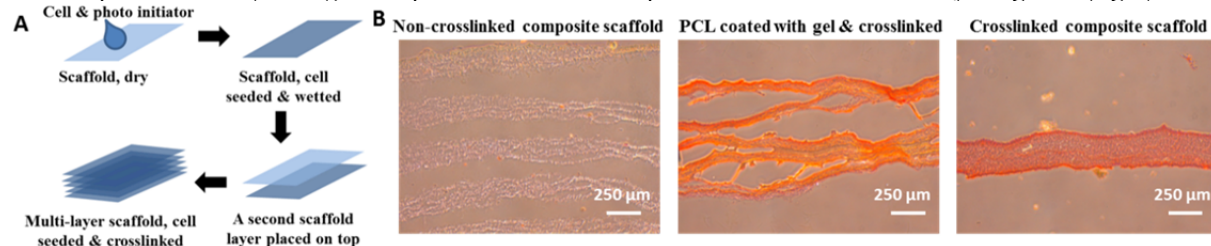


**Fig. 2.** Design and characterization of multilayer construct

## DISCUSSION:

We have developed a photocrosslink-based approach to fabricate a biomimetic multilayer nanofiber-hydrogel biomaterial for functional T&L tissue engineering. Stem/progenitor cell behavior in the scaffold, including attachment, morphology, and differentiation, is currently being investigated. This study is supported in part by the NIH, Commonwealth of Pennsylvania Dept. of Health, and the U.S. Department of Defense.

## IN-VIVO EVALUATION OF A BIORESORBABLE PLLA DEVICE FOR REGENERATION OF THE ACL

William R Walsh<sup>1</sup>, Nicky Bertollo<sup>1</sup>, Robert Arciero<sup>2</sup>, Robert Stanton<sup>3</sup>, and Robert Poggie<sup>4</sup>

<sup>1</sup>*Prince of Wales Clinical School, University of New South Wales, Prince of Wales Hospital, Randwick, Australia,*

<sup>2</sup>*The University of Connecticut Medical Center, Farmington, CT, USA,* <sup>3</sup>*Orthopaedic Specialty Group, Fairfield, CT, USA,* <sup>4</sup>*BioVera, Inc., Notre-Dame-de-L'Île-Perrot, QC, Canada*

### INTRODUCTION:

Anterior cruciate ligament reconstruction (ACL) is an effective surgical procedure. However, pain and morbidity associated with harvest of autograft, and the potential for disease transmission and variable outcomes of allograft are of concern. A synthetic alternative to human tissues has long been sought to address these issues, with mostly poor clinical outcomes. The ideal synthetic device would temporarily replace the ACL, facilitate the regeneration of host tissue into a fully functional ACL, and be bioresorbed without adverse effects. This abstract describes the 6 weeks through 4 years performance of a bioresorbable poly-L-lactic-acid (PLLA) device used to reconstruct and regenerate the ACL in an acute functional knee model in sheep.

### METHODS:

The PLLA implant is made of multiple 3-D braided bundles of PLLA fibers (15 µm), with a loose braid intra articularly and a tight braid for whip stitching with non-resorbable suture and insertion into the bone tunnels. The human implant is 6 mm in diameter, 120 mm long; the ovine implant 4 mm in diameter, 80 mm long.

ACL reconstructions were performed with PLLA devices in 48 adult sheep and autograft extensor tendons in 28 sheep with titanium alloy interference screws on the femur and tibia. The reconstructions were evaluated at 3, 6, 12, 18, 24, and 48 months for clinical function, synovitis, serology, gross reaction, scoring of cartilage and menisci, histology, radiography, micro-CT, MRI, and pathology of major and filter organs. The ultimate strength, stiffness, and energy to failure of the bone-ligament-bone (BLB) complex were measured at time zero, and 6 & 12 months via testing in an anterior draw orientation (45 degrees) using a preconditioning profile of 10 cycles, followed by a stress relaxation period prior to testing to failure at a rate of 50 mm/minute.

### RESULTS:

Micro-CT, radiographs, MRI, and histology indicated resorption of the grafts and regeneration of the ACL at 12 months, and continued maturation of intra articular tissue through 18 and 24 months, and gradual envelopment of the PLLA scaffold by bone through 48 months. The sheep with PLLA devices were fully functional post-op and at all time points, while the autograft sheep exhibited early post-op morbidity. There was no evidence of synovitis and serology and gross findings were normal. Histology of the intra articular portion of the PLLA implants and autograft showed neo ligamentization at 3 months, increased collagenous deposition and cellularity with time, a reconstituted ACL at 1 year, and continued graft maturation. Intra-articularly, PLLA devices were intact at 3 and 6 months, and nearly fully resorbed at 1 year; remnant PLLA was observed at 12, 18, and 24 months.

Histology of the tibial tunnel at 6 through 48 months showed the more proximal portion of the graft (distal from the screw) filled with new collagenous tissue and progression of tendon-bone healing. Pathology of lymph nodes and organs indicated occasional presence of PLLA particulate. The ultimate load to failure for the PLLA device with outside-in fixation for the tibia and femur at 6 and 12 months was 320N (n=6, SD 142N) and 601N (n=6, SD 186N). Likewise, load to failure for autograft at 6 and 12 months was 358N (n=1) and 422N (n=3, SD 164N). The strength of the human device is 1952 N, stiffness 960 N/mm, and fatigue strength 500N. In-vitro degradation in phosphate buffered saline for 24 months showed >85% retention of strength and molecular weight.

### DISCUSSION:

Histology of sheep with PLLA devices at 12, 24, and 48 months showed a regenerated ACL that resembled autograft reconstructions. Histology was consistent for auto and PLLA grafts, which is ascribed to the PLLA resembling autograft in terms of early load bearing, gradual resorption and consequent load transfer to newly formed tissue (absence of stress shielding), and maturation of tissue after 6 months. The absence of adverse tissue reaction to PLLA is ascribed to the biocompatibility and high ratio of surface area to volume of the PLLA fibers. The difference in resorption observed in the bone tunnels versus intra articularly is ascribed to the more vascular, biologically dynamic healing environment of the ACL. This PLLA scaffold possesses the requisite biomechanical properties for ACL reconstruction based on a fatigue strength of 500 N exceeding the maximum ACL load of 450 N. This is the first study to demonstrate complete regeneration of ACL tissue, resorption of an implant intra articularly using a degradable polymeric scaffold, and is the longest in-vivo evaluation of PLLA in ligament repair that we are aware.

## PLATELET BASED BLOOD PRODUCTS FOR STIMULATION OF TENDON HEALING AN IN VITRO CELL CULTURE STUDY

<sup>1</sup>Schmidt, T; <sup>1</sup>Klatte-Schulz, F; <sup>1</sup>Ueckert, M.; <sup>1</sup>Wildemann, B; <sup>2</sup>Scheffler, S; <sup>3</sup>Kalus, U; <sup>3</sup>Pruss, A,  
<sup>1</sup>Julius Wolff Institute, Center for Musculoskeletal Surgery, Charité-Universitätsmedizin Berlin, Germany  
<sup>2</sup>sportthopaedicum Berlin, Germany;  
<sup>3</sup>Institute of Transfusion Medicine, Charité-Universitätsmedizin Berlin, Germany

**INTRODUCTION:** Tendon healing is limited due to poor vascularity and low intrinsic healing capacity. Platelet rich blood products contain a variety of growth factors, which are known to trigger or even be involved in angiogenesis and tissue regeneration. Because different protocols and systems are available to prepare PRP, currently used PRP's vary in platelet, leukocyte and growth factor content. Platelet lysate (PL) can be prepared by freezing and thawing PRP to lyse the platelets and release the growth factors, which can be harvested after centrifugation and used to stimulate tendon healing. This study aimed to investigate the effect of PL and different PRPs on human tenocytes to validate their capability as therapeutic agent to promote tendon healing.

**MATERIAL AND METHODS:** Platelet concentrate (PC), platelet lysate (PL), platelet rich plasma (PRP; BCT tubes, RegenLab) and autologous conditioned plasma (ACP, Arthrex) from 12 male donors (30-50 years) were prepared following standard protocols or the instructions of the manufacturer. PC was produced by apheresis. PL was produced from PC by one cycle of freezing (-80°C), thawing and centrifugation. Platelet and leukocyte concentration was determined using a standard blood cell counter (Sysmex K-4500). Tenocytes from 4 male donors (mean age 69.5 years) were isolated from supraspinatus tendon biopsies by collagenase digestion and pooled. A total of  $1 \times 10^4$  cells per well were seeded into 24-well plates. After 2 days an Alamar blue test was performed to analyse cell activity. Afterwards cells were stimulated with PRP, ACP, PC or PL each 10% v/v in cell culture medium with 10% human serum using cell culture inserts with 0.4µm pore size. Cells cultures in medium with 10% human serum served as negative control. After 5 days, cell activity was again analysed by Alamar Blue test. Furthermore, RNA was isolated and gene expression of collagen I, III, scleraxis, tumor necrosis factor-alpha (TNF-α) and Interleukin-1 beta (IL-1β) was analysed by Real-Time PCR. **Statistics:** Mann-Whitney U test, Bonferroni-Holm correction,  $p \leq 0.05$ .

**RESULTS:** Platelet content was significantly higher in PC ( $1.17 \times 10^9$ /ml) compared to ACP ( $5.7 \times 10^8$ /ml) and PRP ( $2.3 \times 10^8$ ;  $p \leq 0.0001$ ). Furthermore, platelet content was significantly higher in ACP compared to PRP ( $p \leq 0.0001$ ). Leucocyte content was significantly lower in ACP ( $1.9 \times 10^5$ /ml) and PC ( $1.3 \times 10^5$ /ml) compared to PRP ( $8.7 \times 10^5$ /ml;  $p \leq 0.0001$ ).

Cell activity and collagen I expression was significantly increased in all groups except PL compared to negative control ( $p \leq 0.04$ ). Collagen III expression was significantly increased after stimulation with PRP. Gene expression of the tendon marker scleraxis was significantly decreased in all groups with exception of ACP group ( $p \leq 0.03$ ) compared to negative control (fig. A). Analysis of the inflammatory cytokines showed a highly increased IL-1β gene expression in 4 out of 12 cell cultures stimulated with PRP. Gene expression of TNF-α was not affected in any group.

### DISCUSSION:

This study showed that platelet based blood products may be beneficial in tendon healing by increasing cell activity and collagen I gene expression. However the significantly decreased scleraxis gene expression, a tendon marker which is involved in tendon differentiation and maturation, in all groups except ACP may underline the limited capability. These results might explain partially the unsatisfactory results of clinical studies using PRPs to stimulate tendon healing [1, 2]. Platelet lysate was not able to overcome standard PRP limitations and the poorer results regarding cell activity and collagen I expression may be based on negative effects of freezing. The highly increased gene expression of IL-1β, especially after stimulation with PRP, could indicate inflammatory effects. This may be due to the significantly higher leukocyte content in PRP.

The use of platelet preparations for tendon repair is a promising, safe and easy method to use the body's own growth factors and it is capable to increase cell activity and extracellular matrix gene expression. However, the impact is limited and the influence of preparation and platelet, leukocyte and growth factor content are still poorly understood, so further studies are needed to clarify the mechanisms to improve clinical outcomes.

**REFERENCES:** [1] De Vos et. al 2011, Br J Sports Med, [2] Rodeo et. al 2011, Am J Sports Med

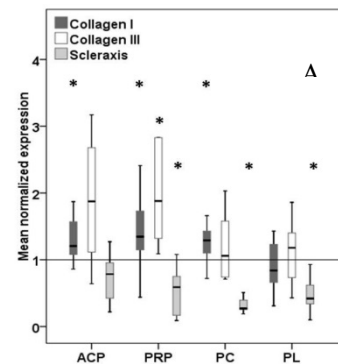


**Fig. A** shows gene expression of collagen I, III and scleraxis after 5 days of stimulation

# BIAXIALLY ALIGNED TENDON-DERIVED MATRIX-POLY(E-CAPROLACTONE) (PCL) ELECTROSPUN SCAFFOLDS FOR ROTATOR CUFF TENDON TISSUE ENGINEERING.

T. Tseng\*, S. Meehan\*, A. Chainani, S.B. Orr, C.L. Gilchrist and D. Little.

*Orthopaedic Research Laboratories, Departments of Orthopaedic Surgery and Biomedical Engineering, Duke University, Durham, NC. \*Co-first authors*

## INTRODUCTION:

Electrospun scaffolds have been evaluated for rotator cuff tendon tissue engineering,<sup>1-5</sup> and we have recently used a multi-layered electrospinning approach<sup>6, 7</sup> to achieve growth of human adipose stem cells (hASCs) through the full thickness of aligned and non-aligned scaffolds.<sup>7, 8</sup> We and others have shown that tendon-derived extracellular matrix (TDM) can stimulate tenogenesis.<sup>7, 9-14</sup> However it remains unclear whether the biomimetic effects of TDM are retained with electrospinning. The normal rotator cuff is composed of collagen fibers running both parallel to the axis of predominant loading and at 45 degrees to this axis,<sup>15, 16</sup> which allows for distribution of multi-axial loads over a wide area. Consideration of this complex arrangement of collagen fibers may reduce stress concentration and potential for failure in tissue engineered rotator cuff. The objectives of this study were two-fold: To evaluate tissue engineered tendon development on multi-layered scaffolds with biaxial alignment,  $\pm 45$  degrees (45-offset) to the expected principal axis of loading compared to scaffolds aligned only in the axis of principal loading (0-offset). Second, to compare the biomimetic effects of electrospun TDM-PCL composite fibers (fTDM-PCL) to TDM-coated electrospun PCL fibers (cTDM-PCL) and PCL fiber only (PCL).

## METHODS:

TDM was prepared as described previously.<sup>14</sup> 10% w/v PCL scaffolds were prepared by electrospinning individual aligned layers using a hybrid alignment technique as described previously.<sup>8</sup> fTDM-PCL scaffolds were electrospun from 1% w/v TDM and 10% w/v PCL, and cTDM-PCL scaffolds were prepared by electrospinning PCL layers then coating alternate layers with 1% TDM. 0-offset scaffolds were prepared by collecting each aligned layer sequentially onto a collection slide in the same orientation. 45-offset scaffolds were prepared by alternately collecting each aligned layer at  $\pm 45$  degrees to the axis of the 0-offset scaffolds generating biaxial instead of uniaxial alignment. Scaffolds were seeded with hASCs and cultured for 28 days in media without exogenous growth factors. Outcomes of biochemical content were evaluated, together with expression of tendon-related genes, tensile mechanical properties, and development of aligned collagen. Results were assessed by factorial ANOVA with Neuman-Keuls post-hoc test ( $p < 0.05$ ).

## RESULTS:

Cell infiltration and matrix synthesis was observed through the full thickness of all seeded scaffolds. There was no effect of scaffold alignment direction on DNA, s-GAG content or gene expression. DNA content increased to the greatest extent in fTDM-PCL after seeding. Seeded fTDM-PCL scaffolds demonstrated the greatest increase in collagen content, particularly in 0-offset scaffolds. Tendon-related gene expression was upregulated, in particular tenomodulin in cTDM-PCL. s-GAG content increased with cell seeding over time, especially in cTDM-PCL. Collagen alignment was greatest in x-y and y-z planes in 0- compared to 45-offset scaffolds, and through the thickness of the scaffolds, alignment index as assessed by polarized light imaging was greatest in cTDM-PCL. Modulus and yield stress were greatest for fTDM-PCL with no effect of scaffold alignment direction.

## DISCUSSION:

Incorporation of TDM into scaffolds was biomimetic but effects differed depending on whether fibers were coated with TDM or if TDM was incorporated into the electrospun fibers. As expected, 45-offset scaffolds induced less overall collagen alignment than 0-offset scaffolds, but this was generally not reflected in mechanical properties. These data confirm TDM is beneficial to development of tendon-like properties in electrospun scaffolds and suggest that biaxial alignment patterns and manipulation of the vertical gradient of multi-layered scaffolds should be investigated further for their ability to distribute multi-axial stress in rotator cuff tendon tissue engineering.

**REFERENCES:** 1) Xie J et al, *Nanoscale* (2010) 2:923-6. 2) Moffat KL et al, *Tissue Eng Part A* (2009) 15: 115-26. 3) Hakimi O et al, *Eur Cell Mater* (2012) 24:344-57. 4) Baker BM et al, *Biomaterials* (2008) 29:2348-58. 5) Taylor ED et al, *J Bone Joint Surg Am* (2010) 92 (Suppl 2):170-9. 6) Tzezana R et al, *Tissue Eng Part C Methods* (2008) 14:281-8. 7) Chainani A et al, *Tissue Eng Part A* (2013) 19:2594-604. 8) Orr SB et al, *Proc Ortho Res Soc* (2014) 39:508. 9) Zhang J et al, *Biomaterials* (2011) 32:6972-81. 10) Yin Z et al, *Acta Biomater* (2013) 12:9317-29. 11) Youngstrom DW et al, *PLoS One* (2013) 8:e64151. 12) Little D et al, *Tissue Eng Part A* (2010) 16:2307-19. 13) Omae H et al, *J Tissue Eng Regen Med* (2012) 6:238-44. 14) Orr SB *Proc Orthoped Res Soc* (2014) 39:507. 15) Clark JM & Harryman DT, *J Bone Joint Surg Am* (1992) 74:713-25. 16) Fallon J et al *J Orthop Res* (2002) 20: 920-6.

**ACKNOWLEDGEMENTS:** This work was supported by NIH grants AR059784, AR065764 and AR065888.

## A NOVEL MURINE MODEL OF AUTOGRAFT ANTERIOR CRUCIATE LIGAMENT RECONSTRUCTION

Brian Grawe; Hongsheng Wang; Boyce Collins; Jeffrey S Willey; Camila Carballo, Andrew Carbone; Ian Hutchinson; Xiang-Hua Deng; Scott A Rodeo.

**INTRODUCTION:** The distinct advantages of using the mouse model in translational research relate to expense, ease of handling and the abundant availability of transgenic strains. To date, a reproducible murine model to study bone-tendon autograft healing in Anterior Cruciate Ligament (ACL) reconstruction has been lacking. Therefore, the aim of this study was to develop a novel murine ACL reconstruction model using a tendon autograft.

**METHODS:** A total of 25 male mice (C57B16/inbred wild-type) were utilized for this study. All mice were 12 weeks old, and weighed between 22-30 grams. ACL autograft strength and integration were assessed at 2 week and 4 week time points, and compared to the native murine ACL. **Microsurgical Approach:** The hindlimb flexor tendon was harvested and controlled with 6-0 prolene suture placed in a Mason-Allen configuration. Using an open medial parapatellar arthrotomy, the ipsilateral ACL was disrupted and tunnels were prepared in the tibia and femur using a 23 gauge needle (0.64 mm diameter). The autograft was passed from the femoral side to the tibial tunnel and excess graft was tenodesed to the surrounding soft tissue for secure fixation. **Biomechanical Testing:** Graft stiffness and load to failure testing were performed (N=7 for week 2 and week 4) using established lab protocols. **Nanofocus CT:** Imaging was conducted with a GE Phoenix Nanotom-MTM instrument (GE Inspection Technologies; Lewiston, PA, USA) (N=2 for day 2, week 2 and week 4). The x-ray emission parameters for ~5  $\mu\text{m}$  voxel resolution were 60 kV and 60 mA, and the number of acquired projections was 1,800. Correlative decalcified histological analysis was undertaken in the remaining specimens.

**RESULTS:** The microsurgical ACL reconstruction technique was reproducible and resulted in anatomic trans-articular graft passage and secure fixation. Mean graft stiffness was  $2.28\text{N} \pm 1.41$  at 2 weeks and  $2.59\text{N} \pm 0.87$  at 4 weeks. This finding was co-incident with a progressive increase in load to failure testing from 2 to 4 weeks, ( $1.29\text{N} \pm 0.47$  and  $1.79\text{N} \pm 0.40$  respectively) approximating the native ACL at the 4 week time point. Graft failure resulted in the graft being pulled out of the tunnel at 2 weeks, while 4 week specimens failed at the mid-substance of the graft. NanoCT confirmed reproducible tunnel placement along the tibia and femur and demonstrated new trabecular bone formation at the healing interface at 4 weeks. Tunnel remodeling was evidenced by an increased intra-specimen variation in tunnel diameter at both 2 and 4 weeks, compared to day 2 controls (**Fig.1**). Histologic evaluation demonstrated fibrovascular granulation tissue with progressive cell ingrowth from the interface towards the inner tendon.

**CONCLUSION:** A reproducible model of ACL reconstruction using a flexor tendon autograft was established using the mouse model creating a biological *in vivo* platform to study graft ligamentization and graft-bone tunnel integration using transgenic animals. Therein, a comprehensive investigational paradigm was created using functional biomechanical measures, nanofocus CT imaging and correlative histology. Ultimately, it is hoped that this model can be applied to transgenic and knockout murine strains to further characterize the complex cellular and molecular events that control tendon-bone healing.

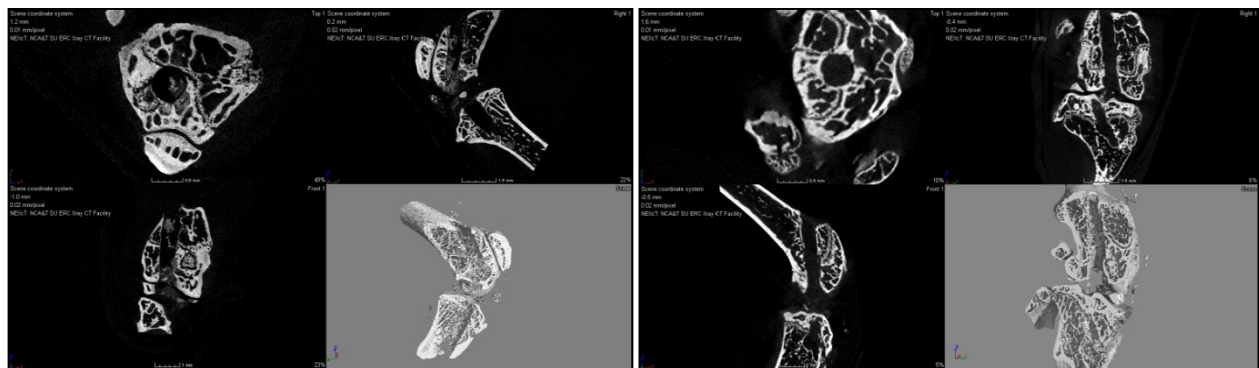


**Figure 1:** A) Day 2 specimen aligned with the axis of the femoral tunnel. The bone tunnels are sharply cut out from the trabecular bone and are anatomic in the knee joint; they are regularly shaped (femoral tunnel,  $704 \pm 28 \mu\text{m}$ ) and some debris is seen. B) Week 4 specimen aligned at the proximal tibia tunnel segment. There is evidence of interfacial bone formation and increased integration with the trabecular network. The diameter of the bone tunnels is more variable and has decreased on average from the  $640 \mu\text{m}$  surgical preparation (femoral tunnel  $622 \pm 68 \mu\text{m}$ ).

## INDIAN HEDGEHOG SIGNALING IN TENDON-BONE HEALING: A POTENTIAL REGULATOR OF ENTHESES REPAIR

A.D. Carbone, C.B. Carballo, X. Gu, H. Wang, L. Ying, R. Ma, X. Deng, S. Rodeo  
*Tissue Engineering Regeneration and Repair Lab, Hospital for Special Surgery, New York, NY*

**INTRODUCTION:** Tendon to bone healing is required for many common sports injuries, and healing between the repaired tendon and bone does not recapitulate a normal enthesis. Indian Hedgehog (Ihh) is a signaling protein which has recently been shown to be important in the development of enthesis tissue in a mouse model.<sup>1</sup> It is also a recognized regulator of matrix proteins expressed during tendon-to-bone repair and has a role in differentiation of tendon- progenitor stem cells (TPSC).<sup>2</sup> Based on our knowledge this is the first study to quantitatively evaluate the role of Ihh signaling during tendon-bone healing in the post-natal animal using a rat ACL reconstruction model.

**METHODS:** 14 adult male Sprague Dawley rats (300-350g) underwent surgical ACL transection and subsequent reconstruction using a flexor tendon graft. Rats were placed into two groups: 1. those whose graft was fixed under 0N of tension; 2. those whose grafts were fixed under 10N of tension. Animals were sacrificed at 3 and 6 weeks post-operatively. Specimens were evaluated using immunohistochemistry (IHC) for three different proteins of Ihh signaling whose expression level is increased when Ihh signaling is activated: Ihh, Patched 1, (Ptch1), and GLI1. Images were analyzed independently by two observers using a custom MatLab software designed to quantify staining.<sup>3</sup>

**RESULTS:** Qualitative analysis of all three stains demonstrated that Ihh signaling is active in granulation tissue formed at the healing tendon-bone interface. This was confirmed through IHC stains which demonstrated significantly greater staining in terms of area of staining as well as staining intensity when compared to negative controls. Staining was not uniformly distributed along the tendon bone interface; staining intensity was increased in areas of increased tendon graft-bone contact, with one side of the graft-bone interface generally showing more complete integration with the surrounding bone. We were also able to show increased staining intensity of Ptch1 ( $p=.035$ ) and Gli1 ( $p=.05$ ) at 3 weeks in animals that received a pre-tensioned tendon graft. There were also statistically significant differences between these same two groups in terms of area of the graft-bone interface stained, with Ptch1 ( $p=0.02$ ) and Gli1 ( $p=0.03$ ) showing increased staining in rats whose grafts were fixed under 10N of tension. No significant differences were seen between the three and six week time points when comparing the two groups.

**DISCUSSION:** We suggest that the Ihh signaling pathway is active during the tendon-bone healing process. The intensity and amount of staining may be related to the amount of contact between graft and bone as well as strain on the graft. Our analysis shows that pre-tensioning of the graft at the time of surgery resulted in increased Ihh signaling at 3 weeks. We also suggest that Ptch1, due to its increased expression levels, is the best protein marker to study Ihh signaling. Further studies are necessary to characterize the exact role of Ihh signaling during the tendon-bone healing process.

**REFERENCES:** 1. Liu C-F, et.al 2013, *PLoS One* 13;8(6):e65411; 2. Bi Y, et al. 2007, *Nat. Med.* 2007;13(10):1219-27; 3. Matkowskyj K. et al. 2000, *J. Histochem Cytochem*;48:303-311.

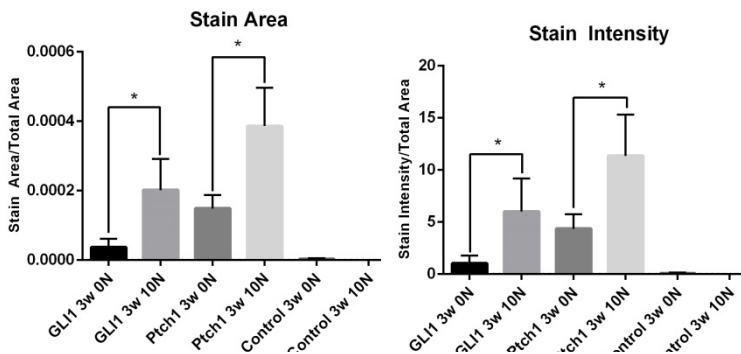


**Figure 1: Quantitative Analysis of Ihh signaling in terms of both area (A) and intensity (B) of stain. \*- denotes p-value < 0.05.**

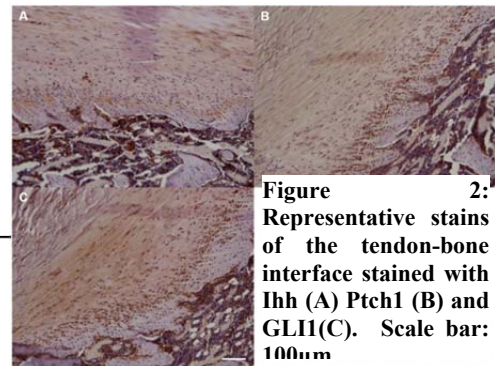


**Figure 2: Representative stains of the tendon-bone interface stained with Ihh (A) Ptch1 (B) and GLI1(C). Scale bar: 100µm**

## ENTHESIS MINERAL APPPOSITION DURING POSTNATAL GROWTH AND FOLLOWING JOINT DESTABILIZATION IN THE ADULT

<sup>1</sup>Nathaniel A Dymant, <sup>2</sup>Yusuke Hagiwara, <sup>1</sup>Xi Jiang, <sup>1</sup>Jianping Huang, <sup>1</sup>Douglas J Adams, <sup>1</sup>David W Rowe  
<sup>1</sup>University of Connecticut Health Center, Farmington, CT; <sup>2</sup>Nippon Medical School Hospital, Tokyo, Japan

**INTRODUCTION:** Several pathologies, including osteoarthritis and ankylosing spondylitis [1], yield increased mineralization of enthesis fibrocartilage. However, the mechanism of this process is largely unknown. Therefore, the objective of this study is to measure the mineral apposition within fibrocartilage of tendon and ligament entheses during postnatal growth and following joint destabilization in the adult to gain insight into the mineralization process and whether it is affected by altered loading during post-traumatic osteoarthritis pathogenesis.

**METHODS:** Transgenic Mice. Col1a1-CFP (unmineralized fibrochondrocytes) and ColX-RFP (mineralized fibrochondrocytes) double reporter mice were used for this study. Experimental Design. *Postnatal Growth.* Mice were injected with mineralization labels at 2.5 (demeclocycline), 4.5 (calcein), 6.5 (alizarin complexone), and 8.5 (demeclocycline) weeks of age. Limbs were harvested at 10.5 weeks of age to measure mineral apposition (i.e., distance between labels) within entheses of the patellar (PT), supraspinatus (ST), Achilles (AT) tendons and medial collateral ligament (MCL). *Joint Destabilization.* The ACL was transected (ACLT) in 10-week-old mice. Mineralization labels were delivered on the day before surgery (demeclocycline), 2 weeks postsurgery (calcein), and 4 weeks post-surgery (alizarin complexone). MCL entheses were assessed at 2 and 4 weeks post-surgery and compared to intact or sham controls. Sample Preparation. Limbs were fixed, embedded, and cryo-sectioned using cryofilm [2]. Enzymatic Activity. Sections were stained for alkaline phosphatase (AP) and tartrateresistant acid phosphatase (TRAP). Imaging. Each section was imaged repeatedly in this order: 1) GFP reporters and mineralization labels, 2) TRAP, 3) AP, and 4) toluidine blue (TB). Images from each round were aligned and constructed into multi-layer composites in Photoshop.

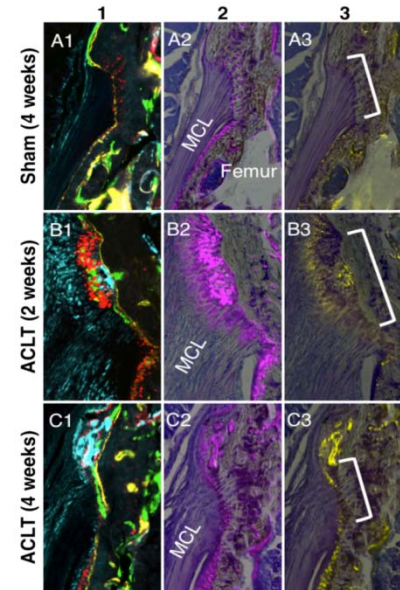


**Fig. 1.** Proximal MCL enthesis after ACL transection (ACLT). Top row is sham limb at 4 weeks, 2nd row is ACLT at 2 weeks, and 3rd row is ACLT at 4 weeks. Column 1 is Col1-CFP and ColX-RFP with mineral labels. Column 2 is AP with TB. Column 3 is TRAP with TB. Brackets denote enthesis width.

**RESULTS:** Postnatal Growth. Cells at the base of the enthesis were first to mineralize and mineral apposition progressed towards the midsubstance as cells in unmineralized fibrocartilage adjacent to the tidemark became encapsulated in mineral with time. These cells were AP<sup>+</sup> and a subset was AP<sup>+</sup>/TRAP<sup>+</sup>. Total mineral apposition was highest in the PT (162±29µm) followed by the MCL (118±15µm), ST (82±12µm), and AT (58±5µm) (p < 0.05). By 10.5 weeks of age, mineral apposition rate had dropped below detectable levels. Joint Destabilization. Unmineralized fibrochondrocytes adjacent to original tidemark (yellow) displayed increased Col1-CFP and ColX-RFP with a strong calcein label, indicating active mineral deposition (Fig. 1B1). These cells were AP<sup>+</sup> (magenta) and a subset was TRAP<sup>+</sup> (yellow) (Fig. 1B2-3). There was continued mineral apposition at 4 weeks, demonstrated by the alizarin complexone label that was advanced from the prior calcein label (Fig. 1C1). However, mineral apposition between 0 and 2 weeks was greater than between 2 and 4 weeks, indicating that mineral apposition was slowing. In addition, Col1-CFP, ColXRFP, AP, and TRAP signals were all reduced (Fig. 1C1-3), further demonstrating the reduction in mineralization.

**DISCUSSION:** Unmineralized fibrochondrocytes of the enthesis mature into mineralized fibrochondrocytes during postnatal growth to yield a fully developed zonal enthesis. These cells reduce Col1-CFP and increase AP, TRAP, and ColX-RFP when mineralizing. Once cells finish depositing mineral, they express only ColX-RFP. Mineralization initiates at the base of the enthesis and propagates towards the tendon midsubstance, yielding a maturation gradient with most mature cells at the bottom and least mature cells near the midsubstance. Mineralization activates again in the MCL enthesis following joint destabilization with increased AP, TRAP, and ColX expression by fibrochondrocytes. TRAP expression in these cells is particularly interesting as genetic mutation of TRAP leads to chondrodystrophy [3]. Related research by our lab and others suggest that hedgehog signaling regulates cartilage mineralization [4-5], which may be a potential drug target in these chronic pathologies.

**ACKNOWLEDGEMENTS:** NIH T90-DE021989, R01-AR54713, and R01-AR052374.

**REFERENCES:** 1. McGonagle et al, J Anat, 2010; 2. Dymant et al, PLOS One, 2013; 3. Hayman et al, J Bo

# INSERTION FIBROCHONDROCYTE GROWTH AND BIOSYNTHESIS ON NANOFIBER SCAFFOLDS

D. Qu, H. Park, J.P. Zhu, and H.H. Lu

Department of Biomedical Engineering, Columbia University, New York, NY, USA

**INTRODUCTION:** The fibrocartilaginous entheses through which the anterior cruciate ligament (ACL) connects to bone1-2 are not regenerated following current ACL reconstructions, compromising long-term stability and function3. Nanofibers have been explored for soft tissue-to-bone integration with promising results4-6. In order to establish benchmark criteria for interface tissue engineering, the objective of this study is to characterize the response of ACL insertion fibrochondrocytes on nanofiber scaffolds. Specifically, as the native enthesis consists of both non-mineralized and mineralized regions, cell response to hydroxyapatite (HA)-doped nanofibers will also be determined. It is hypothesized that both 3-D culture and HA incorporation will modulate cell growth and biosynthesis.

**METHODS:** *Scaffold fabrication:* Aligned poly-ε-caprolactone (PCL, Sigma-Aldrich)-poly(lactide-co-glycolide) (PLGA, 85:15, Lakeshore) nanofiber scaffolds were produced by electrospinning. HA nanoparticles (100-150 nm, Nanocerox) were incorporated (15% w/w) to produce PCL-PLGA/HA scaffolds. *Cell isolation and culture:* Fibrochondrocytes were obtained via enzymatic digestion of ACL entheses harvested from neonatal bovine tibiofemoral joints (n=3)7. Fibrochondrocyte-seeded scaffolds were cultured for up to 28 days. *End-point analyses:* At 1, 7, 14, and 28 days, cell viability (n=2) was evaluated and total DNA, alkaline phosphatase (ALP) activity, collagen deposition, and glycosaminoglycan (GAG) production were quantified (n=5/group per outcome) and assessed histologically. Mechanical properties (n=5) were evaluated by loading samples in uniaxial tension until failure. *Statistical analysis:* ANOVA and the Tukey-Kramer post-hoc test were used (\*, ^, p<0.05).

**RESULTS:** Cells remained viable on all nanofiber scaffolds over time and grew much faster compared to monolayer controls (Fig. 1). Cell ALP activity was initially enhanced on scaffold groups and more prominent mineral deposition was observed on the HA-containing scaffolds (Fig. 2). Both scaffold groups supported the deposition of collagen (including collagen II) and GAG, with higher matrix production found on the PCL-PLGA/HA scaffolds (Fig. 3). Tensile mechanical properties were maintained over time (Fig. 4). Similar trends in proliferation and biosynthesis were observed between tibial- and femoral-derived cells (data not shown).

**DISCUSSION:** Culturing on 3-D nanofiber scaffolds enhanced fibrochondrocyte growth and mineralization potential. Furthermore, the production of a collagen and GAG-rich matrix was also higher on nanofiber scaffolds, and, similar to articular chondrocytes9, biosynthesis was further enhanced by the addition of HA. These results demonstrate that nanofiber scaffolds support the deposition of a fibrocartilaginous insertion-like matrix.

**ACKNOWLEDGMENTS:** NIH/NIAMS (5R01AR055280)

**REFERENCES:** 1) Benjamin *et al.*, 1986; 2) Woo *et al.*, 1988; 3) Friedman *et al.*, 1985; 4) Li *et al.*, 2009; 5) Subramony *et al.*, 2011; 6) Liu *et al.*, 2014; 7) Sun *et al.*, 2007; 8) Subramony *et al.*, 2014; 9) Khanarian *et al.*, 2012

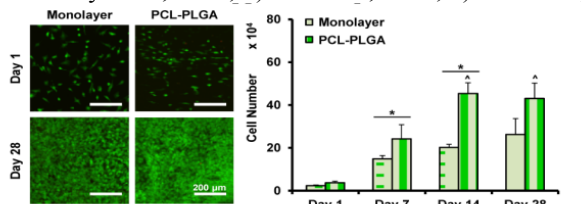


**Fig 1.** PCL-PLGA nanofibers support fibrochondrocyte viability, and cell proliferation is enhanced compared to monolayer culture.

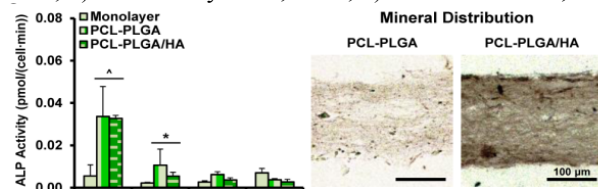


**Fig 2.** ALP activity is initially higher on scaffold groups and enhanced mineral deposition is observed on PCL-PLGA/HA nanofibers.

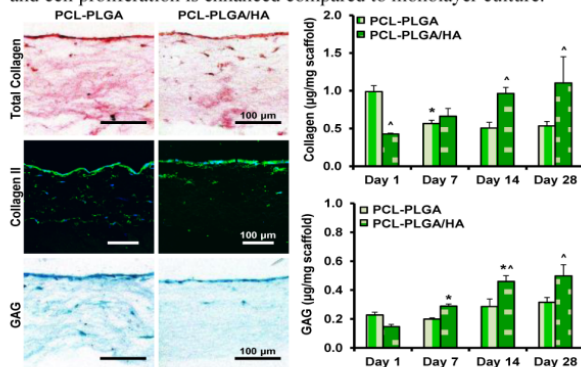


**Fig 3.** Nanofiber scaffolds support both collagen and GAG deposition.

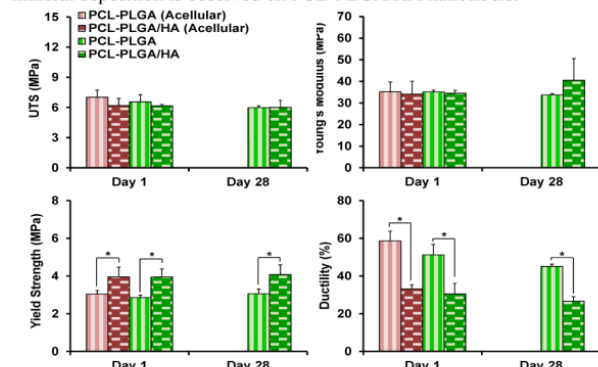


**Fig 4.** Tensile mechanical properties are maintained over 28 days.

# ENGINEERING AND CHARACTERIZING NANOFIBROUS COMPOSITE SCAFFOLDS WITH SPATIALLY-VARYING ARCHITECTURE

A.A. Oberai<sup>2</sup>, J.A. Cooper<sup>1</sup>, M. Tyagi<sup>2</sup>, K.L. Lee<sup>1</sup>, T.J. Anderson<sup>1</sup>, D.T. Corr<sup>1</sup>

Departments of<sup>1</sup> Biomedical Engineering, <sup>2</sup> Mechanical Engineering, Rensselaer Polytechnic Institute, Troy, NY

**INTRODUCTION:** While many new fabrication techniques aim to mimic the hierarchical structure of collagen networks found in connective tissues such as tendon and ligament, it is also important to consider the changes in stiffness (or modulus) present throughout the tissue, particularly at interfaces with neighboring tissues (e.g., ligament-bone, muscle-tendon, tendon-bone). Engineered ligament replacements, for example, should not only mimic the mid-substance modulus, but also strive to capture the gradually increasing stiffness throughout the ligament-bone transition. Our work aims to engineer such spatially-graded properties into a nanofibrous scaffold. To that end, we have developed both a novel strategy to fabricate nanofibrous structures, and create multi-layered scaffolds with graded stiffness, as well as a unique approach to characterize the material property heterogeneity in these scaffolds (not simply deformation). Such characterization methods are critical to assess engineered materials with spatially-varying properties, as well as the biologic tissues they seek to replace.

**METHODS:** Electrospun nanofiber mats were made of a 12% (w/v) poly( $\epsilon$ -caprolactone) (PCL, 80,000 MW) in a 3:1 chloroform to methanol solvent solution. The polymer solution was expelled from a glass syringe with an 18 gauge needle at 12  $\mu$ L/min, by a programmable syringe pump, through an applied 18 keV field, using a custom electrospinning apparatus, and the resulting nanofibers were collected on a mandrel rotating at 2000 rpm to achieve aligned nanofibers. To create scaffolds with graded properties, a 7-layer design (Fig. 1) was used in which sections of the mandrel were masked during deposition of select layers to prevent nanofiber accumulation. The resulting multilayer structure is symmetric in specimen thickness, with uniform continuous surfaces and aligned nanofiber topography (Fig. 2), with 80% of fiber diameters between 200-425 nm. Nanofiber mats were then removed from the mandrel and cut into individual samples using a 0.6 x 3.6 cm rectangular punch (C.S. Osborne & Co., Harrison, NJ). Samples were taken with fibers were aligned to the long axis of the sample, and the masked regions centered within the gauge length (i.e., samples were stiffest at ends and most compliant in center). *Characterization:* Material test specimens were speckle-coated with an anisotropic, high-contrast pattern (for video strain measurements), then mounted in a Universal Materials Test Machine equipped with a 100 N load cell with 0.5 N resolution (Test Resources Inc., Shakopee, MN). Once secured in the pneumatic grips, each specimen was given a slight positive preload (0.1 N), and stretched to failure at a constant rate (0.2 mm/s). All data were recorded a rate of 50 Hz. A two-camera digital image correlation (DIC) system (Correlated Solutions, Inc., Columbia, SC) was employed to measure strains in the material, in a non-contacting manner, using a texture-mapping algorithm. Video was collected at 7 frames/second, and analyzed with VIC-3D 2010 DIC software. The specimen geometry was discretized using a rectangular virtual grid, and 3D positions for every node were exported at each time step to determine the measured displacements. *Modulus Determination:* Spatial distribution of the Young's modulus for the specimen was determined by minimizing the difference between a predicted displacement and the measured displacement field. The former was constrained to satisfy the equations of equilibrium for a linear isotropic solid in a state of plane stress. The spatial variation of the Young's modulus was varied in order to minimize the difference between the predicted and measured displacement fields [1].

**RESULTS & DISCUSSION:** Using this combined approach, we were able to determine the scaffold's modulus and how it varies spatially throughout the specimen (Fig. 2). This is particularly useful for validating the material property distribution in engineered ligament scaffolds, in which stiffness is graded to increase significantly toward the bony ends.

**REFERENCES:** 1. Oberai A.A. et. al, Solution of inverse problems in elasticity imaging using the adjoint method. *Inverse Probl*, 19(2),297, 2003.

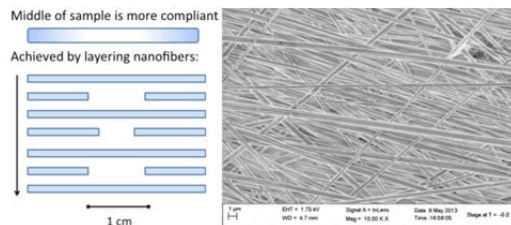


**Fig 1.** Multi-layer scaffold schematic and SEM showing aligned nanofiber

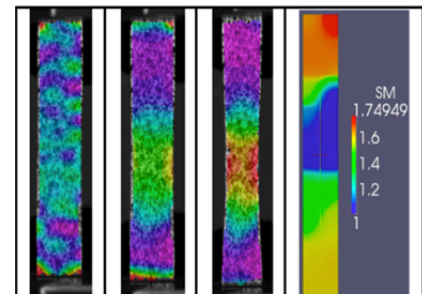


**Fig 2.** (L to R) Scaffold axial strain with increasing displacement, and calculated

# MULTIPLE-TECHNIQUES TO EVALUATE THE FIBROUS INTERZONE DURING THE BONE-TENDON JUNCTION HEALING FOR ANTERIOR CRUCIATE LIGAMENT RECONSTRUCTION (ACLR) MODEL IN RABBITS

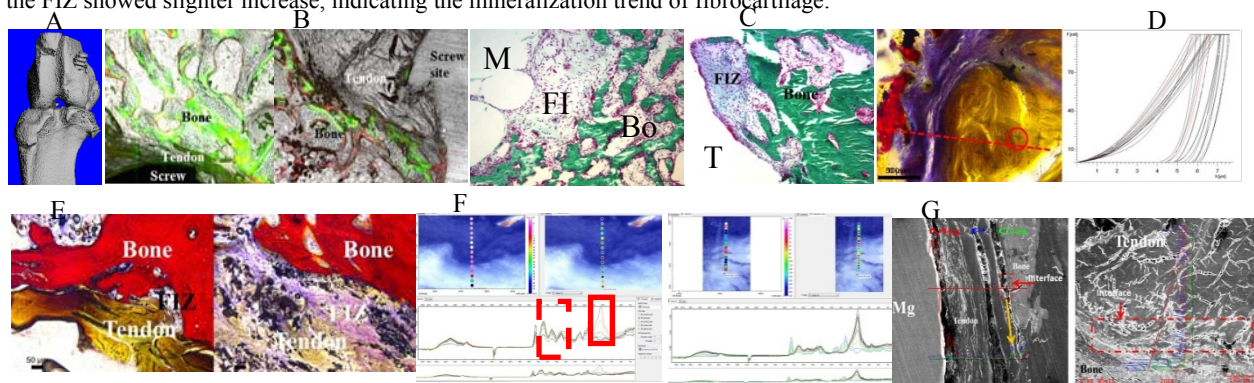
Jiali Wang, Jiankun Xu, DHK Chow, Kaiming Chan, Ling Qin\*

*Musculoskeletal Research Laboratory, Department of Orthopaedics & Traumatology, The Chinese University of Hong Kong, Hong Kong SAR, PR China.*

**INTRODUCTION:** It's estimated that the number of patients suffering from ACL tear is more than 20,000 annually, with over 10,000 ACL reconstruction performed. Regeneration of fibrocartilage in the transitional zone may be involved after the fixation of new tendon grafts in the bone tunnel during the tendon-bone junction healing process. However, due to huge differences for the two dissimilar tissues, the formation of fibrocartilage seems very difficult and slow, leading to poor attachment for the newly inserted grafts in the bone. Currently, biological (e.g. injection of growth factors, etc.) and biophysical treatments (e.g. low intensity pulsed ultrasound stimulation, etc.) are more and more widely used as potential therapeutic approaches to accelerate regeneration of tendon-bone fibrous interzone (FIZ). Therefore, how to evaluate the bio-efficacy of these novel treatments is critical for the selection of appropriate intervention approaches. Therefore, in this study, we introduced some relevant technologies for assessment of the healing level of tendon grafts-bone junction in ACLR model in rabbits.

**METHODS:** 8 rabbits were performed ACLR surgery in their left knee using titanium or Mg based interference screws for fixation of grafts (extensor digitorum ligament) in the lateral side of the femurs, while the other end of grafts in the tibia tunnel was fixed with suture due to insufficient cancellous bone (Figure 1A). Calcein green and xylenol orange were subcutaneously injected into rabbits at the 14<sup>th</sup> day and 19<sup>th</sup> day for labeling of new formed bone, separately. After 3 weeks, the samples were harvested and embedded with methyl methacrylate (MMA) for testing of fluorescent imaging, scanning electron microscopy (SEM) /energy dispersive x-ray analysis (EDAX), micro-Fourier transform infrared spectroscopy (FTIR), micro-indentation and also histological analysis in the FIZ. The intensities of elements of calcium (Ca) and phosphorus (P) in the EDAX were recorded to distinguish the CF area. The values of Vickers hardness in the FIZ were also tested along the direction between the tendon grafts and bone. Besides, spectra were acquired between 350-3500 cm<sup>-1</sup> via line scanning for characterization of special peaks corresponding to collagen and minerals. Goldner Trichrome and Stevenel's blue staining were both explored to distinguish the components located in the FIZ.

**RESULTS:** More bone formation around bone tunnels could be observed for Mg screw fixed group in Figure 1B ( $3.14 \pm 0.84$  vs.  $2.28 \pm 0.42$   $\mu\text{m}/\text{day}$ ,  $p=0.195$ ), indicating osteopromotion role for Mg ions. Fibrocartilage was regenerated in the transitional region, which could be clearly shown in the Figure 1C and 1E. The hardness distribution along the direction from tendon to bone also confirmed the presence of fibrocartilage as higher values were observed towards the direction of bone via line scanning of indentation. Peaks for phosphate (900-1200 cm<sup>-1</sup>) and amide I/II (1500-1700 cm<sup>-1</sup>) could be detected via micro-FTIR analysis. Mineral distribution could be acquired via calculation of relative intensities of these peaks. Besides, the intensities of Ca and P in the FIZ showed slighter increase, indicating the mineralization trend of fibrocartilage.



**DISCUSSION:** The results showed that current technologies including histological staining, hardness testing, fluorescent imaging and elements distribution could be effectively combined for qualitative and quantitative evaluation of tendon grafts-bone junction healing process. The underlying mechanism could be also explored via multiple scales of testing. Actually, more time points have been selected to evaluate the biocompatibility and bio-efficacy of novel biodegradable Mg screws as potential medical devices and more relevant data is under analysis. We hope that these technologies could help us to dig out more than current information.

**ACKNOWLEDGEMENTS:** Guangdong Innovation Team Grant on Biodegradable Magnesium and Medical Implants (Ref. 201001C0104669453) and National Natural Science Foundation of China (NSFC)/Research Grants Council (RGC) Joint Research Scheme (Ref. N\_CUHK449/13), and SMART Program, Lui Che Woo Institute of Innovative Medicine, Faculty of Medicine, the Chinese University of Hong Kong supported by Lui Che Woo Foundation Limited are acknowledged.

**REFERENCES:** 1. L.Y. Dave, et al., *European journal of orthopaedic surgery & traumatology : orthopedie traumatologie*. 2013. 2. J.P. Spalazzi, et al, *PLOS ONE*. 8(9): e74349-64. 2013. 3. C. Aga, et al., *Am J Sports Med*. 41(4): 841-8. 2013.

# GRADIENT POLYURETHANE SCAFFOLDS FOR IMPROVED REGENERATION OF THE TENDON ENTHESIS

Tyler Touchet<sup>1</sup>, Alysha Kishan<sup>1</sup>, Michael Detamore<sup>2</sup>, and Elizabeth Cosgriff-Hernandez<sup>1</sup>  
<sup>1</sup>Texas A&M University, College Station, TX, <sup>2</sup>University of Kansas, Lawrence, KS

**INTRODUCTION:** Although many biomaterial scaffolds show promise as tendon grafts, current designs lack the complexity and mechanical properties of native tendons. Specifically, these scaffolds fail to mimic the innate transition of mechanical properties that make up entheses through discrete transitions in properties that can lead to failure at these junctions. To address these limitations, we have developed a library of biodegradable poly(ether ester urethane)ureas that allows for appropriate selection of material by correlating tensile properties with reported tissue values. We then developed a co-electrospinning technique to form scaffolds with gradient properties that more accurately mimics the tendon to bone interface.

**METHODS:** Biodegradable poly(ether ester urethane)ureas (B-PURs) were synthesized by first end-capping a polyether-ester triblock polyol with hexamethylene diisocyanate to form the prepolymer and then chain extending with diaminopropane or ethylene diamine to complete the polymerization. Hard segment content was varied from 10-50% by stoichiometry and chemical structure confirmed using infrared spectroscopy. The B-PURs were purified, dried and then dissolved 2,2,2-trifluoroethanol (TFE) or 1,1,1,3,3,3-Hexafluoro-2-propanol (HFIP) for further characterization and electrospinning. Films were cast and cut into microtensile bars. Mechanical properties were characterized using a uniaxial tensile apparatus. For gradient electrospinning, 18 wt% B-PUR 10% HS in TFE was placed 35 cm from a collector, pumped at a rate of 0.2 mL/hr at a voltage of 10 kV applied to the needle tip and -10 kV applied to the collector. Simultaneously, B-PUR 50% HS in HFIP was placed 18 cm from the collector parallel to the B-PUR 10% HS solution, pumped at a rate of 0.3 mL/hr with voltage of 9 kV applied to the needle tip. To produce a gradient, the syringe pumps were offset by 5 cm to generate two discrete zones with a transition zone. Fiber morphology was characterized with scanning electron microscopy (SEM). Mechanical properties of electrospun meshes were characterized using a uniaxial tensile tester.

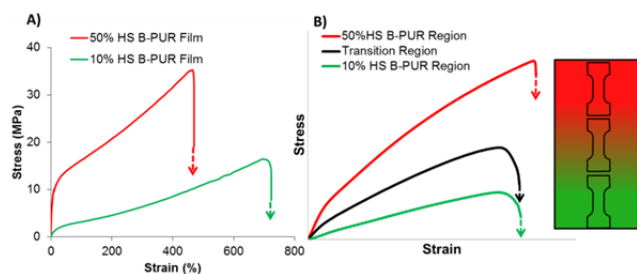


**Figure 1:** Stress-Strain curves of A) the typical B-PUR films and B) the gradient electrospun meshes.

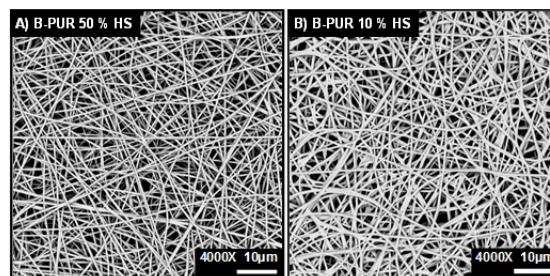


**Figure 2:** SEM images of A) B-PUR 50 % HS and B) B-PUR 10 % HS electrospun meshes.

**RESULTS:** Successful B-PUR synthesis was confirmed with infrared spectroscopy, focusing on the formation of the urethane and urea linkage. Mechanical testing of the B-PUR films with varying hard segment content (10-50%) displayed a wide range in modulus ranging from 18 MPa to 233 MPa and ultimate tensile strength (17-33 MPa), **Figure 1A**. Co-spun meshes were sectioned into 3 zones: 50% HS B-PUR, 10% HS B-PUR, and a transition region. As expected from film testing, the electrospun 50% HS B-PUR zone had a 9-fold increase modulus and a 4-fold increase in ultimate tensile strength over the 10% HS zone. Samples from the transition zone displayed both an intermediate modulus and ultimate tensile strength when compared to the 10% HS and 50% HS B-PUR zones, **Figure 1B**. Despite having different mechanical properties, uniform fiber diameter and distribution was maintained across the zones, **Figure 2**.

**DISCUSSION:** In this study, we were able to fabricate a scaffold with gradient mechanical properties by co-electrospinning B-PURs with varying hard segment content without changing scaffold architecture. This allows for a more gradual transition region without effects from different geometries and stress concentrators that can lead to mechanical failure at the interface. This scaffold shows promise in mimicking the natural gradient of enthesis. Current studies are probing these gradient properties in more detail and the effect of fiber alignment on mesh properties. Future studies will investigate cell viability, adhesion, proliferation on these grafts. Overall, these meshes could provide improved integration at the tendon to bone interface and other musculoskeletal defects.

# AGEING, DEEP VENOUS THROMBOSIS AND MALE GENDER IMPAIR OUTCOME AFTER ACHILLES TENDON RUPTURE

Arverud E.<sup>1</sup>, Anundsson P<sup>1</sup>, Hardell E<sup>1</sup>, Barreng G<sup>1</sup>, Edman G<sup>1</sup>, Latifi A<sup>1</sup>, Ackermann P.W.<sup>1</sup>

<sup>1</sup>*Karolinska Institutet, Stockholm, Sweden*

## INTRODUCTION:

Patients with acute Achilles Tendon rupture (ATR) exhibit prolonged healing and extensive functional deficits in outcome. Knowledge on predictive factors of functional outcome is unsatisfying. One study suggested gender, pain, and physical functioning during rehab as important factors for functional outcome. Recently, a very high rate of deep venous thrombosis (DVT) 36-50%, irrespective of operative or non-operative treatment, has been demonstrated after ATR<sup>1</sup>. Yet, whether common complications with DVT are associated with impaired outcome of ATR patients remains unclear. In the present study we hypothesized that DVT and gender as well as multiple variables including age, BMI, physical activity score and smoking would influence the outcome of ATR. The aim of this prospective cohort study was to assess intrinsic and extrinsic factors that could predict the combined objective and subjective outcome as assessed with validated scores of lower limb function and patient-related outcome at one year after ATR.

## METHODS:

One hundred nine patients (94 men, 15 women; mean age 40.8±9.0) with acute total ATR were prospectively assessed. The main outcome measures consisted of the functional heel-rise test (Heel-rise height and LSI-height) and the Achilles tendon Total Rupture Score (ATRS) for symptoms. These three validated outcome measures after ATR, exhibiting distinct statistical differences were combined to yield the Achilles Functional Outcome Score (AFOS). At 2 weeks post-operatively DVT-incidence was assessed using color duplex sonography (CDU) by two blinded ultrasonographers. The analysis examined the unique contribution of earlier identified predictors of outcome age, body mass index (BMI), physical activity score (PAS) as well as new factors deep venous thrombosis (DVT), gender and smoking.

## RESULTS:

A multiple linear regression analysis was performed based on the AFOS being >1 (n=59) or less than one (n=50). The multiple linear regression analysis demonstrated that three independent variables correlated significantly with AFOS at one year; age, gender and deep venous thrombosis after two weeks.

**Table 1. Relationship between gender, age, deep venous thrombosis, and outcome**

<i>Independent variable</i>	<i>B</i>	<i>S.E.</i>	<i>df</i>	<i>p</i>	<i>OR<sup>2</sup></i>	<i>95% C. I.<sup>1</sup> for OR<sup>2</sup></i>	
						<i>Lower</i>	<i>Upper</i>
<b>Gender</b> (Man= 1; Woman= 2)	1.43	0.724	1	0.048	4.18	1.01	17.24
<b>Age</b> (40 or less= 0; above 40= 1)	-1.59	0.462	1	0.001	0.20	0.08	0.51
<b>Deep venous thrombosis after two weeks?</b> (No= 0, Yes= 1)	-1.19	0.491	1	0.016	0.31	0.12	0.80
Constant	-0.36	0.784					

<sup>1</sup> C.I. = Confidence Interval

<sup>2</sup> OR = Odds Ratio

## CONCLUSIONS:

Postoperative DVT during leg immobilization, ageing and male gender are predictive factors for impaired outcome of the patient at one year post Achilles tendon rupture. Specifically, we hypothesize that the chain-reaction of ageing and DVT leading to immobilization, pain, and impaired blood supply negatively affect Achilles tendon healing, leading to a prolonged tendon length with impaired function. The results suggest that doctors should identify the patients' risk factors and address them in a targeted manner, eg. by improving mobilization and blood supply.

## REFERENCES:

1. Lapidus, L. et al., Prolonged thromboprophylaxis with dalteparin after surgical treatment of achilles tendon rupture: a randomized placebo-controlled study. *J Orthop Trauma.* 200;21(1):52-7. Epub 2007/01/11

# SILK SCAFFOLD WITH OSTEOCONDUCTIVE AND OSTEOINDUCTIVE CUES FOR ENTHESIS REGENERATION IN ANTERIOR CRUCIATE LIGAMENT RECONSTRUCTION

T.K.H. Teh<sup>1</sup>, P. Shi<sup>1</sup>, K. Chen<sup>1</sup>, X. Ren<sup>2</sup>, S.L. Toh<sup>1,3</sup>, J.H.P. Hui<sup>2</sup>, J. Li<sup>1,4</sup> and J.C.H. Goh<sup>1,2</sup>

<sup>1</sup> Department of Biomedical Engineering, National University of Singapore, Singapore

<sup>2</sup> Department of Orthopedic Surgery, National University of Singapore, Singapore

<sup>3</sup> Department of Mechanical Engineering, National University of Singapore, Singapore

<sup>4</sup> Institute of Materials Research and Engineering, Agency for Science, Technology and Research (A\*STAR)

**INTRODUCTION:** Graft-to-host tissue integration remains to be a significant clinical problem in ACL reconstruction. One tissue engineering strategy to this problem looks at improving bone ingrowth into the ACL graft through biological cues that are osteoconductive, osteoinductive or a concoction of the two. With the aim to understand the synergistic effects of these biological cues, composite silk scaffold systems incorporated with nanoparticles of low crystallinity hydroxyapatite (nHA, osteoconductive) and/or loaded with bone morphogenetic protein 2 (BMP-2, osteoinductive) will be compared in their effects to stimulate bone tunnel and entheses regeneration.

**METHODS:** Knitted scaffolds (240 fibroins, 20 × 20 mm for in vitro characterization and 60 × 20 mm for rabbit implantation; 480 fibroins, 100 × 20 mm for pig implantation) were first fabricated from raw Bombyx mori silk and subsequently degummed. Aqueous silk fibroin (SF) solution was obtained by dissolution. Four different types of SF-based scaffolds were made by solution blending for in vitro characterization: SF (2.6 %w/v), SF/nHA (0.78 mg/ml nHA), SF/BMP2 (29 µg/ml BMP2) and SF/nHA/BMP2 (0.78 mg/ml nHA and 29 µg/ml BMP2). Porcine bone marrow derived MSCs (P3, 1 × 10<sup>6</sup>/scaffold) were seeded into the scaffolds and statically cultured over 28 days. For implantation, composite knit-sponge scaffolds were made with central one-third pure SF and the ends either SF/nHA (Ctrl) or SF/nHA/BMP2 (Exp), and were each seeded with rabbit MSCs (P3, 3 × 10<sup>6</sup>/scaffold for rabbit implantation) or porcine MSCs (P2, 10 × 10<sup>6</sup>/scaffold for pig implantation), prior to classic ACL reconstruction of seeded constructs after excision of the native tissue. The animal experiments were approved by IACUC, NUS.

**RESULTS:** MSCs were observed to be viable and proliferative in all four groups of the in vitro study. Upregulation of osteogenic genes (such as COL I, COL III, ON, OPN), translating to phenotypic outcomes, persisted in the SF/nHA, SF/BMP2 and SF/nHA/BMP2 groups compared to pure SF, with BMP2 shown to not stimulate a persistent (beyond 21 days) upregulation of osteogenic genes and increase in collagen production. Gross observation of the excised rabbit and porcine knee joints showed no signs of osteoarthritis and that the ligament portion was regenerated (Fig. 1A, B). Bone tunnel narrowing was observed in Exp compared to Ctrl as indicated by micro-CT images (Fig. 1C,D), with significantly better bone tunnel healing in the Exp group (~68%) as compared to Ctrl (~6%). Histological characterizations further indicated presence of new bone formation in Exp with development of Sharpey's fibers in the earlier post-implantation stages. Better graft to bone integration was also observed from the superior pull-out strength of Exp compared to Ctrl in the rabbit models, while for the Exp in the porcine model mechanical failure initiated at the mid-substance of the ligament portion during tensile testing and not due to pull out.

**DISCUSSION:** It was found that BMP2 and nHA synergistically complemented each other in stimulating osteogenic differentiation of MSCs, resulting in bone tunnel narrowing with new mineralized tissues observed in both the small and large animal models. Consequently, there was enhanced graft-host integration by 6 months resulting in mechanical properties closer to that of the native bone-ACL-bone construct. Based on our knowledge, this study is the first to investigate the biphasic silk scaffold enhanced with blended osteoinductive BMP2 and osteoconductive HA nanoparticles, and carried through in vitro analysis, small and large animal preclinical studies. The results indicate that this strategy is a promising tissue engineering solution for complete ACL-entheses-bone regeneration.

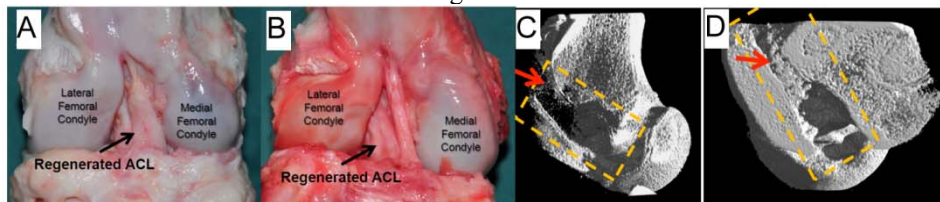


Fig. 1: Gross observation and micro-CT images of excised porcine knee joints of Ctrl (A, C) and Exp (B, D) at 6 months post-implantation. Rectangle: original bone tunnel location, arrow: new calcified tissue deposition.

## BIOMECHANICS OF THE TRANSVERSE CARPAL LIGAMENT

Zong-Ming Li

*Hand Research Laboratory*

*Departments of Biomedical Engineering, Orthopaedic Surgery, and Physical Medicine and Rehabilitation*

*Cleveland Clinic, Cleveland, Ohio*

*liz4@ccf.org*

The transverse carpal ligament (TCL) is a significant constituent of the wrist and forms the volar boundary of the carpal tunnel. It has biomechanical and physiological functions that include serving as a pulley for the flexor tendons, anchoring the thenar and hypothenar muscles for hand strength, stabilizing the bony structure, and providing wrist proprioception. The TCL has attracted extensive research attention during the past two decades, and considerable knowledge has been gained from basic science research and its clinical implications in hand surgery. The science of this ligament has progressively evolved with regard to its cellular mechanisms, histological composition, fiber architecture, neural anatomy, morphological characteristics, material properties, and structural mechanics.

This presentation will review our recent studies regarding the biomechanical role of the TCL in the compliant characteristics of the carpal tunnel. First, force applied to the TCL from within the carpal tunnel increased the arch height and area due to arch width narrowing from the migration of the bony insertion sites of the TCL. These experimental findings were further elucidated through geometric modeling which revealed the relationships among arch width, height, and area. Second, carpal arch deformation showed that the carpal tunnel was more flexible at the proximal level than at the distal level, and was more compliant in the inward direction than in the outward direction. The hamate-capitate joint had larger angular rotations than the capitate-trapezoid and trapezoid-trapezium joints for their contributions to changes of the carpal arch width. Third, pressure application inside the intact and released carpal tunnels led to increased carpal tunnel cross-sectional areas, which were mainly attributable to the expansion of the carpal arch formed by the TCL. Transection of the TCL led to an increase of carpal arch compliance that was nine times greater than that of the intact carpal tunnel. The carpal tunnel, while regarded as a stable structure, demonstrates compliant properties that help to accommodate biomechanical and physiological variants such as changes in carpal tunnel pressure.

Additional discussions will include the areas of future studies and their clinical translation. Transecting the TCL has been shown to benefit patients by relieving symptoms of carpal tunnel syndrome. However, disrupting the tunnel structure may compromise other aspects of hand function; these implications remain to be further clarified. Alternative surgical techniques and non-surgical strategies related to the TCL continue to be explored, each warranting rigorous scientific investigation to establish evidence-based interventions. Regarding the many etiological factors of carpal tunnel syndrome, thickening and stiffening of the TCL are suggested as possible mechanisms of median nerve compression and carpal tunnel syndrome. Future studies are needed to elucidate the potential mechanobiological effects on the TCL resulting from repetitive hand use that involves biomechanical interactions among tissues. For carpal tunnel biomechanics and its relationship to the TCL, a validated computational model of the wrist with high fidelity constitutive components is valuable to assist our understanding of pathomechanisms and to provide patient-specific simulation and intervention. More effort is needed to investigate TCL and wrist function in the *in vivo*, physiological environment with the aid of dynamic imaging modalities, such as ultrasound, fluoroscopy, computed tomography, and magnetic resonance imaging. Such advancement of knowledge in the TCL and its integral structure will further improve clinical management of hand and wrist conditions.

THE INTERFASCICULAR MATRIX ENABLES FASCICLE SLIDING AND RECOIL IN TENDON, AND BEHAVES MORE ELASTICALLY IN ENERGY STORING TENDONS

C T Thorpe<sup>1</sup>, M S C Godinho<sup>1</sup>, G P Riley<sup>2</sup>, H L Birch<sup>3</sup>, P D Clegg<sup>4</sup> and H R C Screen<sup>1</sup>

<sup>1</sup>Queen Mary, University of London, London, UK, <sup>2</sup>University of East Anglia, Norwich, UK, <sup>3</sup>UCL, London, UK.

<sup>4</sup>University of Liverpool, Liverpool, UK  
c.thorpe@qmul.ac.uk

**INTRODUCTION:** Our previous work shows that the interfascicular matrix (IFM) is critical for tendon function, facilitating sliding between fascicles to allow tendons to stretch (1). We have shown that this is particularly important in energy storing tendons such as the human Achilles tendon and equine superficial digital flexor tendon (SDFT), which experience strains as high as 16% during exercise (2), and therefore require the capacity for considerable inter-fascicular sliding. This capacity is not required in positional tendons such as the equine common digital extensor tendon (CDET). Further, we have shown that the IFM in the energy storing SDFT becomes stiffer with age, which may explain why aged tendons are more prone to injury (3). While the failure properties of the IFM have been studied previously (1), it has not been established if the IFM is able to recoil and recover from loading. The aim of this study was therefore to assess the recoil capacity and failure properties of the IFM in the SDFT and CDET from young and old horses. We hypothesised that the IFM has the ability to recoil, and that elasticity is greater in the energy storing SDFT than in the positional CDET. Further, we hypothesised that the recoil capacity of the IFM decreases with ageing and the stiffness of the IFM increases, specifically in the SDFT.

**METHODS:** Groups of 2 intact fascicles (bound together by IFM) were dissected from the SDFT and CDET from young (aged 3-7 years) and old (aged 17-20 years) horses. Using a polarised light microscope and a dissection rig, the opposing end of each fascicle was cut transversely, leaving a 10 mm length of intact IFM (Fig.1). Samples were preconditioned from 0-0.5mm for 10 cycles (Fig.2a), and then pulled apart to failure. Hysteresis and stress relaxation were calculated during preconditioning. A force-extension curve was derived from the failure test data, and IFM extension was calculated from 10-80% failure load (Fig.2b). Statistical significance was tested using an ANOVA.

**RESULTS:** The IFM was able to recoil in both tendon types (Fig.2a). Hysteresis and stress relaxation were significantly greater in CDET than in SDFT IFM samples ( $p < 0.01$ ). IFM failure load and failure extension did not differ between tendon types. At and below 40% of failure force, there was significantly greater extension within the SDFT IFM than the CDET IFM ( $p < 0.01$ , Fig.2b&c). Hysteresis did not change with age, but stress relaxation increased with ageing in both tendon types. Ageing resulted in decreased extension at the interface in SDFT samples ( $p < 0.05$ , Fig.2d).

Fig.2. Response of IFM to cyclic loading (a) and test to failure (b). IFM extension wd calculated at different percentages of failure load (b). Extension at interface differed with tendon type (c) and with age (d)

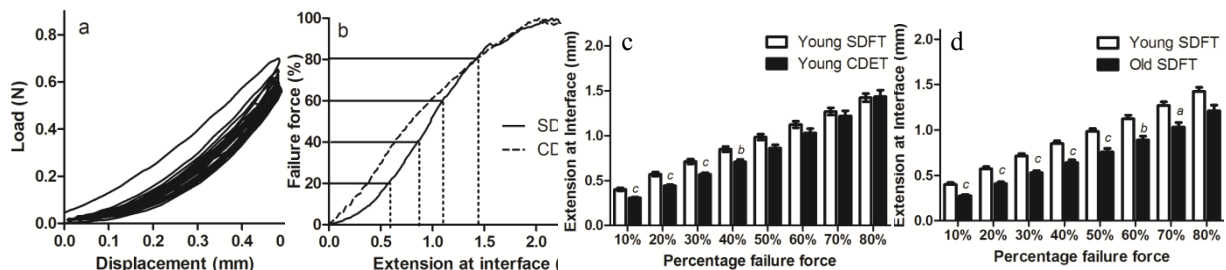


**Fig.1.** Schematic of IFM test. 2 fascicles (white) bound together by IFM (black) were pulled apart, testing the IFM in shear.

**DISCUSSION:** The results support the hypothesis, showing that the IFM exhibits reversible deformation behaviour. Further, the IFM in the SDFT has a greater ability to recoil, with less hysteresis and stress relaxation than in the CDET, providing further evidence that the IFM is crucial for efficient function of energy storing tendons. The results also indicate that the IFM is less able to resist repetitive loading as it ages, becoming stiffer with age in the SDFT. Full understanding of IFM specialisation in energy storing tendons and the age-related changes that result in loss of function is important for the development of effective preventative measures and treatments for age-related tendon injury.

**REFERENCES:** 1. Thorpe et al 2012 J R Soc Interface, 2. Stephens et al 1989 Am J Vet Res, 3. Thorpe et al 2013 eCM.

### 3-D RECONSTRUCTION OF INTACT AND STRESS DEPRIVED RAT TAIL TENDON CELLS

M. Egerbacher<sup>1</sup>, W. Tschulen<sup>1</sup>, I. Kolarov<sup>1</sup>, S. Handschuh<sup>2</sup>

*Institute of Anatomy, Histology & Embryology<sup>1</sup>, VetCore Facility for Research<sup>2</sup>, Vetmeduni Vienna, Austria*

**INTRODUCTION:** Tendon cells can respond to mechanical stimuli like tensile strain, fluid flow and compression via complex mechanotransduction signaling pathways (1) both individually and collectively as they are able to communicate this response between adjacent cells through a 3-dimensional network of cell processes linked by gap junctions (GJ) (2). To date, the effect of various loading parameters on the expression and function of gap junction proteins has been limited to cell culture studies (3, 4, 5). In rat tail tendons (RTTs), connexin-43 (Cx43) has been found to be up-regulated after the loss of homeostatic cellular tension resulting from stress-deprivation (SD) (6). Therefore, the purpose of this study was to examine the 3-dimensional tenocyte morphology and synthesis of Cx43 in an *in vitro* rat tail tendon model in order to document the spatial distribution of communicational structures in healthy and altered tendons using two different approaches (whole mount staining vs. 3D-reconstruction of semithin sections).

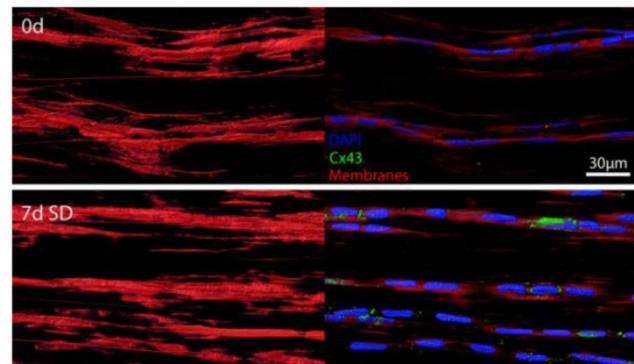
**METHODS:** Rat tail tendon fascicles (RTTs) were harvested immediately after euthanasia from 3 adult (9 to 11 months) male Sprague-Dawley rats and maintained as previously described (7). RTTs were cut in 2 cm pieces and either fixed in 4% buffered formaldehyde for immunostaining or fixed in 2.5% glutaraldehyde for Epon resin embedding at 0d and after 7d of stress-deprivation (SD). Staining for Cx43 on whole RTT fascicles was performed using a rabbit pc antibody (dilution 1:2000) with subsequent detection with anti-rabbit Alexa Fluor 488 antibody. After washing with PBS, tendons were submerged in a 5µg/ml solution of CellMask<sup>TM</sup> Deep Red plasma membrane stain in PBS and incubated for 15 minutes in the dark; nuclei were counterstained with DAPI. Confocal image stacks (ZEISS LSM 510 Meta) of whole mounts showing nuclei, membranes and Cx43 expression were visualized by multichannel 3D volume rendering. For each group, 100-200 serial semithin sections were cut at 0.8 µm thickness and stained with toluidine blue. All 3D image processing and rendering procedures were done using the 3D software Amira. Serial section images were aligned, and tenocytes and nuclei were segmented using manual image segmentation tools. Based on segmented materials, polygon surface models were created and rendered.

**RESULTS:** The number of tenocytes per volume doubled during 7d SD and cells show more compact cell bodies. Even their lateral processes appeared shorter and thicker, seemed to have increased in number, however not all interconnect.

In fresh RTTs (0d), strands of slender cells communicated preferentially at their end-to-end contacts and along their lateral wing-like protrusions. Up-regulation of Cx43 synthesis in 7d SD RTTs involved specific cell groups where the protein was detected in the Golgi field and membrane-bound on their lateral processes. In addition to the flat wing-like cytoplasmic processes, we found straight thin longitudinal processes (Ø 1-3µm) reaching up to several 100 µm in length in both fresh RTTs and after 7d SD which were completely devoid of Cx43.

**DISCUSSION:** The formation of additional cell processes after loss of homeostatic tension secondary to SD concurrent with an increased synthesis of Cx43 can be due to a loss of orientation and interpreted as proactive “search” for cell-to-cell communication. Cell aggregation is due to an actin-mediated contraction to re-establish tensional homeostasis (7). We confirm the presence of membrane nanotubes (NTs) that connect tenocytes longitudinally over a long distance (3) representing a long-range cell-to-cell communication system independent of gap junctions. The existence of NTs mediating functional connectivity between cells *in vivo* has only recently been discovered (8). They allow intercellular transmission of various cell components, offering potential protective effects for the respective tissue. Further studies on structural and functional properties of NTs in tendons are necessary in the future.

**REFERENCES:** 1) Wall and Banes *J Musculoskelet Neuronal Interact* 2005. 2) McNeilly et al. *J Anat* 1996. 3) Waggett et al. *Eur J Cell Biol* 2006. 4) Wall et al. *Cell Motil Cytoskeleton* 2007. 5) Qi et al. *J Appl Physiol* 2011. 6) Egerbacher et al. *Trans ORS* 2008. 7) Gardner et al. *JOR* 2012. 8) Ranzinger et al. *Front Physiol* 2014.



# THE ROLE OF p38 MAPK IN TENDON GROWTH AND REMODELING

KB Sugg, AJ Schwartz, DC Sarver, JP Gumucio, CL Mendias  
*Department of Orthopaedic Surgery, University of Michigan, Ann Arbor, MI, USA*

## INTRODUCTION:

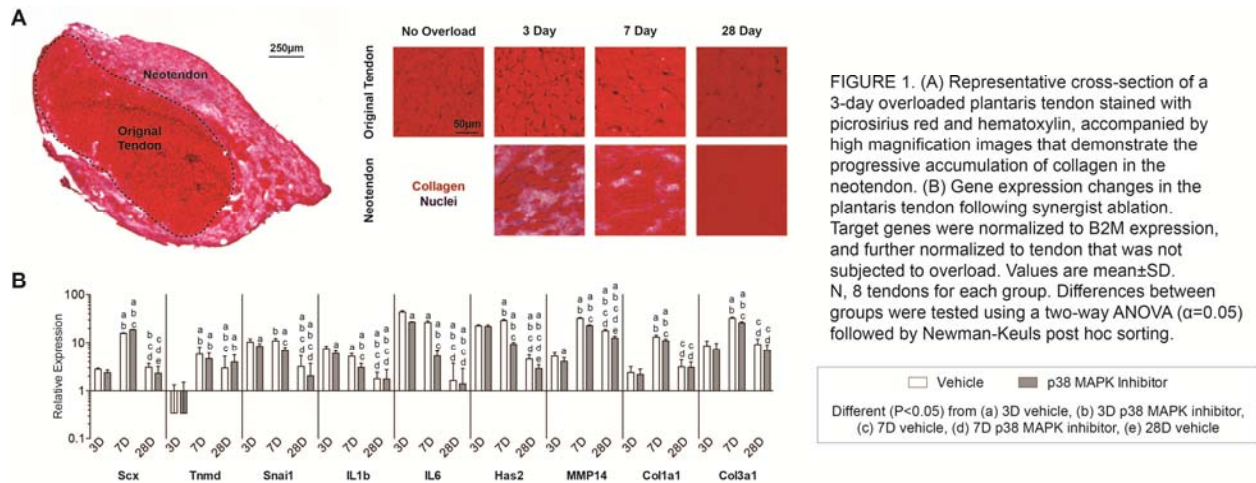
Tendon is a dynamic tissue whose structure and function is influenced by mechanical loading, but little is known about the fundamental mechanisms that regulate tendon growth and remodeling in vivo. Data from cultured tendon fibroblasts indicated the p38 MAPK pathway plays an important role in tendon fibroblast proliferation and collagen synthesis in vitro. To gain greater insight into the mechanisms of tendon growth in vivo, and explore the role of p38 MAPK signaling in this process, we tested the hypotheses that inducing plantaris tendon growth through the ablation of the synergist Achilles tendon would result in rapid expansion of a neotendon matrix surrounding the original tendon, and that treatment with the p38 MAPK inhibitor SB203580 would prevent this growth.

## METHODS:

Six-month-old male Sprague-Dawley rats were treated with vehicle or SB203580, and subjected to synergist ablation by bilateral tenectomy of the Achilles tendon to induce rapid growth of the synergist plantaris tendon. Rats were randomized to receive intraperitoneal injections of a vehicle or SB203580, a specific inhibitor of p38 MAPK. SB-203580 was administered at a dose of 3 mg/kg one day prior to surgical intervention and 1 mg/kg daily for seven days following surgical intervention. Changes in histological and biochemical properties of plantaris tendons were analyzed 3, 7 and 28 days after overload, and comparisons were made to non-overloaded animals.

## RESULTS:

By 28 days after overload, tendon mass had increased by 30% compared to non-overloaded samples, and cross-sectional area (CSA) increased by 50%, with most of the change occurring in the neotendon. The expansion in CSA initially occurred through the synthesis of a hyaluronic acid rich matrix that was progressively replaced with mature collagen (Fig. 1A). Changes in histology were accompanied by quantitative changes in gene expression with significant upregulation of genes involved in fibroblast proliferation, cell cycle control and factors that regulate matrix synthesis and turnover (Fig. 1B). Relative to vehicle, p38 MAPK inhibition during synergist ablation led to an 18% increase in scleraxis gene expression; however, tenomodulin, MMP14 and IL6 expression decreased by 20%, 30% and 80%, respectively.



## DISCUSSION:

These data suggest that p38 MAPK plays an important role in tendon fibroblast cell signaling and motility, as well as the inflammatory response, during tendon adaptation to mechanical growth stimuli in vivo. Inhibition of p38 MAPK resulted in a profound decrease in IL6 expression, and had a modest effect on the expression of other matrix and cell proliferation genes. The combined results from this study provide novel insights into tendon mechanobiology, and suggest that synergist ablation is a useful model for the study of postnatal tendon growth in rats. This work was supported by NIAMS grants F32-AR067086, F31-AR065931 and R01-AR063649.

# EARLY EMBRYONIC TENDON POSSESSES AN ACTIN CYTOSKELETON NETWORK WITH CRIMP MORPHOLOGY

N.R. Schiele, Z.L. Tochka, F. Von Flotow, and C.K. Kuo

*Department of Biomedical Engineering, Tufts University, Medford, MA, USA*

**INTRODUCTION:** A better understanding of embryonic tendon development may improve strategies to engineer, regenerate or heal tendon. We recently characterized embryonic chick tendon mechanical property elaboration during development and found that elastic modulus increases as a function of embryonic stage<sup>1</sup>. Inhibition of enzymatic collagen crosslinks abrogated increases in elastic modulus of late embryonic stage (HH 40-43) tendons, but had no effect on mechanical properties of early stage (HH 28-37) embryonic tendons<sup>1</sup>. Additionally, collagen content of early stage tendons (HH 28-37) was found to account for less than ~1% of the tendon dry mass, despite measurable increases in elastic modulus<sup>1</sup>. We also reported that DNA content at these same stages accounts for ~5-9% of the tendon dry mass<sup>1</sup>. To examine whether embryonic tendon progenitor cells (TPCs) may be significant contributors to early stage embryonic tendon tissue mechanical properties, we chemically disrupted the actin cytoskeleton of cells in HH 36 tendon and measured tissue elastic modulus. We found that disruption of the actin cytoskeleton leads to significant decreases in tendon elastic modulus<sup>2</sup>. In this study, we were interested in characterizing the cell network further to gain insight into how the embryonic TPCs may be regulating developing tissue mechanical properties. We quantitatively and qualitatively characterized cell network components of early stage tendons, with focus on actin organization and cadherin-11 (cad-11), N-cadherin (N-cad), and connexin 43 (cx43) protein content.

**METHODS:** Calcaneus tendons were dissected from HH 35 to 37 embryonic chick limbs. *Actin Imaging:* Tendon cryosections were stained with phalloidin and imaged on a confocal microscope. Actin filament crimp morphology (period and amplitude) was measured using ImageJ and Matlab. *Western Blot:* Whole tendons were lysed, run in electrophoresis gels, and probed with cad-11, N-cad, cx43 and  $\beta$ -actin (loading control) antibodies. *Data Analysis:* Differences were evaluated for significance with a one-way ANOVA and Tukey's post hoc test using  $p < 0.05$ .

**RESULTS:** Early stage embryonic tendons exhibited a well organized actin cytoskeleton network with a crimp pattern (**Fig. 1a**). Notably, actin filaments appeared to be contiguous from one cell to the next. Actin filament crimp period increased significantly from HH 35 to 36 and from HH 35 to 37 (**Fig. 1b**). Actin filament crimp amplitude at HH 36 increased significantly to 2.1  $\mu\text{m}$ , compared to 1.3  $\mu\text{m}$  at HH 35 and 0.9  $\mu\text{m}$  at HH 37. Cell-cell junction proteins cad-11, N-cad, and cx43 were detected in the embryonic tendons (**Fig. 1c**), with no change in protein levels between stages.

**DISCUSSION:** We previously found that disrupting the actin cytoskeleton of cells in embryonic tendon resulted in a significant decrease in tissue elastic modulus<sup>2</sup>. Here, we further examined how TPCs may regulate embryonic tendon mechanical properties. The well organized actin cytoskeleton and the presence of cell-cell junction proteins suggest that TPCs in embryonic tendons form interconnected cell networks. Others have reported cad-11 in later stage (HH 39) embryonic tendon, and that siRNA knockdown of cad-11 in HH 39 tendon resulted in separation between adjacent tendon cells<sup>3</sup>. Here, we demonstrated earlier stage tendons also contain cad-11, as well as N-cad, and cx43. Additionally, actin filaments and their crimp pattern appeared contiguous between adjacent TPCs, suggesting the actin may be linked between TPCs. In other cell types, cadherins and connexins bind to actin intracellularly<sup>4, 5</sup>. Taken together, our results suggest that cad-11, N-cad and cx43 contribute to connections between the actin filaments of adjacent embryonic TPCs. These results motivate future studies to investigate how interactions between cell-cell junctions and the actin cytoskeleton network influence embryonic tendon mechanical properties.

**REFERENCES:** 1. Marturano Proc Natl Acad Sci 2013. 2. Schiele et al., ORS Trans 2013. 3. Richardson et al., Mol Cell Biol 2007. 4. Desai et al., Nat Cell Biol 2013. 5. Butkevich et al., Current Biology 2004.

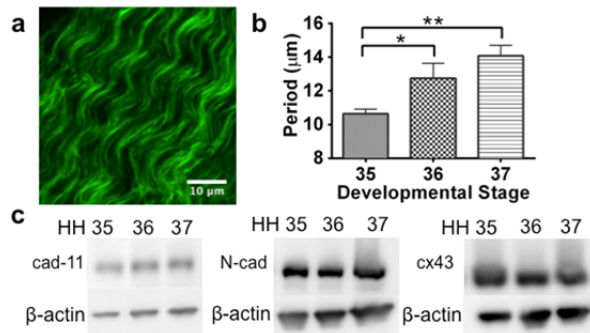


**Fig 1.** a) A well organized actin cytoskeleton network with crimp in HH 36 tendon. b) Actin filament crimp period increased with stage. c) Western blot of cad-11, N-cad, cx43 and  $\beta$ -actin in HH 35 to 37 tendons.

# FULL-FIELD METHODS FOR ANTERIOR CRUCIATE AND OTHER LIGAMENT BIOMECHANICAL CHARACTERIZATION

Kaitlyn F Mallett, Callan Luetkemeyer, and Ellen M Arruda

The anterior cruciate ligament (ACL) is comprised of two primary bundles, both of which are non-linear, anisotropic, viscoelastic, fibrous tissue structures. These anteromedial (AM) and posterolateral (PL) bundles twist around each other as they course anteriorly, medially, and distally from the femur to the tibia, spiraling laterally (i.e. counter-clockwise in the right knee). Characterization of the biomechanical response of the ACL has remained elusive because of the geometries and fibrous nature of the two bundles, and their complicated tibial and femoral insertions, which render establishment of well-posed experimental boundary conditions extremely challenging. In our approach to characterizing the biomechanical properties of the individual bundles of the ACL, we first separate the two bundles by cutting through the tibial to the enthesis along the line separating the two bundles, and then gently pulling the bundles apart, keeping the femoral attachments intact. We then retract the PL bundle to test the AM bundle, and then retract or remove the AM bundle to test the PL bundle. Each bundle's orientation is manipulated until an unloaded configuration providing the closest approximation to uniaxial loading is established. The specimens are coated with graphite particles to provide a speckle pattern and load-unload tests and stress relaxation tests are conducted. Two high-speed digital cameras capture the motion of the speckle pattern, and these images are synchronized with the force response data. Digital image correlation (DIC) analysis is utilized to compute the strain fields within the entire field of view of the high-speed digital cameras. This approach affords us unprecedented detail in examining the deformation response of the ACL bundles during uniaxial testing. Axial, transverse, and shear strain contours on the AM bundle at a globally applied axial strain of 8% are shown in Figure 1. The axial strain (A) evolves fairly homogeneously during loading with a maximum average tissue level strain of about  $4.5\% \pm 1.5\%$  due to uniform stretching of stiff collagen fibrils. The transverse strain contours demonstrate that some fibrils expand laterally (red and green bands in B) while others contract (blue and purple bands in B) during uniaxial loading. The shear strain patterns (C) also demonstrate the heterogeneous response of individual fibrils. As powerful as the DIC method is in the analysis of deforming materials it is clearly limited as it provides only surface deformation information from less than half of the full perimeter of the ACL bundle. The boundary conditions at the bone attachments and deformation response of the interior fibrils must accommodate these surface strains and it is likely the interior fibrils are also deforming heterogeneously. Our more recent efforts are focused on acquiring full surface DIC information as well as adapting digital volume correlation (DVC) techniques to ACL characterization. The latter requires an imaging modality that provides contrast within the entire ACL volume. Full surface DIC may be achieved with very good resolution using nano-CT. An example of this approach is demonstrated in Figure 2. Barium particles painted on the surface of the MCL and LCL are imaged at 25-micron resolution and a scan time of 50 minutes. With this method, it is possible to image the entire surface of these ligaments during deformation although the deformation must be applied in time increments that are long compared to the relaxation time of the viscoelastic ligament. This talk will provide an update of our efforts to measure ligament deformation and strain fields using full-field methods such as DIC and DVC together with the virtual fields method of material property characterization. We will discuss the advantages, disadvantages, and challenges associated with treating the ACL as a single, homogeneous structure, vs. two individual bundles that are homogeneous and yet not mechanically similar (see Figure 3), vs. a more detailed description of the individual fibril response of the AM and PL bundles.

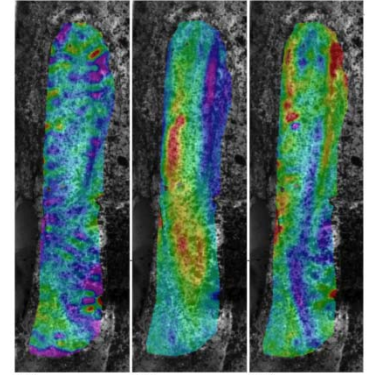


Figure 1: Axial (A) (vertical, 0% - purple to 10% - red), transverse (B) (-15%, purple to 30%, red), and shear (C) (-10%, purple to 5%, red) strain contours during uniaxial loading of the AM bundle via DIC analysis.

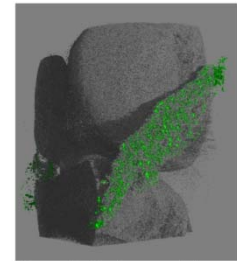


Figure 2: Barium particles (green) on the MCL and LCL imaged via nano-CT.

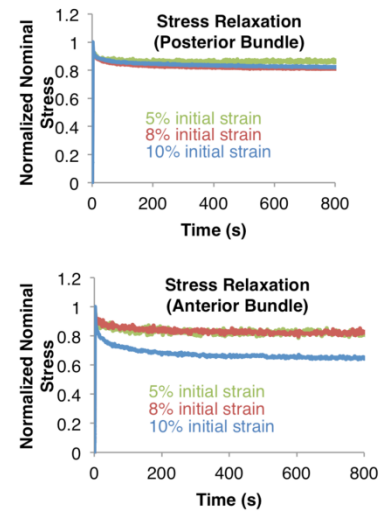


Figure 3: Normalized stress relaxation response of the AM (A) and PL (B) bundles of the ACL. The PL is seen to be linear in its viscoelastic response up to at least 10% strain whereas the AM is non-linear beyond 8% strain.

## NEW BIOMECHANICAL TESTING STANDARDS FOR EVALUATING ADJUSTABLE FEMORAL CORTICAL SUSPENSION DEVICES

AB Peterson<sup>1</sup>, MH McGarry<sup>1</sup>, O Limpisvasti<sup>3</sup>, JS Dines<sup>4</sup> and TQ Lee<sup>1,2</sup>

<sup>1</sup>Orthopaedic Biomechanics Laboratory, VA Long Beach Healthcare System, Long Beach, CA, USA. <sup>2</sup>Department of Orthopaedic Surgery, University of California, Irvine, Orange, CA, USA. <sup>3</sup>Kerlan Jobe Orthopaedic Clinic, Los Angeles, CA, USA. <sup>4</sup>Hospital for Special Surgery, New York, NY, USA.

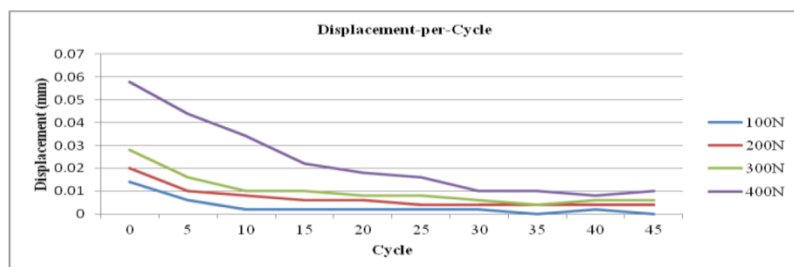
**INTRODUCTION:** Femoral cortical suspension is commonly employed for ACL and PCL graft fixation. Adjustable-loop suspension devices allow greater flexibility in tunnel characteristics, but at the cost of the ability to maintain fixed graft length. With a growing number of adjustable devices with this inherent shortcoming, it becomes imperative that they undergo a proper, comprehensive biomechanical evaluation, as all adjustable cortical suspension devices lack a permanent locking mechanism by design. The literature to date typically focused on few parameters, providing an inadequate characterization of device efficacy. It is the purpose of this study to develop a standardized testing protocol that will provide meaningful biomechanical information for adjustable cortical suspension devices.

**METHODS:** For such a protocol, all necessary functional requirements for adjustable devices must be considered. This includes the structural integrity of the locking mechanism, both from a functional and strength perspective. Specifically, suspension devices are required to withstand forces of routine rehabilitation with limited slippage, including periods of slack (no load), and maximum potential graft forces. ACL forces have been shown to reach up to 240N under passive flexion-extension, 340N with applied tibial torque, and experience complete unloading at mid-range flexion.<sup>1,2</sup> As such, the testing protocol should include cycling at 10-100N, 10-250N, and 10-400N, with 500 cycles of each load and 60 seconds of zero load every 100 cycles. Devices should be preloaded at 50N prior to each set of 500 cycles to simulate initial tightening achieved by the surgeon. Clinically, devices may be seated in a non-ideal position and therefore evaluation at multiple angles is necessary. Specifically, cyclic testing should be performed with the suture loop at -10°, 0°, and 10° from the ideal perpendicular positioning of the adjustable loop device. In addition, to account for the potential effects of bodily fluids on device performance, suture should be kept moist with saline, viscous fluid. Following all cyclic testing, a load to failure test should be performed to quantitatively assess failure characteristics including the failure modes.

**VALIDATION / DISCUSSION:** The testing protocol introduces novel parameters that allow for a more appropriate evaluation of the biomechanical characteristics of cortical suspension devices. With validation testing, depending on the device, the adjustable loop displacement will experience varying increases indefinitely due to slip. Higher cyclic loads yielded greater displacement, demonstrating that slippage is dependent on the load applied. Displacement-per-cycle values decrease and plateau with increasing cycles, which demonstrates the locking mechanism efficiency. These values also are dependent on the loads applied (Figure 1). The plateau values are essential for assessing the safety as well as the potential clinical failure due to slippage. Variation in device angle showed increased slippage with increasing angle, which is dependent on and specific to the locking mechanism design. Consistently, displacement values decreased immediately following rest periods. This also demonstrates the importance of the zero load condition that is experienced clinically during rehabilitation. In summary, the main reason necessitating this testing protocol is that all adjustable cortical suspension devices do not provide a permanent locking mechanism by design.

**REFERENCES:** <sup>1</sup>Markolf KL, Gorek JF, Kabo JM, Shapiro MS. Direct measurement of resultant forces in the anterior cruciate ligament. An in vitro study performed with a new experimental technique. J Bone Joint Surg Am. 1990;72(4):557-67. <sup>2</sup>Wascher DC, Markolf KL, Shapiro MS, Finerman GA. Direct in vitro measurement of forces in the cruciate ligaments. Part I: The effect of multiplane loading in the intact knee. J Bone Joint Surg Am. 1993;75(3):377-86.

Fig 1: Relationship between displacement-per-cycle and cycle number. Higher cyclic loads are associated with higher displacement-per-cycle values. The plateau value represents locking mechanism efficiency.



# ABERRANT DIFFERENTIATION OF TENDON STEM CELLS CAUSES TENDINOPATHY

J. Zhang and JH-C. Wang

MechanoBiology Laboratory, Department of Orthopaedic Surgery, University of Pittsburgh, Pittsburgh, PA.

## INTRODUCTION

Advanced stage tendinopathy is believed to be caused by excessive mechanical loading. We previously found that small mechanical loading induces differentiation of tendon stem cells (TSCs) into tenocytes *in vitro*, but large mechanical loading also induced differentiation of non-tenocytes such as adipocytes, chondrocytes, and osteocytes [1]. *In vivo*, moderate treadmill running (MTR) of mice upregulated tenocyte-related genes but intensive treadmill running (ITR) also induced non-tenocyte differentiation of TSCs [2]. In this study, we aimed to test the hypothesis that TSCs *in vivo* undergo non-tenocyte differentiation when subjected to ITR.

## METHODS

**Irradiation and Injection of GFP TSCs** – First, we eliminated resident tendon cells from the patellar tendons of 12 C57BL/6J mice by irradiating with 6 Gy from a Gamma cell 40 (cerium). A live/dead cell viability assay (Life Technologies) revealed that cell killing was > 99% in tendon. Then, GFP-TSCs (P1,  $1 \times 10^4/\mu\text{l}$ ) from C57BL/6 transgenic mice (GFP-mice) [C57BL/6-TgN (ACTbEGFP) 10sb mice, Jackson Labs] were injected into the irradiated tendons using a 30G syringe.

**Mouse treadmill running experiment** – Six irradiated and GFP-TSC injected mice were subjected to a ITR (1 week training, then running at 13 meters/min, 1-5 hrs/day, 5 days/week for 3 weeks). Then, tendon sections were immunostained to evaluate the presence of GFP-TSCs and non-tenocyte proteins. Tendon cells in the injected area were also isolated for qRT-PCR.

## RESULTS

Fluorescence microscopic observations and immunohistochemical analysis of irradiated and injected mice tendons revealed that the ITR increased the expression of non-tenocyte specific proteins (PPAR $\gamma$ , Sox-9 and Runx-2) (Fig. 1). Further, qRT-PCR analysis demonstrated that ITR upregulated the expression of non-tenocyte related genes, LPL, Sox-9 and Runx-2, and tenocyte related genes, collagen I and Scx (Fig. 2A, B).

## DISCUSSION

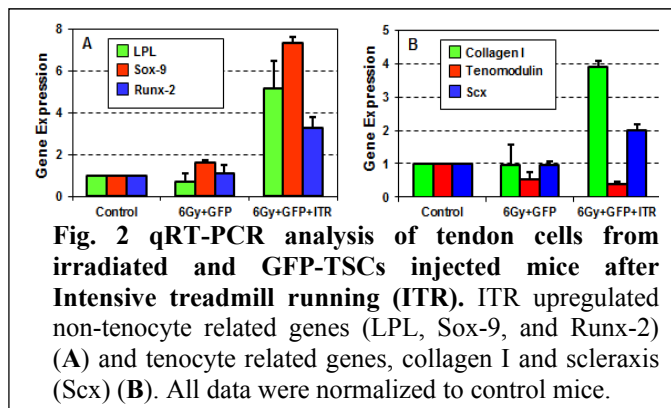
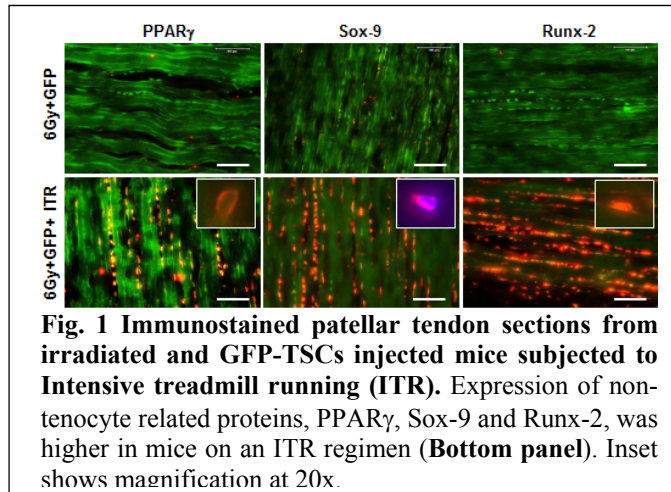
Immunohistochemistry and qRT-PCR revealed that ITR regimen enhances non-tenocyte differentiation of mice TSCs *in vivo* similar to our previous *in vitro* findings [1]. Also, ITR not MTR induced the aberrant differentiation of TSCs. Our irradiation and injection approach also proved feasible to test our hypothesis that *only* TSCs induce non-tenocyte differentiation and therefore major contributors to the development of tendinopathy.

## ACKNOWLEDGEMENTS

This work was supported in part by the NIH awards AR061395 and AR060920.

## REFERENCES

1. Zhang, J. and J.H. Wang, J Orthop Res, 2010. 28(5): p. 639-43.
2. Zhang, J. and J.H. Wang, PLoS ONE, 2013. 8(8): p. e71740.



# THE ROLE OF NF- $\kappa$ B SIGNALING IN ROTATOR CUFF TENDINOPATHY

S.A. Shah, Y. Abu-Amer, and S. Thomopoulos

Department of Orthopaedic Surgery, Washington University in St. Louis, St. Louis, MO

## INTRODUCTION:

Conditions such as overuse can lead to rotator cuff degeneration and eventual rupture. The molecular mechanisms driving these effects, however, are largely unknown. In particular, the role of inflammation in rotator cuff tendinopathy remains unclear [1], and the therapeutic potential of modulating inflammation for rotator cuff disease remains unexplored [2]. The objective of the current study was to examine the role of nuclear factor- $\kappa$ B (NF- $\kappa$ B) signalling, a downstream regulator of inflammatory cytokines such as IL-1 $\beta$  and TNF- $\alpha$ , in overuse-induced tendinopathy [3]. Specifically, we examined the effect of increased and decreased expression of IKK $\beta$  (key member of the NF- $\kappa$ B pathway) under tendinopathy conditions. We hypothesized that tendon-specific deletion of IKK $\beta$  will protect tendon from overuse whereas increased expression of IKK $\beta$  will exacerbate overuse-induced tendinopathy.

## METHODS:

Floxed IKK $\beta$  (IKK $\beta^{fl}$ ) mice and constitutively activated IKK $\beta$  (IKK $\beta^{ca}$ ) mice were crossed with mice expressing Cre-recombinase under the tendon specific scleraxis (Scx) promoter [4-5]. After an initial training week, mice (N=16; 4 per group) were subjected to 4 weeks of overuse treadmill running (20m/min, 30min/day, 5 times/week, 10 $^\circ$  decline). Cage activity (CA) mice were age matched to overuse mice. The humerus with the supraspinatus (SS) tendon attached was dissected from each forelimb for histology, bone morphometry, and biomechanical testing. For histology, 5  $\mu$ m sections were stained with hematoxylin and eosin (HE) or toluidine blue. For bone morphometry, SS-humeral head samples were scanned at a resolution of 12  $\mu$ m to determine bone volume (BV), bone mineral density (BMD), bone volume of the mineralized supraspinatus insertion (SSI-TV), and trabecular bone parameters in the humeral head distal to the growth plate. For biomechanics, uniaxial failure tests were performed in a saline bath at 37  $^\circ$ C. The effects of group and activity level were compared using an ANOVA followed by post-hoc LSD tests when appropriate.

## RESULTS:

In IKK $\beta^{ca}$ ;ScxCre mice (i.e., with IKK $\beta$  constitutively active in Scx-expressing cells), there were significant decreases, relative to wild type (WT) controls, in BV/TV (53% of WT), BMD (69% of WT), trabecular thickness (55% of WT), and SSI-TV/TV (54% of WT). No significant differences in bone morphometry were observed between IKK $\beta^{fl}$ ;ScxCre mice (i.e., with IKK $\beta$  deleted from Scx-expressing cells) compared to WT controls. Overuse activity caused significant decreases in BV/TV (84% of CA) and trabecular thickness (86% of CA), and an increase in trabecular spacing (111% of CA). Overuse activity led to significantly lower modulus/stiffness and maximum stress/load compared to cage activity (Fig. 1A). IKK $\beta^{fl}$ ;ScxCre mice had significantly higher maximum stress, stiffness, and resilience compared to IKK $\beta^{ca}$ ;ScxCre mice (Fig. 1B). Cellularity (including inflammatory cells) was highest at the tendon insertions of IKK $\beta^{ca}$ ;ScxCre mice subjected to overuse (Fig. 1C,D).

## DISCUSSION:

An overuse protocol was implemented to induce rotator cuff tendinopathy in mice. We showed that:

- Overuse led to tendinopathy, as demonstrated by reduced rotator cuff mechanical properties.
- NF- $\kappa$ B signaling played an important role in overuse-induced tendinopathy: deletion of IKK $\beta$  in tendon fibroblasts (effectively making these cells unresponsive to common cytokines such as IL-1 $\beta$ ) protected the rotator cuff from tendinopathy; activation of IKK $\beta$  in tendon fibroblasts amplified tendinopathy and led to reduction of mineral in the adjacent bone.

Based on these results, modulation of inflammation in tendon via IKK $\beta$  is a promising therapeutic target.

**REFERENCES:** [1] Millar, NL. JBS, 2009. **91**(3):417-24 [2] Riley, G. Rheumatology. 2004. **43**(2): p. 131-42. [3] Soslowsky LJ. JSES, 2000. **9**(2):79-84. [4] Otero, JE. PLoS One, 2012. **7**(6): p. e38694. [5] Blitz, E. Dev Cell, 2009. **17**(6): p. 861-73. **ACKNOWLEDGMENTS:** NIH F31-AR066452 and R01-AR057836.

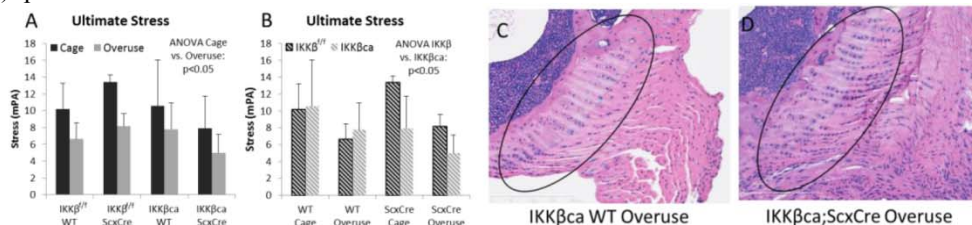


**Figure 1:** (A) Overuse activity led to reduced mechanical properties. (B) IKK $\beta^{fl}$ ;ScxCre mice had higher ultimate stress than IKK $\beta^{ca}$ ;ScxCre mice. (C-D) Cellularity at the enthesis (circle) was highest in IKK $\beta^{ca}$ ;ScxCre mice.

## CATHEPSIN ACTIVITY IN HUMAN AND RAT SUPRASPINATUS TENDINOPATHY

Parks, Akia<sup>1</sup>; Seto, Song<sup>1</sup>; McFaline-Figueroa, Jennifer<sup>1</sup>; Soslowsky, Louis J.<sup>2</sup>; Karas, Spero<sup>3</sup>; Ghattas, Timothy<sup>3</sup>; Sloan, Harris<sup>3</sup>; Tayrose, Gregory<sup>3</sup>; Platt, Manu<sup>1</sup>; Temenoff, Johnna<sup>1</sup>

1. Coulter Dept. of Biomedical Engineering, Georgia Tech and Emory University, Atlanta, GA 2. McKay Laboratory, University of Pennsylvania, Philadelphia, PA, 3. Dept. of Orthopaedics, Emory University, Atlanta, GA

**INTRODUCTION:** Though generally attributed to overuse, the exact mechanisms behind matrix degeneration in tendinopathy are still not well understood [1]. Cysteine cathepsins are a family of proteases that include cathepsin K, a powerful human collagenase that has been shown to be involved in many tissue-destructive diseases [2]. It is hypothesized that cathepsins are upregulated in damaged supraspinatus tendon tissue, degrading the collagen ECM and leading to deterioration of supraspinatus tendon structure. Multiplex cathepsin zymography was used to analyze cathepsin activity in tissues from human patients with chronic supraspinatus tears, and in a rat supraspinatus tendon overuse model after 4 and 10 weeks of overuse. Structural damage was also assessed via histology.

**METHODS:** Procedures were approved by the IACUC at both Georgia Tech and Emory. Human tissue samples were isolated from surgical patients with chronic (symptoms 3+ months) tears. Male Dahl Salt Resistant rats (Harlan Labs) were subjected to a daily downhill running regime described previously [3] for 4 or 10 weeks (n=12 tendons/timepoint) or served as age-matched controls (n=12 tendons/timepoint). For histology, running and control tendons (n=3/group/timepoint) were cryosectioned and stained with hematoxylin and eosin (H&E).

For cathepsin zymography, the rat supraspinatus tendons were systematically divided into the insertion (17% of the total tendon length from the bone attachment point) and midsubstance (the remaining tendon) regions. Human tendon samples were processed without division into regions. Protein from sample homogenates (n=4) were loaded into gelatin-embedded SDS-polyacrylamide gels with cathepsin V as a positive control. After electrophoresis proteins were renatured, degraded ECM, and quantified with densitometry using ImageJ (NIH) normalized to cathepsin V. Data (4 week rodent samples only, 10 week samples in processing) were Box-Cox transformed and analyzed by t-tests to assess statistical differences (p<0.05). Values are reported as mean ± standard deviation.

**RESULTS:** In 5 of 6 samples, zymography on the human samples demonstrated active cathepsins K, V, S, and L (Fig 1). Zymography of the rat tendon at 4 weeks showed the overuse samples at a 1.8-fold increase in active cathepsin L and a 4.2-fold increase in cathepsin K only in the insertion region (Fig 2B, C). While 10 week samples are still undergoing zymography, from histology, 10 week running samples showed rounded cells at the insertion region (Fig 3) that were not present in the controls (Fig 3) or 4 week samples (not shown due to space constraints).

**DISCUSSION:** This study has demonstrated the effects of overuse on cysteine cathepsin activity both in the supraspinatus tendon tissue of human patients with chronic tears and in overused supraspinatus tendons of rats. The presence of cathepsin activity suggests that these proteases are playing a role in the progressive degeneration of the tissue that is confirmed visually with histological images in the 10 week rodent samples, especially at the insertion region. Because we have shown that similar cathepsins are active in both a rat supraspinatus overuse model and in end-stage human tendinopathy, we will use this animal model in the future to further elucidate proteolytic mechanisms of tendon damage and explore treatment options for chronic tendinopathy.

**REFERENCES:** [1] Maganaris, C.N. et al. *Sports Med.* 2004; 34(14), 1005-17. [2] Garnero, P. et al. *J Biol Chem.* 1998; 278(43), 32347-52. [3] Soslowsky, L.J. et al. *J Shoulder Elbow Surg.* 2000; 9(2), 79-84.

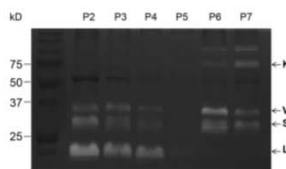


**Figure 1.** Cathepsin activity in human chronic rotator cuff tendon tears. Zymography gel depicts activity of cathepsins K, V, S, and L.

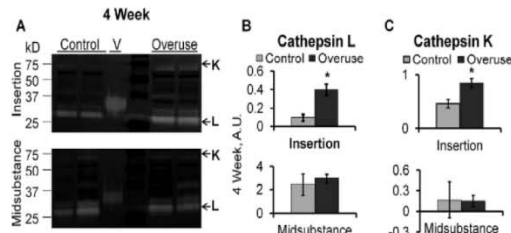


**Figure 2.** Cathepsin activity in rat supraspinatus tendon. Representative gels (A) depict location of cathepsins K and L. Cathepsin L (B) and cathepsin K (C) activity in 4-week overuse tendons compared to age-matched controls. n=3-4, \* indicates significantly greater activity over control at the same time point (P<0.05).

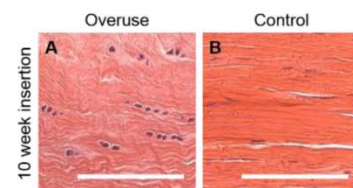


**Figure 3.** Changes to rat supraspinatus tendon structure obvious by 10 weeks of overuse. The cells in the insertion region (A) appear more rounded and misaligned than in the non-running controls (B). (n=3), Scale bar indicates 50 μm.

DISRUPTION OF TGF $\beta$  SIGNALING IN THE *SCLERAXIS* CELL LINEAGE LEADS TO TENOCYTE DEDIFFERENTIATION AND TENDON DEGENERATION

Guak-Kim Tan<sup>1</sup>, Anna G. Stabio<sup>1</sup>, Brian A. Pryce<sup>1</sup>, Doug R. Keene<sup>1</sup>, Ronen Schweitzer<sup>1,2</sup>

<sup>1</sup>Shriners Hospital for Children, Portland, OR, USA. <sup>2</sup>Oregon Health and Science University, Portland, OR, USA.

**INTRODUCTION:** Tendons are connective tissues that attach muscle to bone, and transmit contractile forces from muscles to the skeleton to generate movement. Our group has previously reported that disruption of transforming growth factor- $\beta$  (TGF $\beta$ ) signaling in mouse limb mesenchyme resulted in complete failure of tendon differentiation in mutant embryos [1]. To address the possibility of additional roles for TGF $\beta$  signaling in later stages of tendon development, here, we generated mice with a conditional deletion of TGF $\beta$  type II receptor gene (*Tgfb2*) specifically in *scleraxis* (*Scx*; a distinct marker of tendon progenitors and tenocytes)-expressing cells using the Cre/loxP system [2,3].

**RESULTS:** Most mutant (CKO) pups appeared physically normal at birth but showed movement difficulties and splayed limbs by P3 (Fig.1b). Examination of the *ScxGFP* tendon reporter signal [4] revealed a complex phenotype. At E14.5, the tendons of CKO embryos were indistinguishable from those of wild-type (WT) littermates, and the first indication of a tendon phenotype was detected at or close to E16.5, in which a single flexor tendon snapped and remained disconnected (Fig.1a). Severe disruption of tendons manifested in neonates where some tendons that appeared intact at birth were completely eliminated and could not be detected by P7, likely accounting for the splaying of CKO limbs, whereas other tendons retained structural integrity with a substantial loss of the *ScxGFP* signal (Fig.1c). Transverse sections showed that the loss of *ScxGFP* signal was not due to loss of tendon cells since the *ScxGFP*-negative cells were positive for Cre reporter *Rosa-tdTomato* (*RosaT*) [5] (Fig.2a), indicating they were derived from *Scx*-expressing cells. Moreover, these cells lost other tendon markers, including collagen I and tenomodulin (Fig.2b). Interestingly, the loss of tendon gene expression was not associated with transdifferentiation (not shown). Surprisingly, the cells that retained *ScxGFP* expression became rounded and enlarged (Fig.2a), and preliminary data suggests these cells may be newly recruited tenocytes. Macroscopically, the CKO tendons appeared grey and thin, with disorganization of collagen fibrils as revealed by transmission electron microscopy (Fig.2c). While these findings imply that TGF $\beta$  signaling may have a direct role in maintenance of the tendon cell fate, preliminary results suggest that the loss of tendon markers in CKOs is not due to a cell autonomous requirement for TGF $\beta$  signaling in tenocytes.

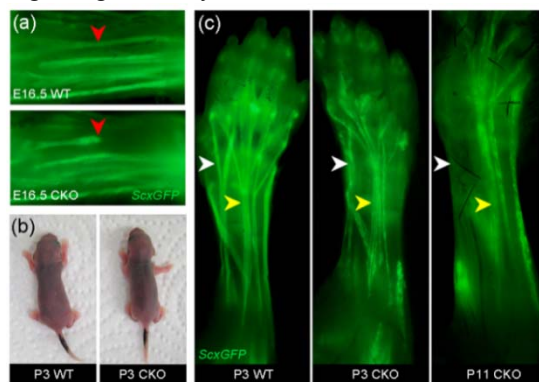


Fig.1: Tendon phenotypes manifested in *Tgfb2* CKOs. (a) Starting at E16.5 flexor carpi radialis tendon (red arrow) tear was noted in the CKO embryo. (b) By P3, all CKO pups displayed physical abnormalities including splayed limbs. (c) From this stage onward, some tendons could not be detected (white arrow) whereas others retained structural integrity with a substantial loss of *ScxGFP* signals (yellow arrow). In P11 CKO pups the tendon phenotype was exacerbated resulting in patchy *ScxGFP* appearance (yellow arrow).

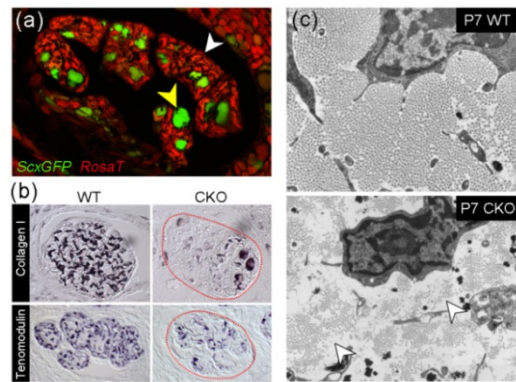


Fig.2: Disruption of *Tgfb2* in *Scx*-expressing cells results in loss of tendon markers and collagen degradation. (a) Most cells in the tendon of *Tgfb2* CKOs were *ScxGFP*-negative cells, but these cells originated from *Scx* lineage, as indicated by *RosaT* signals (white arrow). Meanwhile, tenocytes that retained *ScxGFP* expression became rounded and enlarged (yellow arrow). (b) The *ScxGFP*-negative cells also lost other tendon markers, including collagen I and tenomodulin. (c) Transmission electron microscopy imaging showing degradation of collagen fibrils in the tendons of CKOs (white arrows).

**DISCUSSION:** Our results reveal that disruption of TGF $\beta$  signaling in *Scx*-expressing cells leads to loss of tendon gene expression and degenerative phenotypes starting at late embryonic stage. One striking feature of this process is that the tenocytes lose marker gene expression suggesting a disruption of the cell fate but we do not find indications of tenocyte transdifferentiation. This analysis highlights an unexpected possibility for loss of differentiated characteristics in tenocytes as a key factor in a tendon degeneration process where the underlying cellular and molecular players remain largely unknown [6]. Our data also suggests that the phenotype is not due to a direct requirement for TGF $\beta$  signaling in tenocytes. Taken together these results suggest an essential and non-cell autonomous role for TGF $\beta$  signaling in tenocyte maturation and maintenance of the tendon cell fate.

**REFERENCES:** [1] Pryce et. al. Development. 2009,136:1351-1361. [2] Chytil et. al. Genesis. 2002,32:73-75. [3] Blitz et al. Development. 2013,140, 2680-2690. [4] Pryce et. al. Dev. Dyn. 2007,236:1677-1682. [5] Madisen et. al. Nat. Neurosci. 2010,13:133-140. [6] Sosolowsky et. al. J Shoulder Elbow Surg. 2000,9:79-84.

# INHIBITION OF HIF-2A SIGNALING WITH DIGOXIN DECREASES CALCIFICATION IN TENDINOPATHY

Jiajie Hu (1), Xiao Chen (1), Zi Yin (1), Hongwei Ouyang (1)  
School of Medicine, Zhejiang University, Hangzhou, China

**INTRODUCTION:** Chronic tendon pathology (tendinopathy) is a common but poorly treated disease, due to limited understanding of its pathogenesis. The resident tenocytes undergo continuous renewal from tendon progenitor/stem cells (TSPCs) (Bi, et al.,2007). How TSPCs are maintained and differentiated into tenocytes in healthy individuals and which key molecular events are defective in patients have been largely unknown. Manipulating endogenous stem cells with small molecules has been proposed as a therapeutic strategy, but practical approaches are still unavailable. In this study, our results demonstrate that digoxin represents a potential approach for calcifying tendinopathy therapy through inhibiting HIF-2 $\alpha$  mediated erroneous differentiation of TSPCs.

**METHODS:** Human model of tendinopathy: Calcific Achilles tendon and supraspinatus tendon were collected from patients undergoing surgical procedures. Treatment: Digoxin/saline was injected into rat Achilles tendon subcutaneously every 3 days after collagenase injection.

**RESULTS:** We compared the abundance of HIF-2 $\alpha$  (encoded by *EPAS1*) in uncalcified and calcified regions of human and rat Achilles's tendon. *EPAS1* mRNA and protein levels were elevated in calcific tendons compared with normal tendons. Immunoreactive for stro-1, CD44 and HIF-2 $\alpha$  demonstrated that HIF-2 $\alpha$  was increased in TSPCs which located in the vicinity of calcific sites. These findings demonstrate the HIF-2 $\alpha$  level is increased in TSPCs of calcific tendons.

Knockdown of HIF-2 $\alpha$  by shRNA significantly decreased the activity of alkaline phosphatase (ALP) and Alizarin red staining (ARS) of human TSPCs underwent osteogenesis induction combined with IL1 $\beta$  treatment. In contrast, overexpression of a constitutive active form of HIF-2 $\alpha$  lead to a significant reduction in expression levels of tendon specific markers, such as *SCX*, *EYAI/2*. These data suggest HIF-2 $\alpha$  signaling plays a significant role in the fate specification of tenocytes and osteoblasts from TSPCs.

Digoxin treatment *in vitro* inhibited IL1 $\beta$ -induced elevation of HIF-2 $\alpha$  protein and significantly decreased the activity of ALP and ARS staining of TSPCs (Fig.1 **a,b**) and increased expression level of *SCX*, *EYAI/2*. Moreover, we observed successful inhibition of HIF-2 $\alpha$  *in vivo* by subcutaneously delivery of digoxin. X-ray quantification and histological examination showed that compared with vehicle, digoxin administration led to decreased calcium deposition (Fig.1 **c,d**).

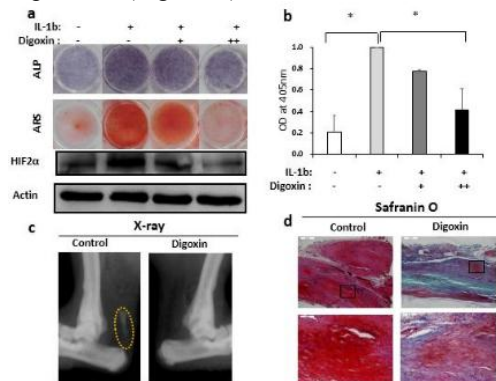


**Figure 1:** Digoxin decreases calcification *in vitro* and *in vivo*. (**a,b**) Western blot, alkaline phosphatase (ALP) activity, Alizarin red staining (**a**) and quantification (**b**) in human TSPCs treated with IL-1 $\beta$  and osteoinduction in the presence of HIF inhibitor: digoxin. (**c**) Calcification deposition assessed by x-ray in rats Achilles tendons at 8 weeks after creating a tendinopathy model combined with or without digoxin treatment. (**d**) Glycosaminoglycan content assessed by safranin O staining in digoxin treated or untreated tendons. Scale bars, 500 $\mu$ m (up), 100 $\mu$ m (down). All data are expressed as mean  $\pm$  s.d. \* $p$ <0.05 versus control groups.

**DISCUSSION:** Our work provides a applicable therapeutic approach for tendon calcification, through manipulation of HIF-2 $\alpha$  pathway in stem/progenitor cells by digoxin.

**REFERNCES:** Bi Y, Ehrlichou D, Kilts TM, et al. 2007. Nat Med. 13(10): 1219-27.

# IS NOD1 ACTIVATION INVOLVED IN TENDINOPATHY? CHARACTERIZATION ON CLINICAL SAMPLES AND IN VITRO STUDIES OF NOD1 ACTIVATION ON CULTURED TENDON CELLS

Hopkins C<sup>1,2</sup>, Fu SC<sup>1,2</sup>, Cheuk YC<sup>1,2</sup>, Chan KM<sup>1,2</sup>, Rolf C<sup>1,3</sup>

<sup>1</sup>Department of Orthopaedics and Traumatology, Faculty of Medicine, The Chinese University of Hong Kong

<sup>2</sup>Lui Che Woo Institute of Innovative Medicine, The Chinese University of Hong Kong

<sup>3</sup>Division of Orthopaedics and Biotechnology, CLINTEC, Karolinska Institute

**INTRODUCTION:** Tendinopathy is a common and disabling disease, but its aetiopathogenesis is not fully understood. Two case reports of tendinopathy have been documented in relation to Lyme disease (*B. burgdorferi*) and in both cases, tendinopathy was successfully treated with a course of antibiotics [1, 2]. A number of studies have demonstrated the involvement of Nucleotide Oligomerization Domain (NOD) proteins in Lyme disease [3]. NOD are intracellular proteins which respond to microbial components that enter the cell. The activation of NOD pathways result in the triggering of host defences against the microbes, including expression of pro-inflammatory mediators. It is unknown if NOD activation was involved in tendinopathy cases that did not experience an overt infection. In this study, we propose to investigate the involvement of NOD1 in tendinopathy by 1) detecting its expression in clinical samples of tendinopathy, and 2) determining the effect of NOD1 activation on cultured human tendon cells.

**METHODS:** This study has been approved by the Clinical Research Ethics Committee of the authors' institution (Ref no.: CRE-2013.479). Ten patellar tendinopathy samples were collected from patients and ten healthy patellar tendon samples were collected from patients undergoing anterior cruciate ligament (ACL) reconstruction surgery. All samples were processed for paraffin embedding and histological sectioning; immunohistochemical (IHC) staining of NOD1 was conducted on consecutive sections in every sample. Cultured tendon progenitor cells were also prepared from healthy tendon samples from patients of ACL reconstruction surgery. After seeding, tendon cells (at passage 5) were incubated with either synthetic NOD1 activator C12-iE-DAP (DAP) at concentrations of 0.1µg/ml and 1µg/ml, or its negative control γ-D-Glu-Lys (Lys) at the same concentrations. An untreated control without DAP or Lys was also included. The cells were harvested at 4 and 24 hours post incubation (n=3), and mRNA was extracted for qPCR to measure the expression levels of NOD1, interleukin-1 beta (IL-1β) and transforming growth factor (TGFβ). A two-way ANOVA was used to detect differences in cell culture study at α=0.05.

**RESULTS:** Eighty percent of tendinopathy samples were positive for NOD1 and none of the healthy tendons expressed IHC detectable NOD1 in interstitial tenocytes and the difference was statistically significant (Fisher's exact test, p = 0.000). No change in cell morphology and cell number was observed after treatment with DAP or Lys over a 24 hour time period. At 4 hours, NOD1 mRNA expression was significantly up-regulated in samples treated with DAP as compared to those treated with Lys, without an obvious dose response (Fig. 2A), but no significant differences in IL-1β (Fig. 2B) and TGFβ mRNA expression (Fig. 2C) were noticed at 4 hours. At 24 hours, IL-1β mRNA expression was up-regulated only in the higher dose 1µg/ml, and there were no significant differences in mRNA expression of NOD1 or TGFβ.

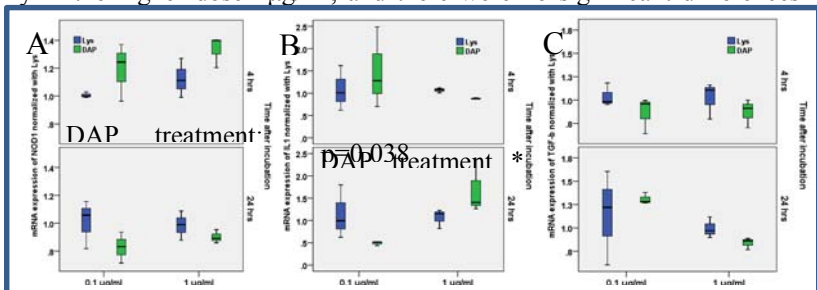
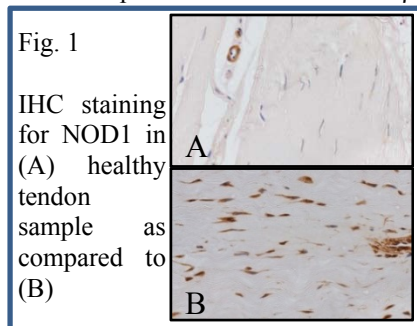


**Fig. 2: Relative mRNA expression levels of (A) NOD1, (B) IL-1β and (C) TGFβ, at 4 (upper panel) and 24 hours (lower panel), with 0.1 and 1µg/ml**

**DISCUSSION:** Increased expression of NOD1 in tendinopathy samples may imply the roles of NOD activation in the pathogenesis. The effects of NOD1 activation on tendon cells were similar to previous reports in other cell types [4]. Further investigation on the relationship of NOD1 activation and tendinopathic changes is necessary. The potential involvement of microbes in tendinopathy may suggest new therapeutic strategies.

**REFERENCES:** [1] Pandya, et al. Am J Orthop. 2008; 37(9): E167-E170; [2] Coulon, et al. Phys Ther. 2012; 92(5): 740-7; [3] Petnicki-Ocwieja, et al. PLoS One. 2011; 6(2); [4] Fernández-Velasco, et al. PLoS One. 2012; 7(9).

## MICRORNA IN TENDINOPATHY- A TRANSLATIONAL TARGET

Neal L Millar<sup>1</sup>, D. S. Gilchrist<sup>1</sup>, Moeed Akbar<sup>1</sup>, Abigail L Campbell<sup>2</sup>, James H Reilly<sup>1</sup>, Shauna C Kerr<sup>1</sup>, William J Leach<sup>3</sup>, Brian P Rooney<sup>3</sup>, George A C Murrell<sup>4</sup> and Iain B McInnes<sup>1</sup>

## MICRORNA IN TENDINOPATHY- A TRANSLATIONAL TARGET

Neal L Millar<sup>1</sup>, D. S. Gilchrist<sup>1</sup>, Moeed Akbar<sup>1</sup>, Abigail L Campbell<sup>2</sup>, James H Reilly<sup>1</sup>, Shauna C Kerr<sup>1</sup>, William J Leach<sup>3</sup>, Brian P Rooney<sup>3</sup>, George A C Murrell<sup>4</sup> and Iain B McInnes<sup>1</sup>

1. Institute of Infection, Immunity and Inflammation, College of Medicine, Veterinary and Life Sciences University of Glasgow, Glasgow, Scotland UK 2. Columbia University College of Physicians & Surgeons, New York, USA 3. Department of Orthopaedic Surgery, Western Infirmary, Glasgow, Scotland, UK 4. Orthopaedic Research Institute, Department of Orthopaedic Surgery, St George Hospital Campus, University of New South Wales, Australia.

**INTRODUCTION:** MicroRNA (miRNA) are a group of short non-coding RNA functioning as regulators of gene expression. Recent evidence has implicated miRNA 29 family as possible posttranscriptional regulators of collagen in diseases such as hepatic fibrosis and systemic sclerosis<sup>1,2</sup>. The key pathological change from type I to type III collagen in supraspinatus tendinopathy remains unanswered at a molecular level. We hypothesized that the miR29 family would be altered in supraspinatus tendinopathy and in an in vivo model of tendon healing.

**METHODS:** Fifteen torn supraspinatus tendon (established pathology) and matched intact subscapularis tendon (representing ‘early pathology’) biopsies were collected from patients undergoing arthroscopic shoulder surgery. Control samples of subscapularis tendon were collected from 10 patients undergoing arthroscopic stabilisation surgery. Human tendon-derived primary cells were derived from hamstring tendon tissue obtained during hamstring tendon ACL reconstruction. The impact of microRNA 29 upon tenocyte biology ex vivo was measured using quantitative RT-PCR, collagen I and III ELISAs and luminex cytokine multiplexes. In vivo work composed of experiments utilising a murine patellar tendon injury model.

**RESULTS:** Down regulation of miR29a expression in tendinopathy: We found that all members of the miR29 family were expressed in control, torn and matched tendon. Control tendon showed the highest level of miR29a expression. Both torn and matched subscapularis showed significantly decreased levels of miR29a compared to control tendon in keeping with collagen type III pathological changes which were confirmed at the message level.

MiR29a selectively targets collagen 3 in tenocytes: miR-29a manipulation selectively regulated collagen 3 but not collagen 1 mRNA and protein expression in primary tenocytes. miR-29a inhibition resulted in a significant increase in col 3a1 expression indicating that miR-29a is not only actively regulating these transcripts in human tenocytes but whose loss is an important factor in the increase of type 3 collagen production observed in tendinopathy. In contrast col 1a1 transcript levels were unchanged. We found through RACE methodology that in tenocytes, miR-29a specifically regulates col 3a1, while both col 1a1 and col 1a2 are rendered insensitive to miR-29a inhibition.

MiR29a altered in tendon healing in vivo: Based on these foregoing experiments we sought to explore the functional relevance of this in an in vivo model of tendon healing. Tendon injury in WT mice resulted in a 22 fold decrease in mir29a on day 1 which was reduced to a 6 fold decrease on day 3. By days 7 and 21 no significant difference was noted in miR29a expression. Thus in WT injured mice at early time points there is concurrent downregulation of miR29a and up regulation of Collagen III production in keeping with our in vitro findings.

Overexpression of miR29a directly regulates collagen matrix changes in in vivo tendon healing: Delivery of miR29a mimic to our in vivo tendon healing model was confirmed by immunofluorescence and qPCR resulting in a significant reduction ( $p < 0.01$ ) of collagen 3 production at Days 1 and 3 post injury. While a transient increase in coll1 message was noted at Day 1 post injury in keeping with our in vitro data we found that miR29a overexpression caused no reduction in coll1 levels in vivo.

**CONCLUSIONS:** This work highlights a novel role for miR-29a as a posttranscriptional regulator of matrix genes in tendon healing and tendinopathy. Our discovery of a single microRNA dependent regulatory pathway in early tissue healing, highlights miR-29a replacement therapy as a promising therapeutic option for tendinopathy with implications for many other human pathologies in which matrix dysregulation is implicated.

**REFERENCES:** 1 Maurer et al Arthritis & Rheumatism June 2010 1733-1743, 2 Rodenburg et al Hepatology Jan 2011 209-1

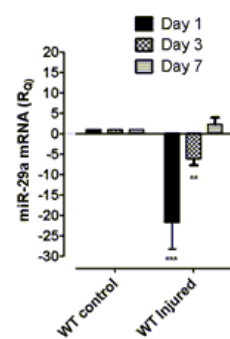


**Fig. 1:** miR29a levels on Days 1, 3 and 7 in rodent patellar

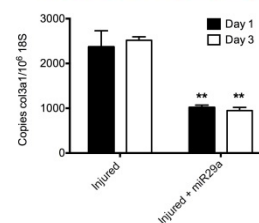
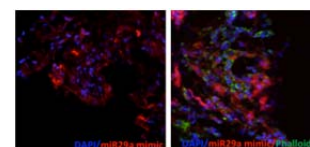


**Fig. 2:** Top panel – IF of miR29a mimic 24 hours post injection in vivo Bottom panel – mRNA

## DOES HYPOXIA CONTRIBUTE TO TENDINOPATHY? EVIDENCE FROM AN IN-VIVO MURINE MODEL

K.J. Trella<sup>1,2</sup>, J. Li<sup>2</sup>, J. Frank<sup>2</sup>, J. Galante<sup>2</sup>, J.D. Sandy<sup>2</sup>, A. Plaas<sup>2</sup>, R. Wysocki<sup>2</sup>, V.M. Wang<sup>1,2</sup>

1. University of Illinois at Chicago, Chicago, IL, United States

2. Rush University Medical Center, Chicago, IL, United States

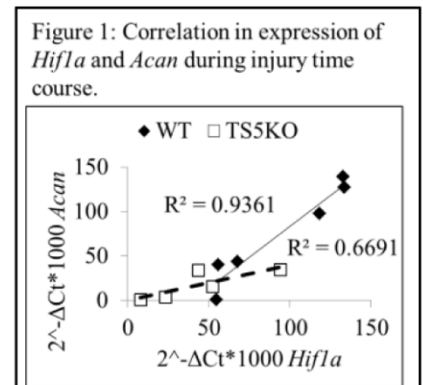
**INTRODUCTION:** Hypoxia has been implicated in numerous histopathologic studies of human tendinopathies [1, 2]. However, the mechanism by which a low oxygen environment may contribute to tendon degeneration (i.e., reduced mechanical properties, chondrogenic gene expression, and chondroid deposits) is poorly understood. We have previously shown in a TGF- $\beta$ 1 induced murine Achilles tendinopathy model that a combination of mechanical loading and the presence of the ADAMTS5 protein are necessary for the removal of aggrecan-rich (chondroid) deposits and the associated recovery of mechanical properties [3]. The objective of this study was to characterize the expression pattern of hypoxia responsive genes in relation to the development of murine Achilles tendinopathy using wild-type (WT, healing) and ADAMTS5-knockout (TS5KO, non-healing) mice.

**METHODS:** Under IACUC approval, 12-wk C57BL/6 WT and TS5KO male mice received two 6- $\mu$ L injections, 2 days apart, of 100ng rhTGF- $\beta$ 1 into the Achilles tendon. Mice were allowed normal cage activity for 3 or 14 days. Injected groups were compared to a control group of naïve mice. 12-20 tendons from each experimental group were combined for RNA preparation using 2-3 pools per experimental group. QPCR for individual matrix-protein genes was performed in triplicate, on cDNA synthesized with the SuperScript<sup>TM</sup> First Strand (Invitrogen) system from 0.5  $\mu$ g of RNA, using inventoried Taqman<sup>®</sup> (Life Technologies) primer-probe sets [3]. For hypoxia gene expression arrays (PAMM-032ZA, Qiagen), cDNA synthesis was performed using the RT<sup>2</sup> First Strand (Qiagen) kit with 0.5  $\mu$ g of mRNA from the same RNA preparations. For analysis,  $\Delta$ Ct (Ct for gene of interest minus Ct for *B2m*) was used to calculate abundance  $2^{-(\Delta$ Ct)\*1000 and fold change,  $2^{-(\Delta\Delta$ Ct)}, relative to naïve levels for each genotype.

**RESULTS:** Overall, TS5KO mice exhibited a higher percentage of up-regulated hypoxia genes (> 2-fold) at both 3 and 14 days post-injury (44% and 56%, respectively) compared to WT mice (38% and 5%, respectively). Naïve TS5KO mice (relative to WT) also had a marked (> 2-fold) down-regulation of 87% of genes related to hypoxia. The 3-day post-injury response in WT mice was accompanied by up-regulation (2.3-fold) in hypoxia inducible factor 1a (*Hif1a*), a master regulator of the cellular homeostatic response to hypoxia [4]. *Hif1a* expression returned to naïve levels (1.1-fold) at 14 days. Conversely, in TS5KO mice, *Hif1a* was up-regulated at both 3 and 14 days post-injury (5-fold and 3.9-fold, respectively). The functional gene groups most affected by injury included genes involved in metabolism and angiogenesis, most notably *Pkm* and *Angptl4*, respectively. At 3 days post-injury, these genes were up-regulated (> 2 fold) in both WT and TS5KO mice. However at 14 days, expression returned to naïve levels in WT mice but remained up-regulated in TS5KO mice. Expression of *Hif1a* was found to be highly correlated to the expression of aggrecan (*Acan*) in both genotypes over the injury time period (Figure 1), while *Pkm* and *Angptl4* were both highly correlated with *Acan* expression in TS5KO ( $R_2=0.91$  and  $0.83$ , respectively) but not WT mice ( $R_2=0.11$  for both).

**DISCUSSION:** The present study implicates hypoxia in an Achilles tendinopathy model, with both WT and TS5KO mice exhibiting an up-regulation in ~40% of hypoxia responsive genes at 3 days post-injury. However at 14 days, >50% of hypoxia genes remain up-regulated in TS5KO, but not WT mice, possibly contributing to its more severe tendinopathic phenotype [5]. Given the pathogenic accumulation of aggrecan in diseased tendon, the high correlation between the expression of *Hif1a* and *Acan* in both genotypes further supports the notion that hypoxia may play a role in the development of tendinopathy. *Pkm* and *Angptl4* are both highly correlated to *Acan* expression in TS5KO but not WT mice, suggesting that the presence of the ADAMTS5 protein may contribute to tendon healing via regulation of the expression of these genes. This study has demonstrated that hypoxia-related pathways regulated by ADAMTS5 may be viable clinical targets in treating tendinopathy. We hypothesize that mechanical stimulation via treadmill running will increase oxygen diffusion throughout the tissue and regulate angiogenic factors, such as *Angptl4*, to promote tendon healing [6].

**REFERENCES:** [1] Millar+, Ann Rheum Dis, 2012. [2] Kannus+, J Bone Joint Surg Am, 1991. [3] Bell+, J Biomech, 2013. [4] Semenza, Ann Rev Cell Dev Bio, 1999. [5] Bell+, JOR 2013. [6] Mousavizadeh+ PLoS One, 2014.



## LOW-DOSE HYDROGEN PEROXIDE IMPAIRED TENDON HEALING AND INDUCED TENDINOPATHIC CHANGES

Man-Yi Yeung<sup>1,2</sup>, Sai-Chuen Fu<sup>1,2</sup>, Christer G Rolf<sup>1,3</sup>, Kai-Ming Chan<sup>1,2</sup>, Leung-Kim Hung<sup>1,2</sup>

<sup>1</sup>Department of Orthopaedics and Traumatology, Faculty of Medicine, The Chinese University of Hong Kong.

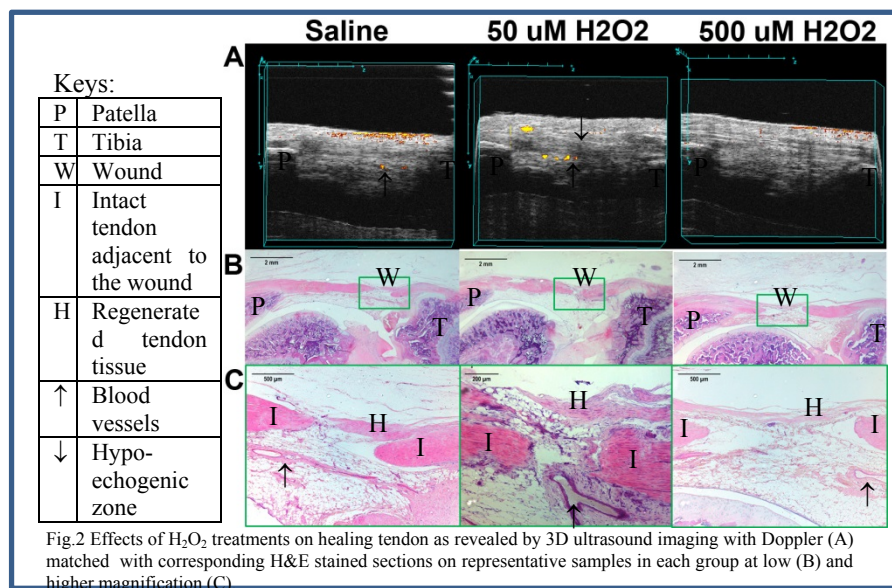
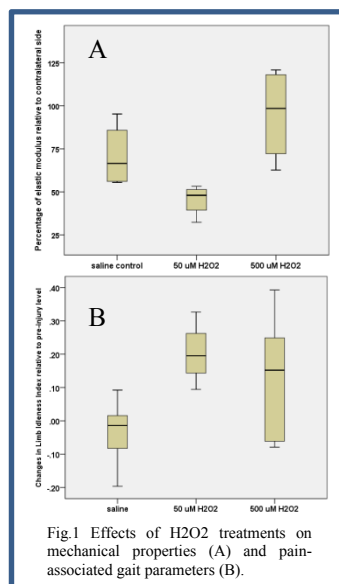
<sup>2</sup>Institute of Innovative Medicine, The Chinese University of Hong Kong.

<sup>3</sup>Department of Orthopaedic Surgery, Huddinge University Hospital, CLINTEC, Karolinska Institutet

**INTRODUCTION:** Oxidative stress is implicated in the development of tendinopathy<sup>1</sup> and it is well-recognised that muscles generate free radicals during exercise that may induce oxidative stress in nearby tendons. Pathogenesis of tendinopathy is now considered as failed tendon healing<sup>2</sup> influenced by a number of risk factors, such as genetics and overuse, but whether oxidative stress would impair tendon healing has not yet been investigated. In this study, the effect of imposed oxidative stress on tendon healing by hydrogen peroxide administration was studied.

**METHODS:** The animal experiments were approved by the Animal Experimentation Ethics Committee in the authors' institution (Ref no.: 12/034/GRF-5). A total of 18 male Sprague Dawley rats (8-10 weeks old, 200-300g) were used in the study. A patellar tendon window injury was created on the right knee according to our previous protocol. The rats were randomly assigned to three groups (n=6). Each group received three subcutaneous injections over the patellar tendon (from the 3<sup>rd</sup> to 5<sup>th</sup> week post operation) of either saline, 50 $\mu$ M or 500 $\mu$ M H<sub>2</sub>O<sub>2</sub> solution (100 $\mu$ l per injection). Collection of animal gait data (CatWalk XT, Noldus) for pain assessment and 3D ultrasound imaging data (Vevo770, Visualsonics) for tendinopathic changes were performed non-invasively at pre-injury and 6-week post operation (n=6). At day 42, the rats were euthanized to harvest knee specimens for either histology (n=2) or tensile mechanical test (n=4). Repeated measures ANOVA and the non-parametric Kruskal Wallis test were used to compare the treatment effects. Statistical significance was accepted at  $\alpha=0.05$ .

**RESULTS:** We found that the elastic modulus of the healing patellar tendons was significantly lower in the group with 50 $\mu$ M H<sub>2</sub>O<sub>2</sub> treatment (p= 0.021) but not in the 500 $\mu$ M H<sub>2</sub>O<sub>2</sub> treatment group (Fig.1A). Similarly, only the 50 $\mu$ M H<sub>2</sub>O<sub>2</sub> group exhibited pain-associated gait asymmetry as compared to the saline control (p=0.038) (Fig.1B). We also observed hypoechoic changes and increased power Doppler signals in and around the tendon wound in the 50 $\mu$ M H<sub>2</sub>O<sub>2</sub> group (Fig. 2A), which was further confirmed by histological examination with significant degenerative changes and hypervascularity (Fig.2 B&C).



**DISCUSSION:** The results demonstrated that H<sub>2</sub>O<sub>2</sub> impaired tendon healing and elicited tendinopathic changes, with respect to pain and structural abnormalities. The high dose of H<sub>2</sub>O<sub>2</sub> did not elicit tendinopathic changes; it may be attributed to the effective triggering of host antioxidant defense mechanisms. The current findings suggest oxidative stress plays a role in the failed tendon healing of tendinopathies.

**ACKNOWLEDGEMENTS:** The current work was kindly supported by the General Research Fund (# 464912).

**REFERENCES:** 1. Longo et al; *Disabil Rehabil* 2008; 2. Fu et al; *Sports Med Arthrosc Rehabil Ther Technol* 2010.

## SHEAR-TENSION RATIO EFFECT ON HEALTHY AND TENDINOPATHIC HUMAN TENOCYTE METABOLISM

Dharmesh Patel (1), Stephanie Bryant (2), Graham Riley (3), Eleanor Jones (3), Hazel Screen (1)

1. Queen Mary University of London, UK; 2. University of Colorado Boulder, US; 3. University of East Anglia, UK.

**INTRODUCTION:** Tendinopathies are common, debilitating tendon disorders, seen among both athletes and non-athletes. Due to the unclear aetiology of tendinopathies, treatment is often generalised, and efficacy limited. Changes in mechanical and cellular interactions after microdamage are thought to be key in developing tendinopathy (Arnoczky et al., 2007). Therefore understanding how the cell strain environment modulates matrix turnover and catabolism is essential. A unique fibre composite system has been developed for this purpose. It mimics the shear/tension tenocyte environment by encapsulating cell-coated polyethylene glycol (PEG)-RGD rods within a PEG matrix, using UV light initiated polymerisation. By recapitulating the specific, tightly controlled strain conditions seen by tenocytes in situ, multiple post-analysis techniques such as gene expression can be explored.

**METHODS:** PEG-RGD rods of two stiffness (20% and 60% PEG) were made and soaked for either 10 or 60 minutes prior to encapsulation to generate four different cellular shear-tension (S-T) ratios. Rods were seeded with either healthy or diseased human tenocytes (obtained following surgery with ethical permissions) prior to encapsulation. 12 composites were made for each condition, of which 6 were loaded and 6 used as non-strained controls. Loaded samples were exposed to 5% cyclic strain (1Hz) for 24 hours using custom-built chambers maintained in an incubator. Once the loading regime ended, all samples were snap frozen and then analysed via RT-qPCR and Taqman Low Density Arrays (TLDA) to investigate the expression levels of 48 matrix related genes.

**RESULTS:** Figure 1 shows the expression levels of a small selection of matrix related genes normalised to TOP1 for fibre composites with tendinopathic cells. S-T ratio dependent changes were seen in COL-11A1 and ADAMTS-3 for both cell types; a significant downregulation of COL-11A1 and upregulation of ADAMTS-3 was evident with increasing levels of shear on the cells. Substrate stiffness dependent differences are also seen in a number of genes including ADAMTS-14, TIMP-3 and PRG4.

**DISCUSSION & CONCLUSION:** Overall, the data suggests tendinopathic cells are more mechano-sensitive than healthy cells showing larger changes in gene expression in response to applied strain. There were also differences in the basal gene expression between tendinopathic and healthy tenocytes. MMP13 was higher and MMP3, ADAMTS-5, PRG4 and VCAN lower in the tendinopathic cells. The S-T dependent change in COL-11A1 is interesting as collagen type XI is found in the interfascicular matrix (IFM) which is a high shear region.

The novel fibre composite system provides the first system able to investigate tenocyte mechanotransduction and physiological and pathological levels of cell shear and tension. Data obtained suggests the cellular S-T ratio is an important factor regulating cell behaviour and hence important in the development and progression of tendinopathies

**ACKNOWLEDGMENTS:** Dharmesh Patel is supported by an Arthritis Research UK studentship. The research is also supported by NIH grant 1R21AR062197.

**REFERENCES:** Arnoczky, et al., *Int J Exp Pathol*, 88:217-26, 2007.

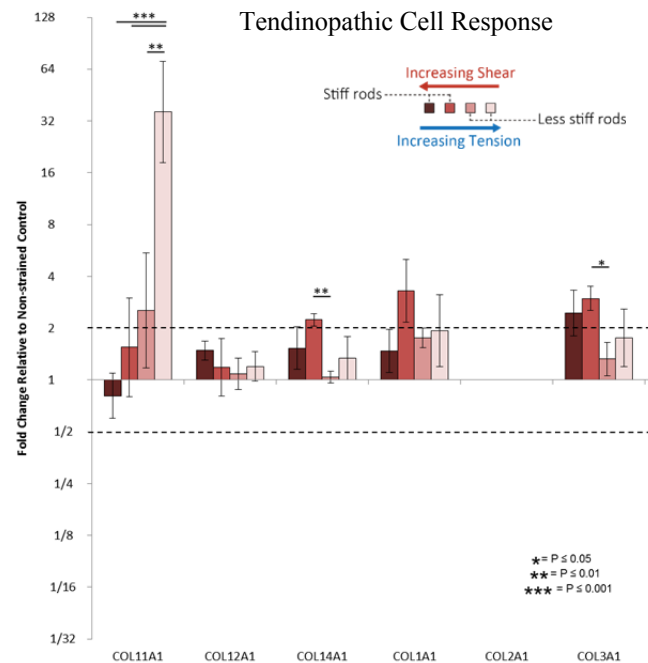


**Fig 1:** S-T ratio effect on tendinopathic cell gene expression (normalised to TOP1).

## PATHOLOGICAL TENDON PROPERTIES: STIFFNESS, STRENGTH AND PROTEOGLYCANS

<sup>1</sup>R.K. Choi, <sup>1</sup>J. Martin, <sup>2</sup>E. Jacobsen, <sup>1</sup>M.M. Smith, <sup>2</sup>A.J. Dart, <sup>1</sup>C.B. Little, <sup>1</sup>E.C. Clarke  
1. Kolling Institute, University of Sydney, Royal North Shore Hospital, St Leonards, NSW, Australia  
2. Camden Vet Hospital, University of Sydney, Camden, NSW, Australia

**INTRODUCTION:** Tendons can be injured or overused in the workplace and in leisure. Subsequently, an insidious and painful degenerative cascade can alter and weaken the previously healthy tendon, resulting in ruptures. Surgical repairs of the Achilles tendon re-rupture in 20% of cases and no current treatments can restore the structure of degenerated tendons.

Our previous research using an equine model demonstrated that focal tendon injury induced histopathological changes, throughout the tendon (up to 10cm from the injury site). Changes included increased tenocyte rounding, inter- and intra-fascicular cell density, neovascularization and increases in proteoglycans and associated glycosaminoglycans (GAGs). This indicates that “healthy” tendon tissue surrounding tears and used in surgical repairs is in fact abnormal.

Whether the widespread histopathological changes are associated with altered mechanical properties throughout the tendon that may contribute to re-injury and surgical failure has not previously been investigated. Furthermore, the contribution of proteoglycan/GAG accumulation, a hallmark of tendon pathology, to altered biomechanics in tendinopathy is unclear. Therefore, our aims were a) to determine whether the widespread tendinopathy developing after a focal injury alters regional modulus and ultimate tensile stress (UTS), and b) to determine the role of GAGs in any changes observed, by comparing with tendons with enzymatically reduced GAG levels.

**METHODS:** The superficial digital flexor tendon (SDFT) was unilaterally hemi-transected mid-metacarpus in six horses (“pathological”). Three horses were sham-operated unilaterally, with the contralateral limb being a non-operated control. Animals were sacrificed after six weeks, at which time no differences were found between sham-operated and non-operated so these tendons were combined as “controls” (n=6). Tendons were divided into 12 separate regions: 3 proximal and 3 distal to the lesion from medial and lateral halves. Replicate samples (~25x1x1mm) from each region of each tendon were harvested and allocated to three groups: (i) no treatment (ex vivo) or incubated for 18 hours at 37°C in Tris-acetate buffer without (ii) or with (iii) chondroitinase ABC (0.3 units/ml to remove GAGs). Specimens were mechanically tested to failure in tension and then papain-digested for measurement of GAGs with spectrophotometry. Biomechanics data were normalised to measured specimen cross-sectional area and gauge-length to calculate elastic modulus and UTS. The relationship between modulus, UTS and GAG content was analysed using mixed models and ranking correlation (correcting for non-independence).

**RESULTS:** Ex vivo comparison of pathological versus control tendons confirmed decreased modulus (-39%,  $p<0.01$ ), UTS (-38%,  $p<0.01$ ), and elevated GAG content (51%,  $p<0.01$ ) in pathological tendons. The regional parameters had minor effects. Modulus ( $p<0.01$ ) and UTS ( $p<0.01$ ) were higher nearest the mid-metacarpus in normal tendons, yet not in pathological tendons. Regions farthest from the lesion were higher in modulus (22%,  $p<0.01$ ) and UTS (4%,  $p<0.01$ ). No tendons were found to differ between the medial and lateral halves or between the proximal and distal tendon.

Chondroitinase digestion reduced GAG content in pathological tendons to 50% ( $p<0.01$ ) of ex vivo levels, and partially restored modulus and UTS to 73% ( $p<0.01$ ) and 72% ( $p<0.01$ ) of normal, respectively. In contrast, the same chondroitinase digestion of normal tendons had no effect on biomechanical properties, despite a significant reduction in GAG levels by 28% ( $p<0.01$ ). Interestingly, chondroitinase digestion reduced GAG levels of pathological and normal tendons to the same level. GAG content was negatively correlated with both modulus ( $p<0.01$ ) and UTS ( $p<0.01$ ) when correcting for incubation treatment and pathological versus normal tendons.

**DISCUSSION:** These studies have confirmed that a focal injury results in altered biomechanical properties throughout the tendon. The elevated GAG, specifically chondroitin/dermatan sulfate, in pathological tendons was in part associated with these biomechanical changes, however further work remains in identifying the specific proteoglycans involved. Differences in the proteoglycans deposited and/or their localisation in pathology compared to normal tendon, may help explain the differential effect of chondroitinase digestion on biomechanics. The role of the chondroitinase-insensitive GAGs present at similar levels in both normal and pathological requires further investigation.

Nevertheless, our data suggests that preventing proteoglycan-accumulation could spare the biomechanical properties of tendons undergoing degenerative biomechanical changes, potentially improving repair and reducing incidence of rupture. Understanding the specific proteoglycans involved in tendon pathology would serve to progress this as a potential therapeutic target.

"DOES MY SHOULDER LOOK FAT TO YOU?" MUSCLE PHENOTYPIC CHANGES AND ROTATOR CUFF  
PATHOLOGY

Ranjan Gupta, MD

*Professor of Orthopaedic Surgery, Anatomy & Neurobiology, and Biomedical Engineering  
Chair of the Department of Orthopaedic Surgery  
University of California, Irvine*

Fatty degeneration of chronically injured muscle is a commonly recognized consequence of massive rotator cuff tears. Current surgical treatments are unable to alter or reverse the progression of fatty degeneration and are associated with poor functional outcomes in these patients. Therefore, a better understanding of the pathophysiology of fatty degeneration is required. As such, recent discoveries in stem cell biology and new animal models have significantly advanced our understanding of the cellular and molecular basis of fatty degeneration. Future studies will facilitate development of novel treatments to prevent the progression of fatty degeneration and improve muscle regeneration in patients with massive rotator cuff tears.

## GENETIC RESPONSE OF RAT SUPRASPINATUS TENDON AND MUSCLE TO EXERCISE

<sup>1</sup>S.I. Rooney, <sup>2</sup>J.W. Tobias, <sup>1</sup>P.R. Bhatt, <sup>1</sup>A.F. Kuntz, <sup>1</sup>L.J. Soslowsky

<sup>1</sup>McKay Orthopaedic Research Lab, <sup>2</sup>Penn Molecular Profiling Core, University of Pennsylvania, Philadelphia, PA

**INTRODUCTION:** Muscle and tendon beneficially adapt to non-injurious exercise. Previous studies suggest that inflammation plays an important role in the regeneration of muscle and tendon following acute injury;<sup>e.g.,1</sup> however, the mechanisms governing the roles of inflammation in the adaptation of muscle and tendon to beneficial loading have not been identified. The **objective** of this study was to screen for acute and chronic inflammatory, as well as ECM genes involved in the beneficial adaptation of rat supraspinatus (supra) tendon and muscle to non-injurious loading. Our global **hypothesis** was that a mild inflammatory response is a normal, physiologic requirement for muscle and tendon to adapt to load. Specifically, 1) a mild inflammatory response (changes in arachidonic acid cascade) would present in the tendon and muscle after a single bout of loading, and 2) the tissue will show adaptive matrix changes (increased collagen expression and MMP/TIMP changes indicating turnover) with chronic loading.

**METHODS:** 20 male, Sprague-Dawley rats (400-450g) were divided into cage activity (CA) or acute or chronic exercise (EX) groups (IACUC approved). Acute groups were divided into 12 or 24 hour euthanasia time points following a single exercise bout, and chronic groups were divided into 1 or 8 weeks of repeated exercise (n=4 each group). EX animals walked on a flat treadmill using a previously validated protocol.<sup>2</sup> Control CA animals maintained cage activity for 5 weeks. Supra tendon and muscle were harvest, RNA was extracted, and a custom Panomics QuantiGene 2.0 Multiplex array was used to detect 48 target genes for inflammation, ECM components, matrix turnover, and factors associated with tissue adaptation or degeneration. Target gene signal was normalized by the geometric mean of 3 housekeeping genes and log<sub>2</sub> transformed. Principal components analysis (PCA) was used to visualize global similarities among the 40 samples and for the 4 separate categories of interest: chronic tendon, chronic muscle, acute tendon, and acute muscle. For each category, a 1-way ANOVA (3 levels) with pairwise contrasts was used to compare CA and EX genes. Because this was a screening experiment, an inclusive analysis was conducted. Significance was set at  $p \leq 0.05$  and genes with a positive or negative fold change  $\geq 1.25$  were included.

**Table 1.** Inflammatory and matrix genes changed with acute exercise.

		Acute Tendon	Acute Muscle
<b>Arachidonic Acid Cascade</b>	CA-EX12	<i>Ptger4</i>	<i>Ptges</i>
	CA-EX24	<i>Ptges</i>	<i>Ptger4, Ptgfr</i>
	EX12-EX24	<i>Ptges, Ptger4</i>	<i>Ptges, Ptgfr</i>
<b>Matrix Turnover</b>	CA-EX12	---	<i>Timp4, Colla1</i>
	CA-EX24	<i>Mmp14, Timp3</i>	<i>Timp3, Colla1</i>
	EX12-EX24	<i>Mmp14, Timp3</i>	<i>Timp3, Timp4</i>

**RESULTS:** PCA confirmed distinctions between tissues and time points supporting the study design (not shown). Supporting our hypotheses, acute exercise caused an altered inflammatory response in muscle and tendon, indicated by changes in arachidonic acid cascade components and MMP/TIMPs (Table 1). As expected, inflammatory genes were more changed acutely than chronically. Chronic tissue had more matrix-related gene changes, suggesting tissue adaptation (Table 2). Several growth factors also significantly changed with acute and chronic exercise (not shown).

**DISCUSSION:** Tendon and muscle showed time-dependent responses to exercise. More chronic gene changes were found at 1 than 8 weeks, indicating that this adaptive process begins soon upon initiation of an exercise routine. Results suggest that tendon response to chronic, beneficial exercise is distinct from overuse. Unlike overuse, we did not find increased expression of cartilage markers (*Sox9, Acan, Col2a1*), heat shock proteins (*Hspa2, Hspb1*), or nitric oxide synthases (*Nos2, Nos3*) in tendon. In conclusion, this study suggests a role of physiologic inflammatory processes and matrix turnover in the response of supra muscle and tendon to acute and chronic beneficial load. Future studies can use these results to distinguish beneficial and detrimental loading effects, identify tissue recovery, and develop new treatments.

**Table 2.** Inflammatory and matrix genes changed with chronic exercise.

		Chronic Tendon	Chronic Muscle
<b>Arachidonic Acid Cascade</b>	CA-EX12	<i>Alox5ap</i>	<i>Ptgfr</i>
	CA-EX24	<i>Alox5ap</i>	<i>Ptgfr</i>
	EX12-EX24	---	---
<b>Matrix Turnover</b>	CA-EX01	<i>Mmp14, Timp1, Timp3, Colla1, Col3a1</i>	<i>Mmp14, Colla1, Col3a1</i>
	CA-EX08	<i>Mmp14, Timp1, Colla1</i>	<i>Mmp14</i>
	EX01-EX08	<i>Mmp14, Timp3, Colla1, Col3a1</i>	<i>Col3a1</i>

**REFERENCES:** 1. Connizzo+: *Clin Orthop Relat Res*, 472:2433-9, 2014. 2. Rooney+: *Muscles Ligaments Tendons J* (in press)

# MATRIX METALLOPROTEASES AND TISSUE INHIBITORS OF METALLOPROTEASES IN TENOCYTES OF THE ROTATOR CUFF DIFFER WITH VARYING DONOR CHARACTERISTICS

Franka Klatte-Schulz<sup>1,2</sup>, Thomas Aleyt<sup>1,2</sup>, Stephan Pauly<sup>1</sup>, Sven Geißler<sup>1,2</sup>, Christian Gerhardt<sup>1</sup>, Markus Scheibel<sup>1</sup>, Britt Wildemann<sup>1,2</sup>

<sup>1</sup>Julius Wolff Institute, Center for Musculoskeletal Surgery, Charité-Universitätsmedizin Berlin, Germany

<sup>2</sup>Berlin-Brandenburg Center for Regenerative Therapies, Charité-Universitätsmedizin Berlin, Germany

**INTRODUCTION:** The healing after rotator cuff reconstruction is associated with high failure rates, mainly linked to the formation of inferior, disorganized scar tissue at the tendon bone insertion site. The mechanisms underlying the poor healing are widely unknown. Since the MMPs and TIMPs regulate tendon modeling and remodeling, it is hypothesized that the development of tendon pathologies is dependent on the balance between MMPs and TIMPs.<sup>1,2</sup> The aim of our project was therefore to analyze MMPs and TIMPs in tenocyte-like cells (TLCs) on mRNA-, protein-, as well as activity-level regarding differences between varying donor characteristics such as age, sex and the degenerative status of the tendon.

**METHODS:** TLCs were isolated from SSP tendon biopsies from 16 male and 14 female donors undergoing arthroscopic or open shoulder surgery. Cells from each donor (passage 1 or 2) were seeded in a 6-well plate and RNA was isolated after 7 days of culture. Quantitative Real-Time PCR was performed to analyze the expression of MMP-1, -2, -3, -9, -10, -13 as well as TIMP-1 to TIMP-4. Protein secretion was analyzed from cell culture supernatants using conventional or multiplex ELISA. MMP activity in cell culture supernatants was analyzed by gelatin and casein zymography. **Statistics:** Mann-Whitney-U Test, Spearman's-Rho correlation,  $p \leq 0.05$ .

**RESULTS:** Gene expression analysis revealed a strong MMP-2 expression in all TLCs, followed by MMP-3 and MMP-1. MMP-9, MMP-10, and MMP-13 were expressed in very low amounts. High expression levels of TIMP-1, TIMP-2 and TIMP-3 were found in all cells, while the TIMP-4 mRNA expression was much weaker. Protein analysis of cell culture supernatants revealed a comparable pattern.

MMP and TIMP expression did not differ significantly between TLCs of male and female donors. An age-dependent increase in the mRNA-expression levels of MMP-2, MMP-9, MMP-13 and TIMP-2, TIMP-3 was found (Figure 1). This could be confirmed at the protein-level for MMP-2. In addition, protein-levels of TIMP-1 were significantly elevated in TLCs from older donors (>65 years). Regarding the degenerative status of the tendon several regulations were found. The mRNA-levels of MMP-2, MMP-9 and TIMP-3 were significantly increased in TLCs from donors with enhanced muscle fatty infiltration. MMP-9 and MMP-13 expression was significantly increased with greater tear size, whereas MMP-10 showed significantly decreased expression rates in these cells. At protein-level, MMP-1 and TIMP-1 secretion was significantly higher in TLCs from donors with greater tear size.

Gelatin zymography reveals proteolytic activity for MMP-2 and MMP-9 in cell culture supernatants. After image analysis, neither the intensity nor the area of the degraded bands showed significant alterations by the implicated donor characteristics. Using casein gels to analyze enzyme activity of MMP-1 and MMP-13, no degraded areas were visible.

**DISCUSSION:** In the present *in vitro* study, TLCs from donors with higher age (>65 years) or degenerative status of the tendon showed increased mRNA- and protein-levels of mainly the gelatinases MMP-2 and MMP-9, but also the TIMPs were up-regulated in these donor groups. The interaction between MMPs and TIMPs is a complex process, since TIMPs are not only inhibitors of MMPs, but are also able to regulate the activation of MMPs.<sup>3</sup> The results of the present study show that MMPs and TIMPs might play an important role in degenerative tendon pathologies, but also highlights the need of more knowledge in this research area.

**REFERENCES:** 1) Del Buono A. et al., J Shoulder Elbow Surg 2012; 2) Riley GP et al., Matrix Biol 2002; 3) Glaeser, J. D. et al., Tissue Eng Part A 2010

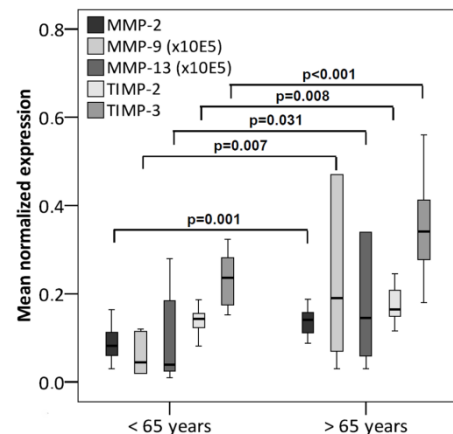


**Figure 1:** MMPs and TIMPs regarding the age of the donors (under 65 years (n=16) and over 65 years (n=14)): mRNA-levels of MMP-2, -9, -13 and TIMP-2, -3 are significantly increased with higher age.

## EFFECT OF BONE MINERAL DENSITY ON ROTATOR CUFF TEAR: AN OSTEOPOROTIC RABBIT MODEL

Hugo Giambinia<sup>a\*\*</sup>; Xiaobin Chen<sup>a, b\*\*</sup>; Ephraim Ben-Abraham<sup>a</sup>; Kai-Nan Ana<sup>a</sup>; Ahmad Nassra<sup>a</sup>; Chunfeng Zhao<sup>\*a</sup>

<sup>a</sup>Department of Orthopedic Surgery, Mayo Clinic, Rochester, MN, USA, 55905

<sup>b</sup>Institute of Orthopaedics, Chinese PLA, Beijing Army General Hospital, Beijing, China, 100700

<sup>\*\*</sup>these authors contributed equally to this work

### INTRODUCTION:

Rotator cuff tear is a common shoulder disorder associated with aging. Bone mineral density (BMD) of the humeral head affects rotator cuff repair healing. An increased BMD and trabecular structure in the greater tuberosity and in the proximity to the insertion site can improve rotator cuff repair and healing. However, it is still unclear how degenerative changes on bone of the humeral head affect the biomechanical properties of the rotator cuff tendon and a possible occurrence of tear. Using an ovariectomy (OVX) rabbit model, the objective of this study was to explore the correlation between humeral head BMD and infraspinatus (ISP) tendon insertion strength, and if an increase in bone quantity of the humeral head can improve the strength of the rotator cuff insertion and potentially decrease the likelihood of a rotator cuff tear in patients with osteoporosis.

### METHODS:

Eighteen New England white rabbits were divided into the 3 groups: Control (normal rabbit), Ovariectomy-Saline (OVX-Saline), and Ovariectomy-PTH (OVX-PTH). The OVX-Saline group and the OVX-PTH were administered daily saline and Teriparatide injections for 8 weeks starting at 17 weeks of OVX. Then, the rabbits were sacrificed and the bilateral shoulders were dissected leaving the ISP tendon-bone complex intact. BMD of the humeral head was measured using dual-energy X-ray absorptiometry (DEXA). The ISP tendon failure load was tested and the failure stress was calculated. One shoulder specimen from each group was left intact for histological analysis. Linear regression analysis was used to derive equations for the BMD and failure stress.

### RESULTS:

Significant differences were observed in the measured humeral head BMD of the Control and OVX-PTH groups compared to the OVX-Saline group (\* $P=0.0004$  and \*\* $P=0.0024$ , respectively) (Fig 1A). No significant difference was found in failure stress among the three groups (Fig 1B). However, there is an expected trend with the control group and OVX-PTH group presenting higher failure strength compared to the OVX-Saline group. The OVX-PTH group presented similar results when compared to control values. BMD at the humeral head showed a positive linear correlation with failure stress ( $r^2 = 0.54$ ) (Fig 1C). Histology results showed the OVX-PTH group to have a well-organized 4-layered tendon-bone interface of ISP enthesis (e.g. tendon, non-mineralized fibrocartilage, mineralized fibrocartilage, and bone) with abundant cells of non-mineralized and mineralized fibrocartilage when compared to the OVX-Saline group (Fig 1D).

### DISCUSSION:

Estrogen deficiency induces bone loss of the humeral head and changes in the architecture of the infraspinatus tendon enthesis that leads to decreased tendon/bone insertion strength. Teriparatide administration can increase bone density of the humeral head and may improve the composition of the mineralized interface of infraspinatus tendon enthesis. These changes result in improved mechanical properties of the infraspinatus tendon enthesis. These results imply bone loss progression may increase the risk factor for rotator cuff tears, and improving humeral bone density in patients with osteoporosis or osteopenia may help to increase the tendon/bone insertion strength.

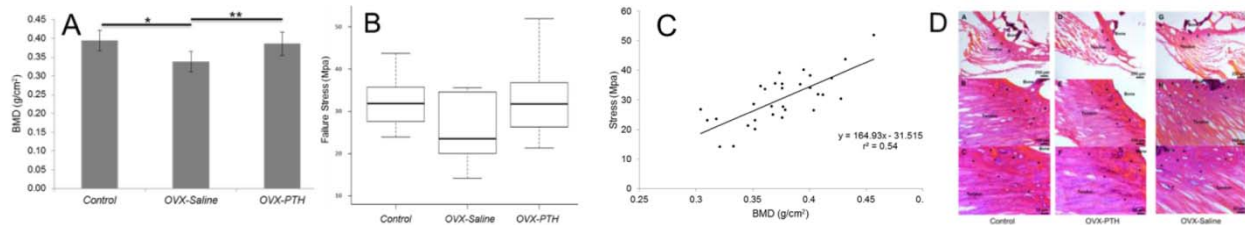


**Fig.1.** **A)** Bone mineral density in the OVX-PTH group was significantly higher than in the OVX-Saline group but similar to that of the Control group. **B)** Failure stress for all groups. Although not significant, a visual trend can be observed where the OVX-Saline group presents smaller failure loads when compared to the Control and OVX-PTH specimens. **C)** Failure stress vs. BMD. A positive linear correlation was observed between failure stress and bone mineral density measured at the humeral head ( $r^2 = 0.54$ ). **D)** The OVX-PTH group had a well-organized tendon-bone interface of ISP enthesis with abundant cells compared to the OVX-Saline group

## BIOMECHANICAL ROLE OF CAPSULAR CONTINUITY IN SUPERIOR CAPSULE RECONSTRUCTION FOR IRREPARABLE ROTATOR CUFF TEARS

Teruhisa Mihata<sup>\*,\*\*</sup>, Michelle H. McGarry<sup>\*</sup>, Timothy Kahn<sup>\*</sup>, Iliya Goldberg<sup>\*</sup>, Masashi Neo<sup>\*\*</sup>, Thay Q Lee<sup>\*</sup>

<sup>\*</sup>*Orthopaedic Biomechanics Laboratory, VA Long Beach Healthcare System and UC Irvine*

<sup>\*\*</sup>*Department of Orthopaedic Surgery, Osaka Medical College, Japan*

### INTRODUCTION:

Patients with irreparable rotator cuff tears have a defect of the superior capsule, which creates discontinuity of the shoulder capsule in the transverse direction. This effect is one of the reasons underlying the shoulder instability after rotator cuff tears. For irreparable rotator cuff tears, superior capsule reconstruction (SCR) has been reported to restore superior glenohumeral stability and function in the shoulder joint. In that surgery, the graft is attached medially to the superior glenoid and laterally to the greater tuberosity; this is followed by side-to-side suturing between the graft and infraspinatus–teres minor tendon and the graft and subscapularis tendon. The biomechanical role of medial attachment of the graft on the superior glenoid was confirmed by a previous study. In that study, superior glenohumeral translation after SCR in which the graft was attached medially to the superior glenoid was significantly less than that after a tendon patch graft in which the graft was attached medially to the torn rotator cuff tendon. However, the biomechanical role of capsular continuity in the transverse direction after arthroscopic SCR has not been investigated. Our objective here was to assess the effects of anterior and posterior continuity on shoulder biomechanics after SCR. We hypothesized that capsular continuity in the transverse direction improves glenohumeral stability after SCR.

### METHODS:

Eight fresh-frozen cadaveric shoulders were tested by using a custom shoulder-testing system. Subacromial peak contact pressure, glenohumeral superior translation, glenohumeral joint force, and glenohumeral range of motion (ROM) were compared among 5 conditions: (1) intact shoulder; (2) simulated irreparable supraspinatus tendon tear; (3) SCR without side-to-side suturing; (4) SCR with posterior side-to-side suturing; and (5) SCR with both anterior and posterior side-to-side suturing. Statistical comparisons were made by using Tukey's post hoc test.

### RESULTS:

Creation of an irreparable supraspinatus tear significantly increased superior translation ( $P < .05$ ) and subacromial peak contact pressure ( $P < .001$ ), decreased glenohumeral compression force ( $P < .001$ ), and increased total ROM ( $P < .01$ ). Superior capsule reconstruction without side-to-side suturing significantly decreased subacromial peak contact pressure ( $P < .001$ ) but did not inhibit superior translation. By adding posterior side-to-side sutures, both superior translation ( $P < .05$ ) and subacromial peak contact pressure decreased significantly ( $P < .001$ ). Neither SCR with nor without side-to-side suturing ameliorated the tear-associated decrease in glenohumeral compression force and increase in total ROM. Adding anterior side-to-side sutures did not change all measurements compared to SCR with posterior side-to-side suturing. In condition 3 (SCR without side-to-side suturing), four of eight shoulders had posterior–superior subluxation of the humeral head during internal rotation. By adding posterior side-to-side suturing (conditions 4 and 5), the humeral head rotated without subluxation in all shoulders.

### CONCLUSION:

SCR with side-to-side suturing completely restored the superior stability of the shoulder joint by establishing posterior continuity between the graft, residual infraspinatus tendon, and underlying residual shoulder capsule. Therefore, we recommend side-to-side suturing between the graft and infraspinatus tendon–underlying shoulder capsule for patients undergoing SCR for irreparable supraspinatus tendon tears to restore superior stability after surgery.

# OPTIMUM TENSION FOR THE BRIDGING SUTURES IN TRANS-OSSEOUS EQUIVALENT ROTATOR CUFF REPAIR

Joo Han Oh<sup>a</sup>, Ji Soon Park<sup>b</sup>, Michelle H. McGarry<sup>c</sup>, Sean T. Campbell<sup>c</sup>, Yeon Soo Lee<sup>d</sup>, Thay Q. Lee<sup>e</sup>

<sup>a</sup>Department of Orthopaedic surgery, Seoul National University College of Medicine,  
Seoul National University Bundang Hospital, Korea

<sup>b</sup>Department of Orthopaedic Surgery, Korea University Anam Hospital, Korea

<sup>c</sup>Orthopaedic Biomechanics Laboratory, Long Beach VA Healthcare System,  
Long Beach and University of California, Irvine, CA, USA

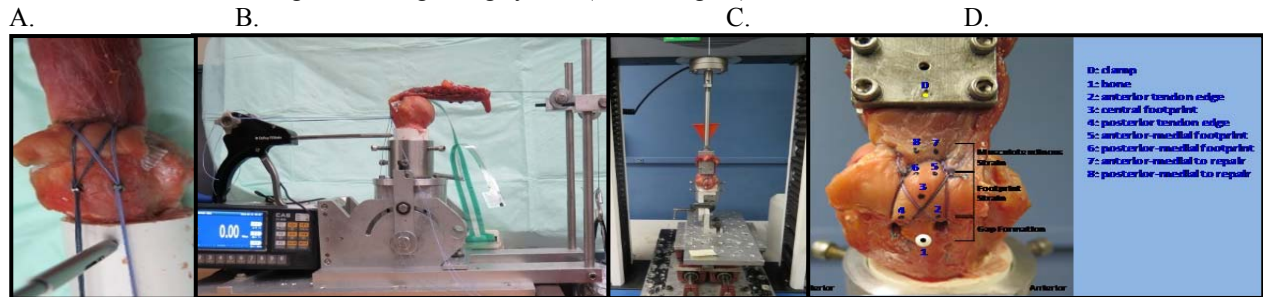
<sup>d</sup>Department of Biomedical Engineering, College of Medical Science,  
Catholic University of Daegu, Korea

## INTRODUCTION:

The trans-osseous equivalent (TOE) rotator cuff repair is known to increase contact area and mean contact pressure between repaired cuff tendon and bony footprint, and show higher ultimate load to failure and smaller gap formation compare to various rotator cuff repair techniques. However, some studies have reported medial rotator cuff failure after TOE repair and too much increased bridging suture tension can be a risk factor for this failure. Therefore, authors would like to determine the optimum bridging suture tension in TOE repair by evaluating supraspinatus footprint contact and construct failure characteristics at different bridging suture tensions.

## METHODS:

Eighteen fresh frozen cadaveric shoulders were prepared. All cadaveric shoulders were constructed with TOE configuration using same medial anchor placing a pressure sensing pad between repaired cuff tendon and footprint (Fig. A). Among them, nine cadaveric shoulders were used in footprint contact characteristics measurement. Using a Tekscan<sup>®</sup> measurement system (Tekscan Inc, South Boston, Massachusetts), the contact force, mean pressure, peak pressure and area between rotator cuff tendon and footprint were quantified for bridging suture tension of 60, 90, 120N under various shoulder positions (abduction 0°, 30° and rotation -30°, 0°, 30°) (Fig. B). After that, Tekscan<sup>®</sup> pad was removed and the eighteen shoulders were randomly divided into three groups. Final TOE construct were made with designated bridging suture tension and anchor type according to groups (60N, 120N of Versalok<sup>®</sup> and maximum tension of Reelx<sup>®</sup>). And then, all the eighteen TOE construct were tested at a cyclic loading and then a load-to-failure using an Instron<sup>®</sup> materials testing machine (Fig. C). Superficial deformation of the sutured tendon was monitored in situ using a video digitizing system (VDS<sup>®</sup>; Fig. D).



## RESULTS:

With increase of the bridging suture tension, contact force, mean and peak pressures increased significantly at all positions (all  $p < 0.05$ ). However, regarding contact area, even though there were significant differences between 60N and 90N, no significant differences between 90N and 120N at all positions. Regarding construct failure test, there were no significant differences in any parameters according to different tensions or anchor types (all  $p > 0.05$ ).

## DISCUSSION:

According to the current data, increasing bridging suture tension over 90N did not improve contact area, although it did increase contact force and pressure. Furthermore, the level of the bridging suture tension did not significantly affect the ultimate failure loads. Therefore, considering the risks for over-tensioning of bridging sutures, it might be clinically more beneficial to not setting the bridging suture tension over 90 N.

# NON-GENETIC FABRICATION OF A NOVEL TENDON-DERIVED STEM CELL (TDSC) SHEET FOR THE BIOLOGICAL REPAIR OF ROTATOR CUFF TEAR

Jian-kun XU, Yi-feng ZHANG, Jia-li WANG, Bruma Sai-chuen FU, Yuk-wa Lee, Kai-ming CHAN, Ling QIN  
*Department of Orthopaedics and Traumatology, Faculty of Medicine, The Chinese University of Hong Kong, Hong Kong*

**INTRODUCTION:** Rotator cuff (RC) tendons are often prone to lesions, as 30% to 50% of the population over fifty suffers of partial- and full-thickness RC tears. A torn rotator cuff is a disruption in the integrity of the tendon at the insertion into the humeral head. Most commonly, tears involve the supraspinatus tendon but can involve any combination or all four of the rotator cuff tendons. Damaged RC heals very slowly and rarely attains the structural integrity and mechanical strength of normal, undamaged RC. Several approaches have been developed to enhance the surgical repaired RC tear over the years, including stem cells therapy. However, it has been reported that addition of bone marrow mesenchymal stem cells (BMSCs) to the injured RC insertion site did not improve the structure, composition, or strength of the healing tendon attachment site despite evidence that they were present and metabolically active (1). Interestingly, the same authors found that BMSCs overexpressed with scleraxis significantly improve the healing of torn RC in rat (2). Tendon derived stem cells, which can be isolated from human, mouse and rat (3, 4), with highly expressed scleraxis, may be an alternative cell source for RC repair. For the first time, our team has fabricated a scaffold-free TDSC sheet by using connective tissue growth factor (CTGF) and vitamin C (5). In addition, the TDSC sheet shows promising healing promotion in tendon injury model (5), while it just improves the early graft healing in anterior cruciate ligament reconstruction model (6). The mentioned results indicated that the previous fabricated TDSC sheet is more favorable for tenogenesis. Thus, for better use of this cell-based strategy, differentiation factors would help in the biological repair of tendon-bone insertion, which consists of tendon, fibrocartilage, mineralized cartilage, and bone. Magnesium ions (Mg<sup>2+</sup>) have been shown of beneficial effects on both cartilage formation of synovial-derived stem cells (7) and osteogenesis of BMSCs (8). Based on these findings, for the first time, we hypothesized that Mg<sup>2+</sup> treated TDSC cell sheet would promote the healing of injured RC and tested our hypothesis accordingly.

**METHODS:** Green fluorescent protein (GFP) rat TDSCs were isolated by our established protocol (5,6). MgCl<sub>2</sub> was dissolved in neutralized culture medium. After confirming the optimal concentration of Mg<sup>2+</sup> using cell proliferation assay (MTT), the effects of Mg<sup>2+</sup> (of optimal dose) on the adhesion and differentiation of TDSCs were investigated by specific staining methods and real-time PCR. Western blotting was used to determine the ion channel, Mg transporter 1 (Magt1) and related signaling pathways. We also used the metafluor system to real-time monitoring the intracellular concentration of Mg<sup>2+</sup>. Rat RC repair model was adopted to test the efficacy of this novel cell sheet in vivo (1,2,9) with the animal ethics approval permitted from the committee of our institution. Harvested samples were used for further tests.

**RESULTS:** The proliferation of TDSC was not affected by addition of Mg<sup>2+</sup> with various concentrations of 1–10mM (n=6 per group). 10mM supplementation of Mg<sup>2+</sup> significantly promoted the adhesion of TDSCs at early time points via up-regulating the expression of phosphorylated focal adhesion kinase (FAK, Fig.1) at the site of tyrosine 397 (4 and 8 hours, n=6). FAK is also suggested to be an osteogenic factor (10), and it helps to explain our observation that Mg<sup>2+</sup> (10 mM) could significantly promote the chondrogenic and osteogenic differentiation of TDSCs (Fig. 1). QRT-PCR showed that the transcriptional expression of Scx, Tnmd, Col 1A1, Acan, and Alp were significantly up-regulated, whereas the expression of Fmod, Col 2A1, Bglap, PPARγ2 and C/EBPα were not affected, in complete medium together with 10 mM Mg<sup>2+</sup>, as compared with control group without supplementation of Mg<sup>2+</sup>. Furthermore, we also identified the mentioned effects were mainly mediated by Mg transporter 1 (Magt1) as the effects of Mg<sup>2+</sup> were almost completely abrogated when the TDSCs were pretreated with adenovirus-mediated Magt1-shRNA or Magt1 blocker, Nitrendipine (Fig. 1). TDSC cell sheet was obtained by addition of vitamin C regardless of Mg<sup>2+</sup> (Fig.2). Eight weeks post the transplantation of the Mg<sup>2+</sup> treated TDSC sheet, significantly more cartilage-like cells (red arrow, Fig. 2) were observed in the regenerated transition in the rat RC injury model as compared to the groups with or without TDSC cell sheet (not Mg<sup>2+</sup> treated) (n=5 per group, Fig. 2).

**DISCUSSION:** In this project, we report the dual effects of Mg on TDSCs, i.e. enhancement of both the chondrogenic and osteogenic differentiation. For the first time, we identified the key molecular mechanism, i.e. Magt1 mediated the activation of FAK signaling pathway, finally lead to the enhancement of chondro-osteogenic differentiation. Preliminary histological result shows that Mg<sup>2+</sup> treated TDSC sheet could improve the healing of injured RC at even late time point (8 weeks). Micro-indentation (micrometer-scale) and Raman microscope will be used to assess the microstructure of the healing site. Together with coming biomechanical tests and functional test using catwalk system (to analysis the alternations of gait), we will gain a better understanding on this novel treatment developed for RC repair before its further clinical application. Our current findings also raise a concern that biodegradable Mg-based sutures may not be appropriate for tendon repair as it may lead to ectopic ossification inside the substance of tendon tissue.

**ACKNOWLEDGEMENT:** This project was supported in part by the General Research Funding from RGC, Hong Kong (Ref. No.: 14112714) and the SMART (Sports Medicine And Regenerative Technology) Program under the Lui Che Woo Institute of Innovative Medicine (LCWIIM).

## REFERENCES:

- (1) Gulotta L.V., et al. *Am J Sports Med.* 2009, 37: 2126-2133;
- (2) Gulotta L.V., et al. *Am J Sports Med.* 2011, 39: 1282-1289;
- (3) Bi Y.M., et al. *Nat Med.* 2007, 13 (10): 1219-1227;
- (4) Tan Q., et al. *Stem Cells Dev.* 2013, 22 (23): 3128-3140;
- (5) Ni M., et al. *Biomaterials.* 2013, 34: 2024-2037;
- (6) Lui P.P., et al. *Am J Sports Med.* 2014, 42 (3): 681-689;
- (7) Shimaya M., et al. *Osteoarthritis Cartilage.* 2010, 18 (10): 1300-1309;
- (8) Yoshizawa S., et al. *Acta Biomater.* 2014, 10 (6): 2832-2842;
- (9) Edelman L., et al. *J Musculoskelet Neuronal Interact.* 2011, 11 (2): 150-162;
- (10) Eskildsen T., et al. *PNAS.* 2011, 108 (15): 6139-6144.

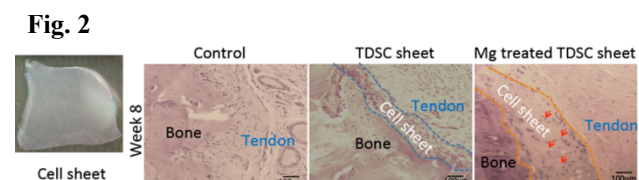
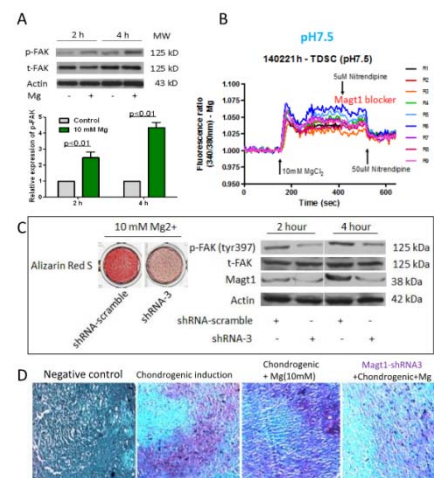


**Fig. 2**

**Fig. 1**



## ULTRASOUND-GUIDED DRY NEEDLING ON HEALTHY RAT SUPRASPINATUS TENDON

<sup>1</sup>C.N. Rigglin, <sup>2</sup>V. Khoury, <sup>1</sup>J.A. Gordon, <sup>2</sup>S.M. Schultz, <sup>1</sup>A.M. Pardes, <sup>2</sup>C.M. Sehgal, <sup>1</sup>L.J. Soslowsky  
<sup>1</sup>McKay Orthopaedic Laboratory and <sup>2</sup>Department of Radiology, University of Pennsylvania, Philadelphia, USA

**INTRODUCTION:** Tendinopathy is a common clinical problem and conservative treatments are often ineffective. Recently, ultrasound-guided dry needling, or repeatedly introducing a needle into the abnormal tissue [1, 2] has been attempted, to disrupt pathological tissues, induce bleeding, and release factors to stimulate healing. However, a controlled laboratory model to study this potential therapy, as well as basic evidence supporting this practice is lacking [3]. Therefore, the objective of this study was to perform ultrasound-guided dry needling in healthy rat supraspinatus tendons to evaluate the acute vascular, biological, and mechanical response in the tendons, to understand the initial effects of dry needling. We hypothesized that dry needling would cause an early increase in blood flow, inflammation, cellularity, and matrix formation, and a decrease in material properties.

**METHODS:** 32 Sprague-Dawley rats were used (IACUC approved). 22 underwent bilateral ultrasound-guided dry needling followed by sacrifice at days 1, 3 or 7 for histology (n=6) and mechanics (n=10). 10 healthy rats served as controls. Color Doppler ultrasound was performed 24 hours prior to needling, as well as 5 and 24 hours after needling (n=6). The rotator cuff was visualized using a 14MHz probe. A 27G needle was inserted posteriorly and guided between the humeral head and acromion to penetrate the supraspinatus tendon 10 times along its length. Color Doppler images were acquired and analyzed for regional and local blood flow (color weighted fractional area (CWFA)). A one-way ANOVA with repeated measures and Bonferroni test were performed (\*p<0.05). The right tendon was mechanically tested [4]. T-tests were performed (\*p<0.05). The left tendon was stained for Safranin-o (Saf-O), hematoxylin and eosin (H&E), interleukin-1 $\beta$  (IL-1 $\beta$ ), tumor necrosis factor  $\alpha$  (TNF $\alpha$ ), and type III collagen. Images were graded by three blinded investigators for cell shape (1-spindle to 3-round), cellularity (1-low to 3-high), Saf-O staining (1-low to 3-high), and DAB staining (1-low to 4-high). A Kruskal-Wallis test and a Dunn's post hoc test were performed (\*p<0.05).

**RESULTS:** The CWFA in local and regional areas were increased 5 hours-post dry needling (Fig 1A). There was an increase in cross sectional area and no change in max load (Fig 1B) or percent relaxation, but a decrease in maximum stress, insertion modulus (Fig 1C), midsubstance modulus, and stiffness. There was an increase in rounded cell shape (Fig 1D), IL-1 $\beta$  (Fig 1E), and type III collagen at day 1, an increase in cellularity at days 1 and 7, and an increase in glycosaminoglycans (GAG) content at days 3 and 7 (Fig. 1F).

**DISCUSSION:** Dry needling the rat supraspinatus tendon caused an acute injury response as hypothesized. Increases in blood flow in the shoulder region and in the needled tendon itself demonstrate systemic and local responses to this micro-damage. There was an early increase in cellularity with a more rounded cell shape. formation of granulation tissue. Additionally, the increase in inflammatory mediators is consistent with a previous study evaluating dry needling in injured rat tendons [5]. Mechanical properties confirm that micro-damage was induced in the tendon, causing an increase in the cross sectional area, a decrease in material properties, but no change in maximum load, supporting that this injury may not dispose the tendon to failure risk. This study demonstrated that the rat supraspinatus tendon can be dry needled consistently under ultrasound guidance, and that a controlled healing response can be elicited. Further studies will evaluate the effect of dry needling on tendonopathic tissue.

**ACKNOWLEDGEMENTS:** The authors thank B Kneeland, J Huegel, and P Bhatt. This study was funded by the NIH/NIAMS supported Penn Center for Musculoskeletal Disorders (P30 AR050950) and a NSF Graduate Research Fellowship.

**REFERENCES:** [1] Rha DW, et al, Clin Rehabil 2012. [2] Housner JA, et al. Clin J Sport Med 2010. [3] Chiavaras MM, et al, Semin Musculoskelet Radiol 2013. [4] Peltz CD, et al, J Orthop Res 2010. [5] Hammerman M, et al, J Appl Physiol 20

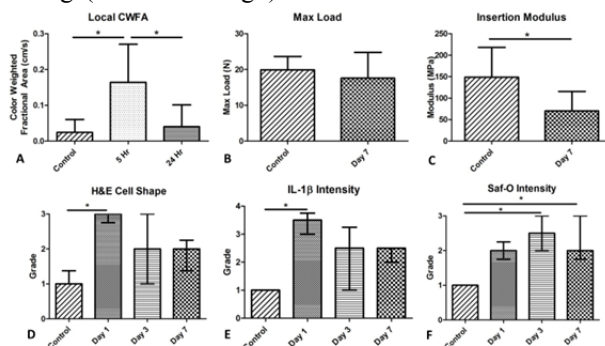


**Figure 1:** (A) Doppler imaging results demonstrate a local increase color weighted fractional area (CWFA) 5 hours after the dry needling procedure. (B, C) Mechanical evaluation of the supraspinatus tendon 7 days after needling demonstrated an increase in insertional modulus and no change in maximum load. (D-F) Histological evaluation demonstrates more rounded cell shape, increased inflammation, and increased GAG production after needling. Data presented as mean  $\pm$  standard deviation with \*p<0.05.

# STEPWISE DIFFERENTIATION OF HUMAN INDUCED PLURIPOTENT STEM CELLS FOR ACHILLES TENDON REGENERATION BY CHANGE OF PHYSICAL SUBSTRATE

Can Zhang, Huanhuan Liu, Xiao Chen, Hongwei Ouyang

*Center for Stem Cell and Tissue Engineering, School of Medicine, Zhejiang University, Hangzhou, China*

## **INTRODUCTION:**

Tendons connect muscles to bone and transmit the force generated during muscle contraction to the skeleton, which are highly prone to injury. Surgical repair is common but natural healing is extremely slow and inefficient. Human-induced pluripotent stem cells (hiPSCs) are highly promising cell source for realizing personalized treatments in regenerative medicine [Lian, Q.2010]. Nevertheless, the utility of these cells for tendon tissue engineering has yet not been adequately explored. This study developed a stepwise strategy to induce hiPSCs differentiation into tenocytes and assessed the efficacy of this tissue-engineered construct in promoting tendon regeneration

## **METHODS:**

Clonogenicity and multi-differentiation potential were revealed by colony-forming unit (CFU) and different mesodermal lineages differentiation assay respectively. Surface markers were detected by flow cytometry. Well-aligned chitosan-based ultrafine fibers were fabricated with stable jet electrospinning (SJES) technique. Gene expressions were analyzed by Q-PCR. A rat Achilles tendon defect model was created and implanted with AC (i.e., aligned fiber scaffold with hiPSC-MSCs) or RC (i.e., random fiber scaffold with hiPSC-MSCs) *in vivo*. The morphology of repaired tissues was analyzed by histological examination and transmission electron microscope. The amount of deposited collagen was quantified using a collagen quantitative assay kit. Mechanical testing was performed for mechanical properties

## **RESULTS AND DISCUSSION:**

hiPSCs were first induce to mesenchymal stem cells (hiPSC-MSCs) as confirmed by differentiation into three mesenchymal lineages. Flow cytometry and CFU assay showed the expression of characteristic MSC surface markers and clonogenicity. Subsequently, hiPSC-MSCs were differentiated into tenocytes by cultivation on the chitosan-based well-aligned ultrafine fiber scaffold. SEM micrographs and immunofluorescence assays showed that hiPSC-MSCs exhibited tenocyte-like morphology and significantly high expression of tendon-specific genes in the hiPSC-MSCs on well-aligned fiber scaffold. ALP and alizarin red staining showed that the random fiber scaffold induced osteogenesis, while the aligned fiber scaffold hindered the process. In addition, aligned cells expressed significantly higher levels of integrin  $\alpha 1$ ,  $\alpha 2$ ,  $\alpha 5$  and  $\beta 1$  subunits, myosin IIB, TGF $\beta 3$  and SDF-1. In rat Achilles tendon repair model, AC-treated tendon had superior structural and mechanical properties than RC-treated tendon. Cell labeling and extracellular matrix expression assays demonstrated that the transplanted hiPSC-MSCs contributed directly to tendon regeneration. Moreover, no teratoma was found in any samples. These findings present a strategy combining well-aligned fiber scaffold with iPSC-MSCs for tendon regeneration and may assist in clinical regenerative medicine to treat tendon diseases.

## **REFERENCES:**

Lian, Q. *et al*, Circulation, 121:1113–1123, 2010.

# MULTIPLE OMICS ANALYSIS REVEALS AGE-RELATED CHANGES IN TENDON DIFFERENTIATION FROM MESENCHYMAL STEM CELLS

<sup>1</sup>Peffers, M.J., <sup>2</sup>Collins, J.A., <sup>1</sup>Fang, X., <sup>3</sup>Rushton, M. D., <sup>1</sup>Clegg, P.D.

<sup>1</sup>*Musculoskeletal Biology, Institute of Ageing and Chronic Disease, University of Liverpool, Leahurst, Neston, Wirral, UK.* <sup>2</sup>*Thurston Arthritis Research Centre, School Of Medicine, University of North Carolina at Chapel Hill, North Carolina, USA,* <sup>3</sup>*Musculoskeletal Research Group, Institute of Cellular Medicine, Newcastle University, UK.*

## INTRODUCTION:

Mesenchymal stem cells (MSCs) have prospective applications in regenerative medicine and tissue engineering, demonstrating promising results, particularly in tendon repair and regeneration. The principles of tissue engineering involve a complex interplay of factors and there is some question as to what extent these cells are subject to ageing. Consequently, any loss in functionality with age would have profound consequences for the maintenance of tissue viability and tissue quality. However no studies have been undertaken on age-related effects on differentiation potential into tendon. This study aims to use an integrated omics approach to evaluate the transcriptome, proteome, and methylome of tendon constructs synthesized from young and old MSCs.

## METHODS:

Human MSCs at passage 4 from young; n=5 (22.2years  $\pm$ 2.3SD) and old; n=6 (64.8years $\pm$ 6.6SD) donors were used to make tenogenic 3-D constructs. Transcriptome analysis using RNA-Seq was undertaken using the Illumina HiSeq 2000 platform. Epigenetic changes were determined firstly by identifying alterations in DNA methylation using the Illumina Infinium HumanMethylation450 BeadChip array and also using small RNASeq on the Illumina HiSeq 2500. Mass spectrometric analysis was undertaken following trypsin digestion using LC-MS/MS with a NanoAcquity LC coupled to a linear ion-trap Orbitrap. Progenesis-QI<sup>TM</sup> was used for label-free relative quantification. The following filters were applied to define differential expression (DE); for transcriptomics a false discovery value-adjusted P-value (FDR) <0.01 and log<sub>2</sub>fold change >2; small RNASeq FDR<0.05 and log<sub>2</sub>fold change >1.4; differential methylation (DM) was defined as FDR<0.01 and a mean methylation difference  $\geq$ 0.15; and proteomic analysis FDR< 0.05 and  $\pm$  2 fold regulation. Bioinformatics was undertaken using Ingenuity Pathway Analysis (IPA), PANTHER, the Database for Annotation, Visualisation, and Integrated Discovery (DAVID) and RAMONA.

## RESULTS:

We identified significant DM and DE of mRNA, microRNAs and proteins due to ageing. Following independent (DAVID, PANTHER, IPA) and simultaneous gene set analysis of combined RNASeq and proteomics datasets using RAMONA we identified alterations in pathways involving actin cytoskeleton, and energy metabolism. Relating to epigenetic changes we found a number developmental transcription factors in which age-related DM impacted on gene expression. In addition microRNAs relating to age-related senescence and DNA methylation were identified. At a number of levels there is evidence for changes in transforming growth factor  $\beta$  signalling in ageing, resulting in changes in extracellular matrix composition at the protein level.

## DISCUSSION:

There is an age-related dysregulation at the transcriptional, post-translational and protein level. We have identified potential age-related mechanisms that could be used to produce improved engineered tendon for therapeutic use and therapeutically target tendon repair in age-related tendon disease.

## ACKNOWLEDGEMENTS:

This study was funded by MRC and Arthritis Research UK as part of the MRC – Arthritis Research UK Centre for Integrated research into Musculoskeletal Ageing (CIMA) and the Wellcome Trust.

# AN IRRADIATION-AND-INJECTION APPROACH TO STUDY TSC DIFFERENTIATION IN MICE

J. Zhang and JH-C. Wang

*MechanoBiology Laboratory, Department of Orthopaedic Surgery, University of Pittsburgh, Pittsburgh, PA.*

## INTRODUCTION:

Tendinopathy is a prevalent tendon disorder affecting millions of Americans. Our previous *in vitro* study showed that tendinopathy is caused by the aberrant differentiation of tendon stem cells (TSCs) into non-tenocytes when subjected to mechanical over-loading [1]. However, tenocytes did not differentiate into non-tenocytes *in vitro* [2]. To understand how tendon cells behave *in vivo*, we used a novel irradiation-and-injection approach to eliminate or reduce resident tendon cells by irradiation thus enabling tracking of GFP-TSCs in the injected region.

## METHODS:

**Isolation of GFP-TSCs** – We isolated TSCs from green fluorescent protein (GFP)-expressing C57BL/6 transgenic mice (GFP-mice) [C57BL/6-TgN (ACTbEGFP)10sb mice, Jackson Labs].

**Injecting GFP-TSCs** – We injected GFP-TSCs (P1,  $1 \times 10^4/\mu\text{l}$ ) into the patellar tendons of 4 C57BL/6J mice using a 30G syringe. After 5 days, mice were killed to harvest the tendons. Then, GFP-TSCs in tendon sections were observed microscopically and by immunostaining with rabbit anti-GFP primary antibody (Cell Signaling), followed by Cy3-conjugated goat anti-rabbit IgG as secondary antibody (Millipore).

**Irradiation and injection approach** – To determine the fate of injected GFP-TSCs *in vivo*, we first eliminated native tendon cells by irradiating 12 C57BL/6J mice with 6 Gy using the Gamma cell 40 (cerium). Cell killing by irradiation was confirmed by the live/dead cell viability assay (Life Technologies). GFP-TSCs were then injected into irradiated mouse patellar tendons. One week later, cell viability in the injected area was determined using semi-quantification methods.

## RESULTS:

First, we successfully injected GFP-TSCs into mice patellar tendons. Abundant GFP-cells were observed by immunohistochemical analyses beneath the paratenon 5 days later. Many cells had also migrated to the central tendon region (**Fig. 1A, B**). These injection experiments demonstrate the feasibility of injecting GFP-TSCs into mice tendons. Second, we established that irradiation of mouse patellar tendons with 6 Gy killed > 99% of resident tendon cells (**Fig. 2A, B**). One week later, > 60% of the cells were live TSCs and the remaining were dead cells (**Fig. 2C**); however, in the un-injected irradiated tendons nearly all cells were dead.

## DISCUSSION:

We have shown the feasibility of cell tracking using the irradiation and injection approach in a mouse tendon model. Irradiation eliminated almost all cells in the tendon region, facilitating cell tracking within the tendon niche. This approach will be effective to determine the role of TSCs in tendon homeostasis and tendon pathology, and is simple enough to be routinely used in laboratories to perform basic science research.

## ACKNOWLEDGEMENTS:

This work was supported in part by the NIH awards AR061395 and AR060920.

## REFERENCES:

1. Zhang, J. and J.H. Wang, *J Orthop Res*, 2010. **28**(5): p. 639-43.
2. Zhang, J. and J.H. Wang, *PLoS ONE*, 2013. **8**(8): p. e71740.

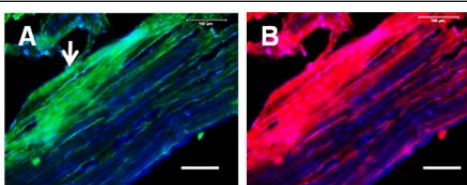


**Fig. 1 Injection of GFP-TSCs into mouse patellar tendons.** Robust GFP-TSCs were observed at the injection site (arrow) (A, green). Confirmation of GFP-TSCs by immunostaining GFP with Cy3-GFP-antibody (B, red). Tissue beneath the label A is a sectioning artifact. Bars: 100  $\mu\text{m}$ .

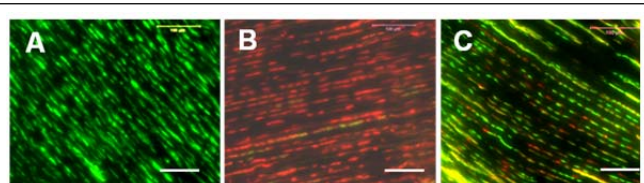


**Fig. 2 Irradiation-and-injection.** A. Intact mouse patellar tendons had ~100% live cells (green). B. Irradiation killed > 99% of cells (red). C. One week later, abundant GFP-TSCs (green) were observed in the tendon. Scale bars: 100  $\mu\text{m}$ .

## AUTOLOGOUS TENOCYTE INJECTION (ATI) FOR GLUTEAL TENDINOPATHY: A PILOT STUDY

Janes G, Bucher T, Ebert J, Bredahl W, Zheng MH

*Centre for Translational Orthopaedic Research, The University of Western Australia, Perth, Australia.*

### **INTRODUCTION:**

Gluteal tendinopathy is a common cause of lateral hip pain. No treatments have effectively improved the poor health outcomes and disability of the condition. Autologous tenocyte injection (ATI) is a novel cell therapy that has shown promise in other tendinopathic conditions. Therefore, this prospective pilot study investigated the effect of ATI in 12 patients with clinical and radiological evidence of gluteal tendinopathy.

### **METHOD:**

A patellar tendon needle biopsy was performed under local anaesthetic and tendon cells were expanded by in vitro culture in a GMP-certified, TGA-licensed facility. Autologous tenocytes were injected into the gluteal tendinopathy under ultrasound guidance on a single occasion. All patients were functionally assessed preoperatively and at 3, 6, 12 and 24 months postoperatively with the Oxford Hip Score (OHS), the Merle d'Aubigne Postel Score (MDP), the 36-item Short-Form Health Survey (SF36) and the Visual Analogue Pain Scale (VAS). A patient satisfaction survey was also given 12 months postoperatively. Magnetic Resonance Imaging (MRI) scans were performed preoperatively and 6 months postoperatively for structural assessment of the gluteus medius tendon.

### **RESULTS:**

Twelve patients, all female, with a mean age of 53 (range 40-65) years and average duration of symptoms of 33 months (range 6-144) were included in the study. All patients had clinical symptoms and signs of gluteal tendinopathy, with diagnosis confirmed by MRI in all patients. No patella biopsy site complications or treatment site infections were noted. Significant ( $p < 0.05$ ) functional improvement to 24 months postoperative was observed across all mean score outcomes: VAS (pre 7.25, post 2.73), OHS (pre 24.00, post 39.45), MDP (pre 11.67, post 16.55) and SF-36 PCS (pre 28.08, post 41.59). One patient did not respond and elected surgery. Patient satisfaction survey results demonstrated that 64% of patients were 'satisfied' or 'highly satisfied' with their ATI outcome. Follow-up MRI scans did not demonstrate notable changes in the radiological appearance of the tendinopathic tissue in most cases.

### **DISCUSSION:**

ATI by single injection significantly improved clinical outcome in this pilot study of gluteal tendinopathy at 24 months follow-up. However, the safety and efficacy of ATI requires substantiation given the small pilot sample size. We believe this study has shown encouraging early outcomes that warrant larger randomised controlled study of ATI for gluteal tendinopathy.

## POSTER PRESENTATIONS

# A NEW APPROACH TO ENHANCE TENDON-BONE JUNCTION HEALING BY REGENERATING FIBROCARILAGE ZONE

J. Zhang and JH-C. Wang

*MechanoBiology Laboratory, Department of Orthopaedic Surgery, University of Pittsburgh, Pittsburgh, PA.*

## INTRODUCTION:

The normal tendon-bone junction (TBJ) is a unique structure protected by the fibrocartilage transition zone. After an injury, the TBJ often heals without regeneration of the transition zone. In this study, we aimed to regenerate the fibrocartilage zone by using KGN composite consisting of KGN, engineered tendon matrix (ETM) and platelet-rich plasma (PRP).

## METHODS:

Materials – KGN solution was prepared in PBS at the concentration of 100  $\mu$ M. ETM was prepared from rabbit patellar tendon and PRP was isolated from fresh whole rabbit blood.

In vivo study - Using a biopsy punch, we made a 1 mm diameter wound on the Achilles tendon-bone junction (ATBJ) areas in the hind legs of 6 rats and immediately injected the following: 10  $\mu$ l saline in the control group, 50  $\mu$ l ETM+50  $\mu$ l PRP, in the second group and 50  $\mu$ l ETM+50  $\mu$ l PRP+10  $\mu$ l KGN (100  $\mu$ M) in the third group. The rats were sacrificed 3 months after the last treatment to collect ATBJ and further analyses.

## RESULTS:

Gross inspection of the saline injected ATBJ 3 months post-treatment looked yellowish with incomplete healing (Fig. 1A). But, ETM+PRP (Fig. 1B) and ETM+PRP+KGN (Fig. 1C) treated wounds healed more completely with more cartilage-like tissues in the wounded ATBJ. The best healing results were found in the ETM+PRP+KGN group (Fig. 1C). In histological analysis, almost 90% of the tissue sections in the ETM+PRP+KGN group positively stained for Safranin O (Fig. 1F), compared to a lack of Safranin O staining in the saline injected sections (Fig. 1D). The KGN-induced cartilage formation was further confirmed by H&E staining (Fig. 1G, H, I). qRT-PCR also showed higher expression of three chondrocyte-related genes, Sox-9, collagen II and aggrecan (Fig. 2A), and the tenocyte-related gene, tenomodulin, in the ETM+PRP+KGN group (Fig. 2B).

## DISCUSSION:

We have shown that KGN composite treatment induces fibrocartilage transition zone formation in rat ATBJ. ETM+PRP in the composite could have confined KGN to the wound area, thereby enhancing the formation of the fibrocartilage transition zone. While ETM+PRP promoted marginal fibrocartilage formation, it was less effective than with KGN. The results suggest that KGN, when implanted with ETM+PRP gels, enhances healing of wounded tendon-bone junction likely because of the following advantages: a) PRP supplies growth factors; b) ETM provides tenogenic matrix to facilitate such healing by forming tendon-like tissue formation; and c) KGN promotes cartilage formation in the interface between tendon and bone. This cell-free tissue engineering approach can readily translate to clinical settings to treat tendon-bone junction injuries more effectively.

**ACKNOWLEDGEMENTS:** - This work was supported by NIH AR061395 and AR060920 (JHW).

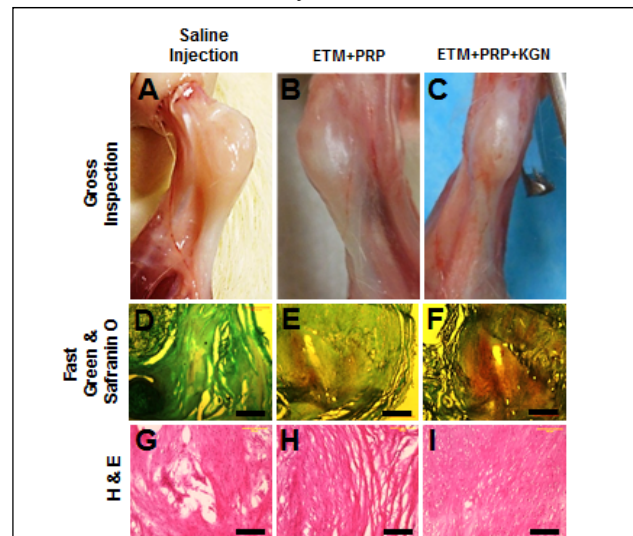


**Fig. 1** KGN composite treatment effects on the wound site at the Achilles tendon-bone junction (ATBJ). Fast green & Safranin O - Bar: 500  $\mu$ m; H&E - Bar: 100  $\mu$ m.

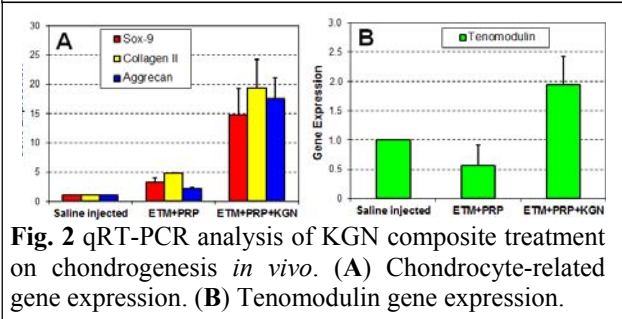


**Fig. 2** qRT-PCR analysis of KGN composite treatment on chondrogenesis *in vivo*. (A) Chondrocyte-related gene expression. (B) Tenomodulin gene expression.

## INVESTIGATING A MOUSE MODEL OF COLLAGENASE-INDUCED TENDINOPATHY

+Lalley AL<sup>1</sup>, Gooch C<sup>1</sup>, Shearn JT<sup>1</sup>

<sup>1</sup>University of Cincinnati, College of Engineering and Applied Science, Biomedical Engineering Program, Cincinnati, Ohio

**INTRODUCTION:** Injuries to the musculoskeletal system, particularly to tendon and ligaments, greatly affect the US population, with 110 million patients reporting an injury in 2008<sup>1</sup>. Overuse injuries constitute a large majority with 50% of all job-related complaints resulting from an overuse or repetitive motion injury<sup>2</sup>. The prevalence of these injuries coupled with lack of effective clinical intervention necessitates further investigation to develop an adequate animal model of tendinopathy and then identify novel therapeutic strategies to treat the condition. Current animal models of tendinopathy are classified as either mechanically-induced or chemically-induced with studies conducted in various species including rat, rabbit, and equine, although each approach and model has limitations<sup>3</sup>. In many studies, the chronic pathology often resolves once the insult is removed, with a return to normal tendon architecture and cellular morphology. These approaches are often classified as a failure, as the insult did not maintain the chronic phenotype in the long-term; however, our group has been interested in understanding the pathways that are activated to restore the tendon to its native structure. Perhaps characterizing the healing process following a collagenase-induced injury could provide insight towards improving tendon healing. We have been developing a mouse model of collagenase-induced tendon damage to investigate this phenomenon.

**METHODS:** All animal protocols were approved by UC IACUC. Experimental Design Gross observations and biomechanical outcomes were measured in 20 week-old male C57BL/6 mouse patellar tendons (PTs) following collagenase (Clostridium histolyticum, Sigma-Aldrich, C6885) injection. A broad range of collagenase concentrations were tested including 2500IU (n=4), 5000IU (n=4), 10000IU (n=3), 15000 (n=3), 20000IU (n=3), 30000IU (n=3), 40000IU (n=3), and 50000IU (n=3) and biomechanically assessed at 24hr post injection. Saline-injected patellar tendons (n=4) served as the control along with normal, uninjured patellar tendons (n=4). Surgical Procedure. A skin incision was made to access the PT. A 0.4  $\mu$ L collagenase injection was administered at the distal end of the patellar tendon just proximal to the tibial insertion. Incisions were closed using 5-0 prolene suture and animals were allowed unrestricted cage activity until the time of sacrifice. Biomechanics. The central-third PT was isolated and the patella-PT-tibia unit was loaded into custom-designed grips in a 37°C PBS bath, preconditioned for 25 cycles from 0-0.02N, and then failed in tension at 0.1%/second. Statistics. Tendon mechanical values for ultimate load (saline, 2500IU, 5000IU, 10000IU, 15000IU, 20000IU) were compared to normal, uninjured values using a two-way Student's t test.

**RESULTS:** Gross Observations. Overall, collagenase-injected tendons appeared hypervascular with increasing vascularity associated with increasing collagenase concentrations. Further, several collagenase injected tendons were ruptured at the site of injection, characterized by abnormal collagen color, proximal translocation of the patella, and visible collagen fraying. Of the tendons observed, 0% of the saline, 2500IU, 5000IU, and 15000IU, 33% of the 10000IU and 20000IU, and 66% of the 30000IU, 40000IU, and 50000IU (not included in statistical analysis) were ruptured. Biomechanics. For ultimate load, saline injected tendons were no different than normal tendons (p=0.65). The low collagenase concentrations (2500IU and 5000IU) also produced no differences with respect to normal ultimate load (p=0.06 and p=0.22). The 10000IU and 20000IU injections also were not statistically different from normal (p=0.08 and p=0.20), although this is based on a low sample number. The 15000IU injection resulted in a 33% reduction in ultimate load, significantly less than normal, uninjured values (p=0.004).

**DISCUSSION:** This study seeks to first identify a suitable collagenase concentration that produces decreased mechanical properties in the short-term while minimizing the number of tendon ruptures so we can investigate the biological pathways that are activated during the repair of this chemically induced injury. Based on the preliminary work reported in this abstract, 15000IU and 20000IU concentrations will be further evaluated. Further, histological evaluation of the repair tissue will be completed to evaluate overall tissue morphology and cellular phenotype. We hypothesize that the initial decrease in mechanical properties at 24 hours post injection will resolve, gradually producing near normal mechanical levels by 2 and 5 weeks. Investigating the mechanisms restoring tissue to normal structure and function has the potential to greatly impact current therapeutic approaches.

**ACKNOWLEDGEMENTS:** NIH R01 AR056943.

**REFERENCES:** 1. US Bone and Joint Decade, AAOS, 2008. 2. United States Bureau of Labor Statistics. Occupational injuries and illnesses, 1995. 3. Lake, Disability and Rehabilitation, 2008.

# HISTOLOGICAL EVALUATION OF THE EQUINE SUPERFICIAL DIGITAL FLEXOR TENDON (SDFT) DURING AGEING

Othman Ali, Eithne Comerford, Elizabeth Canty-Laird and Peter Clegg

*Department of Musculoskeletal Biology, Institute of Ageing and Chronic Disease, University of Liverpool, Leahurst Campus, Neston, Cheshire. CH64 7TE, UK.*

## **INTRODUCTION:**

Normal tendon architecture comprises dense regularly organised longitudinal collagen fibers which are arranged approximately parallel to each other in bundles and having a corrugated (crimped) pattern along the longitudinal fiber axis. Bundles of collagen fibers are called fascicles which are variable in size and shape. Primary, secondary and tertiary fascicles are outlined by the interfascicular tissue (endotenon) which is composed of an irregular loose fibrous connective tissue network containing various structures such as vessels, nerve fibres, cells and both collagenous and non-collagenous extracellular matrix. Intrafascicular tenocytes are distributed regularly between the collagen fibres while their morphology varies between round, elliptical or cigarette shaped to a longitudinal fusiform shape. We aimed to document how the tendons histological structures varied regionally and during ageing.

## **MATERIAL AND METHODS:**

SDFT were taken from horse forelimbs, aged from foetal to 20 years old (n=21), euthanized for non-orthopaedic reasons. Tendon sections of approximately 10 mm length from the proximal, mid and distal metacarpal regions were selected and fixed in 4% paraformaldehyde solution, pH 7.4, at room temperature. The tendon was split sagittally into two equal parts in order to face the central axis of the tendon toward the microtome's knife. Samples were paraffin embedded, sectioned to 5µm thickness and stained with H&E, Toluidine blue and PAS/Alcian blue. A novel scoring method was devised using ImageJ to describe the cellular morphology and extracellular matrix of each tendon and how these altered with anatomical site and ageing.

## **RESULTS**

Histological measurements indicated that percentage of fascicular inclination (degree of fascicular angulation from the longitudinal tendon axis) was approximately (42-61%) in the mid-metacarpal region and (57-91%) in the other two regions but was unaffected by age. A marked difference in interfascicular thickness across regions between tertiary fascicles and secondary fascicles was noted with means of 15.13µm and 4.3µm with a standard deviation of 3.14 and 0.79 respectively and these dimensions were not altered by ageing. Cellular morphology including the lengths of nuclei increased during ageing whilst cell density was decreased. Tendon vascularity did not demonstrate age-related changes. Many inclusion bodies were present in aged horses (17, 18 and 20 years) localised inside the fascicles but without any notable inflammatory reactions. These inclusion bodies were characterized by clusters of large rounded cells which stained positively for mucin and proteoglycans with Toluidine blue and Alcian-blue PAS stains.

## **CONCLUSION**

Histological parameters including interfascicular tissue and nucleus morphology were found to be altered regionally and with ageing respectively in the equine SDFT. In particular we demonstrated that in aged animal chondroid like cells were present which may be indicative of chondroid metaplasia in tendon.

# A HYPERELASTIC FIBRE-REINFORCED CONTINUUM MODEL OF HEALING TENDON WITH DISTRIBUTED COLLAGEN FIBRE ORIENTATIONS

M.N. Bajuri<sup>1</sup>, H. Isaksson<sup>2</sup>, M.S. Thompson<sup>1</sup>

<sup>1</sup>, *Department of Engineering Science, University of Oxford, United Kingdom,* <sup>2</sup>, *Department of Biomedical Engineering, Lund University, Sweden*

## INTRODUCTION:

Mechanical loading has a significant impact on the efficiency of healing tendons. However, the mechanisms for this remain unclear, and until now no constitutive model has been able to represent tendon-mechanics during its healing process. The aim of this study was to test the ability of the hyperelastic fibre-reinforced material model introduced by Gasser-Ogden-Holzapfel (GOH) to simulate tendon tissue during specific time points of healing. This study also aimed to determine which of its three constitutive parameters is the most sensitive in characterising healing process of tendons. This was achieved through a parameter sensitivity study of the model fitted to tendon healing mechanical data.

## METHODS:

The one-dimensional analytical GOH model was fitted with tensile test data on rat Achilles tendon healing at four different time points after transection (5 samples each) [1]. The optimisation was performed using the *lsqnonlin* MATLAB routine [2]. The ability of the GOH model in fitting the data was tested without fixing any of its parameters. Samples with the coefficient of determination ( $r^2$ ) for the model fit greater than 0.98 were considered good. The sensitivity of each parameter was then tested by fixing it during the data fitting process. If it caused poor fitting, that parameter is counted sensitive [3].

## RESULTS:

The GOH model was able to fit the experimental data in all samples with  $r^2 > 0.98$ , ranging from 0.9889 to 0.9940 (Fig. 1). Preliminary results from the sensitivity analyses showed that the  $k_1$ , the fibre stiffness, is the most sensitive parameter as by fixing it during the fitting process had caused 8 out of 20 samples to have poor fitting ( $r^2 < 0.9800$ ).

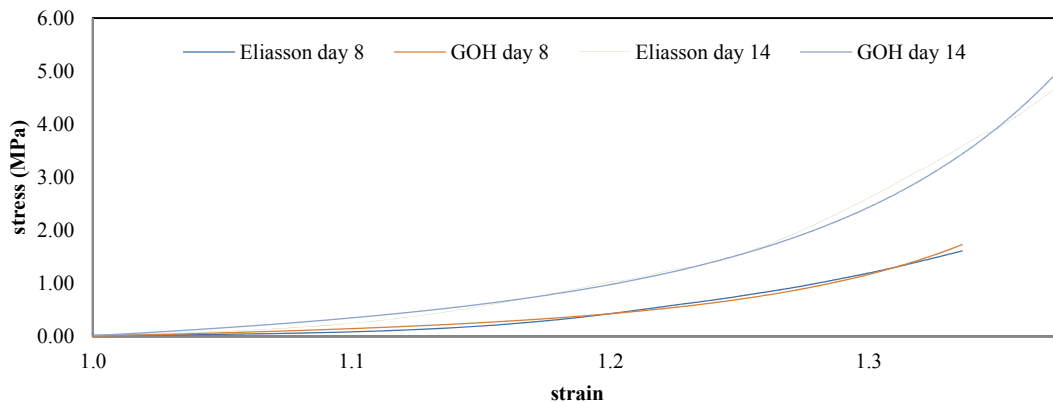


Figure 2: Curve fitting of the GOH model against experimental data at day 8 and 14 of healing

## DISCUSSION:

The GOH model has been used to simulate anisotropic hyperelastic behaviour of various soft tissues including arterial wall, skin and cartilage. The good fits obtained here suggest the capability of the GOH model in simulating tendon tissue at various time points of healing. The preliminary results from the sensitivity study highlight important parameters in the model. Future work will include parametric analyses using the fractional factorial and Box-Behnken designs.

## REFERENCES:

- [1] P. Eliasson, *et al.*, "Rat Achilles tendon healing: mechanical loading and gene expression," *J Appl Physiol*, vol. 107, pp. 399-407, Aug 2009.
- [2] A. Ni Annaidh, *et al.*, "Automated estimation of collagen fibre dispersion in the dermis and its contribution to the anisotropic behaviour of skin," *Annals of Biomedical Engineering*, vol. 40, pp. 1666-1678, 2012/08/01 2012.
- [3] S. J. Welham, *et al.*, *Statistical Methods in Biology: Design and Analysis of Experiments and Regression*: Chapman and Hall/CRC, 2014.

## DIRECT FUNCTIONAL MOBILIZATION AFTER ACHILLES TENDON RUPTURE PROMOTES EARLY HEALING RESPONSE

K.P.Valkering<sup>1</sup>MD, F.Ranucci<sup>1</sup>MD, P.Anundsson<sup>1</sup> BMedSc, S.Aufwärber<sup>1</sup> BSc, E.Domeij-Arverud<sup>1</sup> MD, G.Edman<sup>2</sup> PhD, G.Nilsson<sup>1</sup> MD, PhD, P.W. Ackermann<sup>1</sup> MD, PhD

*1 Integrative Orthopedic Laboratory, Department of Molecular Medicine and Surgery, Karolinska Institutet, 171 76 Stockholm, Sweden;*

*2 Center of Molecular Medicine (CMM), Department of Molecular Medicine and Surgery, Karolinska Institutet, 171 76 Stockholm, Sweden*

### **INTRODUCTION:**

Early mobilization after Achilles tendon rupture (ATR) repair has clinically been reported to improve ATR healing, however, the molecular mechanisms have been unclear. ATR healing entails complex reparative signaling interactions between blood-, nerve- and tissue-derived cells, which all depend on basic metabolites, essential for energy demand and cell proliferation. Therefore, we hypothesized that local metabolites in ATR healing are up regulated by direct post-operative functional mobilization.

### **METHODS:**

A prospective, single-center, randomized controlled trial was conducted comparing direct post-operative functional mobilization (VACOped, OPED GmbH) (n=27), which allows weight bearing and adjustable ankle ROM, with plaster cast immobilization (n=29). Microdialysis was performed 2 weeks post surgery on the sutured ATR and the intact contralateral tendon. Furthermore, 10 healthy individuals were added as an external control group.

### **RESULTS:**

The healing ATR of both groups exhibited at two weeks post-operatively significantly increased levels of glutamate ~200%, lactate ~100%, and pyruvate ~70% as compared to both the contralateral intact tendons and to the healthy tendons, respectively. The levels of glucose, glycerol and the lactate/pyruvate ratio were unaltered during healing.

Direct functional mobilization (mobilized group) as compared to conventional plaster cast (immobilized group) resulted in significantly higher concentrations of glutamate (93.5±35.9 vs. 73.8±34.9 μM, P =0.045). The other metabolite concentrations did not display any significant changes. Metabolite concentrations in the intact contralateral tendons of both study groups, and tendons of the healthy controls were not significantly different.

### **DISCUSSION:**

Early functional mobilization after ATR repair enhances the local levels of the essential metabolite glutamate, which suggests a glutamate-mediated promotion of the early healing response. The up-regulated glutamate levels may reflect a metabotropic coordination of cell proliferation involving angiogenesis and nerve ingrowth.

# A NOVEL MAGNESIUM BASED SUTURE ANCHOR FOR SOFT TISSUE FIXATION

Jonquil R. Flowers, Kwang E. Kim, Antonio Pastrone, Dhir Patwa, Savio L-Y. Woo

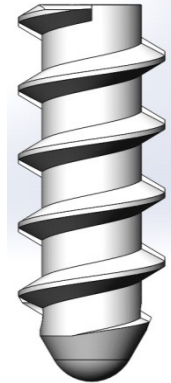
Musculoskeletal Research Center, Department of Bioengineering, University of Pittsburgh, Pittsburgh, PA, USA

## INTRODUCTION:

Metallic and bioreabsorbable polymeric suture anchors have been used successfully for repair of rotator cuff tears in the shoulder and femoroacetabular impingement (FAI) in the hip. However, there are advantages and disadvantages of each of these biomaterials<sup>1</sup>. Titanium anchors could migrate and loosen as well as interfere with magnetic resonance imaging. They also present difficulties during revision surgery. Complications with polyglycolic and polylactic acid suture anchors include osteolysis and breakage during insertion<sup>2</sup>. Thus, efforts aim to develop a metallic suture anchor using Mg-based alloys, which have the potential to be the “best of both worlds” because it is biodegradable, has the desirable mechanical properties and could promote bone remodeling<sup>3</sup>. Thus, the objective of this research was to design a novel Mg-based suture anchor that could have secure soft tissue fixation as well as prevent its breakage at the eyelet and premature pullout.

## METHODS:

Using a computer aided design software, SolidWorks, a 3D computer model of a commercially available suture anchor (6.5 mm x 16.5 mm) was generated. The geometry was then imported into ANSYS finite element software. Using mechanical properties for Mg alloy ( $E = 9.60 \times 10^4$  MPa,  $\nu = 0.36$ ), a parametric analysis includes thread pitch of 2.0 mm, 2.5 mm, 3.0 mm and thread depth of 0.4 mm, 0.7 mm, and 1.0 mm was conducted. Specifically, a simulation of suture anchor pullout was conducted for each combination of design parameters. The maximum von Mises stress and stress concentrations from each combination of design parameters were recorded. The design combination with the lowest von Mises stress was selected as the optimal design and manufactured. Then, the fixation strength of the Mg-based suture anchor was tested after insertion into polyurethane foam, which is often used as a substitute for human bone in mechanical testing of orthopaedic implants to ensure consistency between tests. The suture anchor underwent pullout by uniaxial tension and the ultimate load and ultimate elongation were recorded. For control, a polymeric suture anchor, was tested in an identical fashion and was used as a comparison with the Mg-based suture anchor.



The 3D model of the Mg-based suture anchor

## RESULTS:

The parametric analysis determined that the thread pitch and thread depth have a significant effect on suture anchor fixation strength. Thus, the thread pitch of 3.0 mm and thread depth of 1.0 mm were found to be optimal. Also, the maximum von Mises stress in the finite element model for this design combination was 159 MPa, which is well below the yield strength of the Mg alloy (193 MPa).

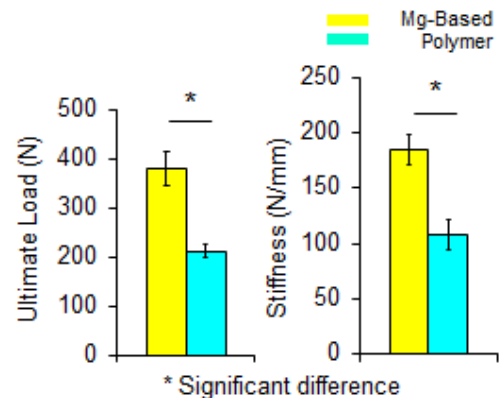
From the mechanical test involving the pullout of the suture anchor from the polyurethane foam, the stiffness, ultimate load, and ultimate elongation were found to be  $185 \pm 13$  N/mm,  $379 \pm 34$  N, and  $2.4 \pm 0.2$  mm, respectively for the Mg-based suture anchor and  $107 \pm 13$  N/mm,  $210 \pm 13$  N, and  $1.9 \pm 0.2$  mm, respectively for the polymeric suture anchor. The stiffness, ultimate load, and ultimate elongation were significantly different between the Mg-based and polymeric suture anchors ( $p < 0.05$ ). The Mg-based suture anchor failed by pullout from the polyurethane foam; whereas, the polymeric suture anchor failed at its eyelet.

## DISCUSSION:

The finite element analyses and parametric optimization had enabled us to achieve a novel Mg-based suture anchor. Its superior mechanical properties led to an improvement in deeper thread profile which resulted in an increased pullout strength. Uniaxial tensile testing showed that the stiffness, ultimate load, and ultimate elongation are superior over the polymeric suture anchor. With these promising results, we believe it may be a superior alternative and are conducting an *in-vivo* animal study to evaluate its performance.

## REFERENCES:

(1) D. J. Beevers, Proc Inst Mech Eng H, 217(1), 59-75. 2003. (2) S. J. Nho, et. al., Arthroscopy. 25(7): p.788-93. 2009. (3) M. P. Staiger, et. al., Biomaterials, 27(9), 1728-1734. 2006.



## DIFFERENTIAL MATRIX TURNOVER OF THE INTERFASCICULAR MATRIX OF TENDONS AT DIFFERENT RISK OF INJURY

<sup>1</sup>Sanders, K., <sup>2</sup>Beynon, R.J., <sup>1</sup>Clegg, P.D., <sup>1</sup>Peffer, M.J.,

<sup>1</sup>*Musculoskeletal Biology, Institute of Ageing and Chronic Disease, University of Liverpool, Leahurst, Neston, Wirral, UK.* <sup>2</sup>*Institute of Integrative Biology, Centre for Proteome Research, University of Liverpool, Crown Street, Liverpool, L69 7ZB.*

### INTRODUCTION:

Tendon injury is a common problem in the human athlete but also a significant cause of loss in the performance horse. Tendons play a key role in locomotion and can be divided into two functional categories; those that primarily have a positional role and those that also act as energy stores. The rate of injury to these two functional types varies; an energy-storing tendon such as the superficial digital flexor tendon (SDFT) is injury prone in contrast to the anatomically opposing common digital extensor tendon (CDET). The tendon is composed of bundles of collagen fibers termed fascicles that are separated by the interfascicular matrix (IFM). Tendon fascicles are composed of collagen type 1, proteoglycans, minor collagens (types III, V, VI, and XII), elastic fibers and glycoproteins. (Peffer et al, 2014) Research into the mechanical properties of the two tendon types have established that the composition of the IFM that facilitates the high strain stretch and recoil characteristics of the energy storing tendons by allowing the tendon fascicles to slide over each other. (Thorpe, et al. 2012) This study primarily aims to characterise the proteins of the IFM within the two structural tendon types and explore the effect of aging processes on the protein complement, in the long term with a better understanding, this may enable preventions/treatments in age related pathologies.

### METHODS:

Our study based on SDFT and CDET samples from young skeletally mature (<4years) and old horses (>15years) collected from the abattoir. Guanidine hydrochloride extracts (4M) were analysed by one-dimensional SDS-PAGE. Mass spectrometry based protein identification was by LC-MS/MS of tryptic peptides after in-gel trypsin digestion using the AMAZON instrument (Bruker)

### RESULTS:

From 40 gel slices a total of 173 proteins were identified. The predominant proteins were multiple collagen variants, cartilage oligomeric protein, filamin, fibronectin, laminin, cartilage intermediate layer protein, and decorin. Mascot scores ranged from over 1600 to 94, reflecting the different degree of coverage and the relative abundance of the proteins.

### DISCUSSION:

From the gel-based LC-MS/MS data our goal is to build a reduced complexity database of diagnostic peptide ions and fragments that can be used to generate quantitative profiles of protein abundance in different tendon samples. In addition, a diagnostic, reduced complexity peptide set will continue the work by Peffer *et al*, 2014 by using matrix-assisted laser desorption/ionization mass spectrometry imaging (MALDI-IMS) to obtain a low resolution molecular map of the peptides within tendon tissue to explore spatial protein disposition during ageing, and in different tendons

### REFERENCES:

Peffer, M.J., Thorpe, C.T., Collins, J.A., Eong, R., Wei, T.K., Screen, H.R., Clegg, P.D. (2014) Proteomic analysis reveals age-related changes in tendon matrix composition, with age- and injury-specific matrix fragmentation. *Journal of Biological Chemistry*. **289**, 25867-25878.

Thorpe, C.T., Udeze, C.P., Birch, H.L., Clegg, P.D., Screen, H.R. (2012) Specialization of tendon mechanical properties results from interfascicular differences. *Journal of the Royal Society Interface*. **76**, 3108-17

### ACKNOWLEDGEMENTS:

This study was funded by Wellcome Trust Research Taster Fellowship awarded to Karen Sanders

## DEVELOPMENT OF A NOVEL MURINE ACHILLES TENDON EXPLANT SYSTEM

K.J. Trella<sup>1,2</sup>, J. Li<sup>2</sup>, E.F. Shewman<sup>2</sup>, J.D. Sandy<sup>2</sup>, A. Plaas<sup>2</sup>, V.M. Wang<sup>1,2</sup>

1. University of Illinois at Chicago, Chicago, IL, United States

2. Rush University Medical Center, Chicago, IL, United States

### INTRODUCTION:

A disorganized collagen matrix with aggrecan-rich deposits is a typical histopathologic finding in human tendinopathy [1-2]. Using an *in-vivo* murine Achilles tendon TGF- $\beta$ 1 injury model, we have shown that both mechanical loading and the presence of ADAMTS5 (TS5) protein are necessary for removal of aggrecan rich deposits to achieve tendon healing [3]. In order to study the mechanobiology of tendon explants, we recently optimized *ex-vivo* culture conditions (e.g. media composition, time) for maintenance of the biomechanical and biochemical properties of free-floating (i.e., non-loaded, explanted) murine Achilles tendons relative to those of freshly harvested tendons [4]. The objective of the current study was to design and implement a culture device to enable static loading of murine Achilles tendons *ex-vivo* for future mechanistic studies to investigate the influence of mechanical stimulation on tendon homeostasis and repair.

### METHODS:

**Explant Culture:** 36 Achilles tendons (6 tendons per group, per assay), ~6mm in length, were excised from male, 12-wk C57BL/6 wild type (WT) mice. Dissected tendons were placed into CO<sub>2</sub> Independent MEM and then cultured free floating or statically loaded for 4 days in AMEM [4]. To apply a static load, tissues were gripped individually in a custom device designed for static loading (Figure 1). The load applied (1g) was selected as the load corresponding to the end of the toe region of the stress-strain curve (approximately 1% strain) in pilot studies. **AlamarBlue Assay:** Tendons (free floating, loaded) were removed from culture at 3 days and placed in multi-well plates with 1 mL of culture media and 10% (v/v) alamarBlue (Invitrogen) to determine the apparent glycolytic activity of cells by the total reducing activity (reduction of resazurin to resorufin; an index of viability). Plates were allowed to incubate at 37°C for 24 hours, at which time the media was removed and the fluorescence was read (ex: 530nm, em: 590nm). Each plate contained a reagent blank control with no tissue. The % viability for each genotype was calculated relative to naïve tissues (uncultured), which underwent the same alamarBlue protocol. **Mechanical Testing:** Tendon cross-sectional area (CSA) was measured using precision calipers (width) and a laser displacement sensor (thickness) assuming a rectangular geometry. Tendons were placed in custom clamps at an initial grip-to-grip length of 3.75mm and tested on a Material Testing System (Eden Prairie, MN) using a 44.5 N load cell. Following a preload of 0.05N for 2 minutes, each tendon was loaded to failure at 0.05mm/sec in a room temperature saline bath. 6 tendons were tested per group. **Statistics:** Groups were compared in GraphPad Prism 5 (La Jolle, CA) using a 1-way ANOVA followed by Tukey's post-hoc tests (p<0.05).

### RESULTS:

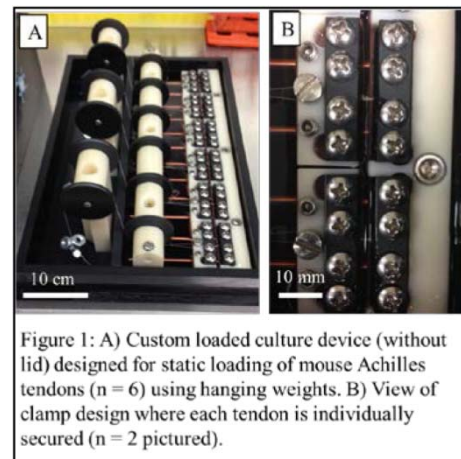
The glycolytic activity (cell viability) of all explants (free floating or loaded) was at or above naïve levels when measured after 3 days in explant. The CSA (naïve – 0.41 ± 0.1 mm<sup>2</sup>, free floating – 0.41 ± 0.04 mm<sup>2</sup>, loaded – 0.38 ± 0.02 mm<sup>2</sup>, p=0.58) and elastic modulus (naïve – 155 ± 48 MPa, free floating -162 ± 33 MPa, loaded – 155 ± 42 MPa, p = 0.94) of loaded tendons was not significantly different than free-floating or naïve tendons.

### CONCLUSIONS:

The present study utilized a novel murine tendon explant system to examine loading effects on Achilles tendons from WT mice. Tendons cultured either free floating or statically loaded achieved viability measurements at or above levels of naïve (uncultured) tendons, indicating reliability of the approach for future biologic assays. In these experiments, the method of culture (naïve, free floating, loaded) did not influence mechanical properties. In future studies, this static loading methodology can be utilized to assess therapeutic strategies to treat tendinopathic tissues (e.g., by injuring tendons prior to loading), such that the independent effects of mechanical loading, at different magnitudes and durations, can be critically examined in healing (WT) and non-healing (TS5KO) genotypes.

### REFERENCES:

[1]Kannus+ JBJS [Am] 1991 [2] Wang+ JOR 2012 [3] Bell+ JOR 2013 [4] Trella+ ORS 2013 [5] Abreu+ JOR 2008 [6] Yamamoto+ J Biomech Eng 2002.



## OUTCOMES FOLLOWING REVISION ROTATOR CUFF REPAIR WITH CONCENTRATED BONE MARROW ASPIRATE OBTAINED FROM THE PROXIMAL HUMERUS

A.H. Voss<sup>1</sup>, M.B. McCarthy<sup>1</sup>, M.P. Cote<sup>1</sup>, A.R. Hoberman<sup>1</sup>, J. DiVenere<sup>1</sup>, A.D. Mazzocca<sup>1</sup>  
<sup>1</sup>University of Connecticut, New England Musculoskeletal Institute, Farmington, Connecticut

**INTRODUCTION:** Over the last few years bone marrow aspirate (BMA) has shown to enhance rotator cuff healing.<sup>1-3</sup> We wanted to look at the difference between fenestrated and non-fenestrated trocars regarding the amount of cells taken by a bone marrow aspiration and the cell number by different aliquots of BMA. Further the purpose of this study was to assess the effectiveness of biologic augmentation of revision massive rotator cuff repair using concentrated bone marrow aspirate (cBMA) obtained from the proximal humerus during surgery and using an allograft patch as a scaffold for the BMA.

**METHODS:** This is a consecutive case series of patients undergoing rotator cuff repair with biological augmentation from a single surgeon's practice. All patients with large or massive rotator cuff tears as well as patients who had failed a primary rotator cuff repair were considered eligible. The decision to pursue repair with biological augmentation was made following a preoperative educational session outlining the senior author's algorithm for operative repair of massive and failed rotator cuff repair. Prior to biological augmentation 16 samples of BMA were obtained with 8 non-fenestrated and 8 fenestrated trocars to show number of CFU/cc of BMA and consecutive 12 cc BMA samples were extracted to determine the CTP/cc of BMA within 0-12cc, 12-24cc, 24-36cc and 36-48cc. Bone marrow was then aspirated during surgery utilizing the 1st anchor hole in the proximal humerus with a non-fenestrated trocar. We biologically augmented the patch with both bone marrow aspirate and autologous concentrated plasma (ACP, Arthrex Inc., Naples FL) through injected into the patch < 30 min prior to implantation. cBMA samples in the patch were sent to the laboratory to obtain cell numbers. The BMA cell concentration within four consecutive 12ml syringes of bone marrow aspiration taken with a non-fenestrated trocar was examined to determine if there was sufficient amount of CTPs within the concentration. All patients followed the same postoperative rehabilitation protocol. For patients whose postoperative physical exam and symptomology at follow up visits was suggestive of repair failure, an additional MRI was obtained.

**RESULTS:** There were 23 repairs in 22 patients. There were 9 supraspinatus repairs, 7 supra+infra+subscap repairs, 6 supra+infra repairs, and 1 supra+subscap repairs. Mean follow up of 21 ± 13 months. Two patients were lost to follow up. Of the remaining 21 procedures in 20 patients, there were 12 failures. Of these 12, 2 went on to undergo a reverse shoulder arthroplasty, 1 underwent latissimus dorsi transfer, 1 was infected and underwent I and D and revision hemiarthroplasty, 1 had a cuff tear arthropathy prosthesis head implanted, and 1 underwent another revision rotator cuff repair with BMA. The remaining 6 had a recurrent defect on postoperative MRI and did not elect for further operative treatment. The non-fenestrated trocar showed a higher number of CFU/cc of BMA compared to the fenestrated trocar (Fig1). The average volume aspirated was 40 ± 9 ml. In patients who had not failed, the average volume was 38 ± 10 ml compared to 42 ± 9 ml in those that did not fail. The average CTP/cc BMA in the first syringe taken was 309 ± 216 cc, in the second syringe was 64 ± 51 cc, in third syringe was 26 ± 62 cc and 11 ± 15 cc in the fourth syringe (Fig. 2). The average CTPs were 20,545 ± 23,316. In patients who had not failed, the average CTPs were 13, 294 ± 3985 compared to 26,476 ± 30,564 in those that did not fail.

**DISCUSSION:** We have previously demonstrated that bone marrow aspiration from the proximal humerus and distal femur is a safe, simple, efficient and reproducible procedure<sup>4,5</sup>. We've also demonstrated that the amount of cells taken from the proximal humerus is comparable to Muschler<sup>6</sup> aspirated bone marrow from the vertebral body and less compared to Hernigou<sup>7</sup> who has aspirated cells from the iliac crest. We've also found that a non-fenestrated trocar is preferable for BMA when looking at the CTP preference (numbers of CFU/cc BMA). In the present study, we did not find a statistical significance in CTPs between those that had failed and those who were stable. This is in contrast to Hernigou<sup>1</sup> who showed higher amounts of CTPs in the aspirated bone marrow of stable patients as compared to those that had failed following primary rotator cuff repair. Future research is needed to address revision massive rotator cuff repair.

### REFERENCES:

- Hernigou P, Flouzat Lachaniette CH, Delambre J, et al. Int Orthop 2014.
- Murphy MB, Moncivais K, Caplan AI. Exp Mol Med 2013.
- Mazzocca AD, McCarthy MB, Chowaniec D, et al. Arthroscopy 2011.
- Beitzel K, McCarthy MB, Cote MP, et al. Arthroscopy 2012.
- Mazzocca AD, McCarthy MB, Chowaniec DM, Cote MP, Arciero RA, Drissi H. Am J Sports Med 2010.
- McLain RF, Fleming JE, Boehm CA, Muschler GF. J Bone Joint Surg Am 2005.
- Hernigou P, Poignard A, Beaujean F, Rouard H. J Bone Joint Surg Am 2005.

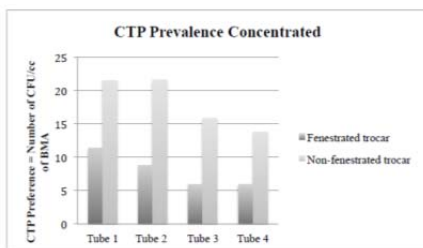


Fig 1. Non-fenestrated trocar showing a higher amount of CFU/cc from BMA compared to fenestrated trocar (Tube1-4 correspond to consecutive 12 cc BMA samples extracted).

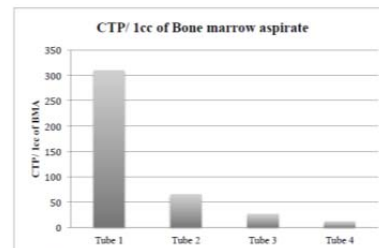


Fig 2. CTP per 1 cc of bone marrow aspirate from proximal humerus. Tube1-4 correspond to consecutive 12 cc BMA samples extracted.

# TRANSPLANTATION OF FETAL INSTEAD OF ADULT FIBROBLASTS DISPLAY INTRINSIC DIFFERENCES IN TENDON REGENERATION AND REDUCE THE PROBABILITY OF ECTOPIC OSSIFICATION

Xiao Chen (1), Tang Qiao-Mei(1), Fang Zhi(1), Zi Yin (1), Hongwei Ouyang (1)  
*1.School of Medicine, Zhejiang University, Hangzhou, China*

## **INTRODUCTION:**

Injured adult tendons do not exhibit optimal healing through a regenerative process, whereas fetal tendons can heal in a regenerative fashion without scar formation. Hence, we compared FFs (mouse fetal fibroblasts) and AFs (mouse adult fibroblasts) as seed cells for the fabrication of scaffold-free engineered tendons. Although cell transplantation therapy can effectively promote functional tendon repair, occasional ectopic ossification during tendon regeneration undermines its efficacy. The effect of transplanted cell types on ectopic ossification has not yet been systematically evaluated. This study also compared the rate of ectopic ossification during tendon repair upon transplantation with fetal fibroblasts and their adult counterparts.

## **RESULTS:**

Our results demonstrated that FFs had more potential for tendon tissue engineering, as shown by higher levels of tendon-related gene expression. In the in situ AT injury model, the FFs group also demonstrated much better structural and functional properties after healing, with higher levels of collagen deposition and better microstructure repair. Moreover, fetal fibroblasts could increase the recruitment of fibroblast-like cells and reduce the infiltration of inflammatory cells to the injury site during the regeneration process.

Alkaline phosphatase (ALP) staining, immunofluorescence, and gene expression analysis were used to compare the spontaneous osteogenic differentiation of FFs and AFs in vitro. X-ray, histology, and gene expression analysis were used to investigate the ectopic ossification in a mouse Achilles tendon repair model in vivo. ALP staining and immunofluorescence data in vitro showed that FFs had less spontaneous osteogenic differentiation capacity, and lower expression of runt-related transcription factor 2 (runx2). For the in vivo study, the FFs transplant group displayed reduced ectopic ossification (2/7 vs. 7/7, Mann-Whitney test  $p < 0.01$ ) at 14 weeks post-transplantation and enhanced tendon repair (general histological score at week 6, 7.53 vs. 10.56,  $p < 0.05$ ). More chondrocytes formed at 6 weeks, and all mice developed bone marrow at 14 weeks post-transplantation in the AFs transplant group. Gene expression analysis of the regenerated tissue showed significantly higher expression levels of transforming growth factor beta1 (TGF-beta1) and transforming growth factor beta3 (TGF-beta3) in the AFs group during the early stages of tendon repair.

## **CONCLUSIONS:**

Our results suggest that the underlying mechanisms of better regeneration with FFs should be elucidated and be used to enhance adult tendon healing. Moreover, transplantation of fetal instead of AFs is more promising for tendon repair, underscoring the importance of the origin of seed cells for tendon repair. This may assist in the development of future strategies to treat tendon injuries.

# MORPHOLOGIC CHANGE OF GLUTEUS MAXIMUS AND MEDIUS AFTER HARVESTING FASCIA LATA: QUANTITATIVE EVALUATION BY MAGNETIC RESONANCE IMAGING

Yasuo Itami\*, Teruhisa Mihata\*, Masashi Neo\*

*\*Department of Orthopedic Surgery, Osaka Medical College, Japan*

## **INTRODUCTION:**

Auto graft of fascia lata is commonly used for reconstructive surgery in the chronic injuries, such as irreparable rotator cuff tears, chronic Achilles tendon rupture, medial patellofemoral ligament injury, and anterior cruciate ligament injury. However, few reports have investigated morphologic change of gluteus maximus and medius after harvesting fascia lata. The objective of this study was to quantitatively assess the effect of harvesting fascia lata on gluteus maximus and medius by magnetic resonance imaging (MRI).

## **METHODS:**

Six patients (mean age 68.5 years; range, 57-81 years) with irreparable rotator cuff tear underwent arthroscopic superior capsule reconstruction using autograft of fascia lata. Gluteus maximus, gluteus medius, and tensor fascia lata muscles were evaluated using preoperative and postoperative (at 3-7 months after surgery) MRI. The size of harvested fascia lata was 10-15 cm in proximal-distal direction and 2.5-4 cm in anterior-posterior direction. With use of SYNAPSE VINCENT software (FUJIFILM, Japan) for axial T1-weighted image, cross sectional areas of the targeted muscles were measured on the slice of sacroiliac joint for gluteus maximus and medius, and on the slice of pubic symphysis for tensor fascia lata muscle. Each cross sectional areas was compared between before and after surgery using Wilcoxon signed-rank sum test.

## **RESULTS:**

After harvesting fascia lata, cross sectional area of gluteus maximus significantly decreased (preoperative  $3235 \pm 534 \text{mm}^2$ , postoperative  $2611 \pm 366 \text{mm}^2$ ,  $p=0.03$ ) and area of gluteus medius significantly increased (preoperative  $4019 \pm 695 \text{mm}^2$ , postoperative  $4730 \pm 848 \text{mm}^2$ ,  $p=0.03$ ). The area of tensor fascia lata muscle did not significantly changed after surgery (preoperative  $760 \pm 264 \text{mm}^2$ , postoperative  $798 \pm 238 \text{mm}^2$ ,  $p=0.16$ ).

## **CONCLUSION:**

Anatomically, the iliotibial band of the fascia lata is formed by a combination of tensor fascia lata muscle and gluteus maximus. Since we harvested fascia lata in the posterior side (gluteus maximus side) for arthroscopic superior capsular reconstruction, the cross sectional area of gluteus maximus decreased in this study. The increased muscle area of gluteus medius may be a compensatory hypertrophy for the progression of gluteus maximus atrophy.

## MANUFACTURE OF SCAFFOLD-FREE TENDON IN AN EX VIVO TISSUE-ENGINEERED SYSTEM

Wang T<sup>1</sup>, Ni M<sup>2</sup>, Thien C<sup>1</sup>, Gao J<sup>1</sup>, Zheng MH<sup>1</sup>.

<sup>1</sup> *Centre for Translational Orthopaedic Research, The University of Western Australia, Perth, Australia.*

<sup>2</sup> *Department of Orthopaedic, the General Hospital of Chinese People's Liberation Army, Beijing, China*

### **INTRODUCTION:**

Tendon cellularity is >90% comprised of tendon progenitor cells, tenoblasts and mature tenocytes, with progenitor cells possessing clonogenicity, multipotency, and self-renewal capacity. These tendon-derived cells (TDCs) have been suggested for tendon repair therapies. We analysed TDCs used in tissue-engineered tendon repair for their isolation, colonisation, characterisation, induced differentiation and induced tendon formation.

### **METHODS:**

TDCs were isolated from mouse flexor tendon and patient patellar tendon. Characterization of isolated cells was then conducted, including expression of progenitor cell and lineage-specific markers by flow cytometry for cell surface markers (CD34, CD44, CD45, CD90, Flk-1, and Sca-1) as well as adipogenesis (oil red-O, C/EBP $\alpha$  and PPAR $\gamma$ 2), osteogenesis (alizarin red, osteopontin and bone morphogenetic protein 2) and chondrogenesis (alcian blue, collagen 2 and aggrecan) assay by cytochemistry and quantitative real-time RT-PCR. The induction of tenocyte differentiation and bioreactor tendon formation after bioreactor static load and dynamic load (6% tensile strength) culture was then assessed by histology, confocal microscopy and both immunohistochemistry and quantitative real-time RT-PCR for osteocalcin, type II collagen, PPAR $\gamma$ 2, type III collagen, type I collagen, elastin, tenomodulin, and scleraxis expression. Bioreactor-engineered tendon was also biomechanically tested for maximum load and elastic modulus force.

### **RESULTS:**

Results showed that TDCs can be successfully isolated from mouse and human tendon and express mesenchymal stem cell lineage cell surface markers and adipo-/osteo-/chondrogenic markers, and were induced to differentiate from multi-lineage cells into tenocytes. TDC cultures were induced to form scaffold-free engineered tendon sheets by static and dynamic bioreactor culture. The application of dynamic load stimulated tenogenic differentiation and the capability to form neo-tendon tissue, as evidenced by improved matrix organisation (uniform and longitudinal fibres), cell morphology (spindle shaped) and significantly ( $p < 0.05-0.0001$ ) elevated tenogenic (tenomodulin, collagen I, and scleraxis) gene/protein expression after 7 days compared to non-tenogenic markers. Biomechanically, the dynamic-load tendon tissue formed was significantly stronger than static culture under both maximum load ( $p < 0.001$ ) and elastic modulus ( $p < 0.05$ ) assessment.

### **DISCUSSION:**

This study demonstrates that although a mixed population of cells (TDCs) may exist in tendon tissues used in tenocyte injection for treating tendinopathy. These tendon lineage cells commit to tendon formation when induced by stimuli that simulates the in vivo environment upon TDC injection into the repairing tendon matrix. Hence, TDCs are effective for use in tendon repair and regeneration.

## **NOTES**

---

## **ISL&T-XIV Supporters**

---

We gratefully acknowledge the support of the following individuals, whose generosity helped make ISL&T-XIV possible:

Dr. Kai-Ming Chan

Dr. Ranjan Gupta

Dr. Thay Lee

Dr. Helen H. Lu

Dr. Lou Soslowsky

Dr. Stavros Thomopoulos

Dr. James Wang

Dr. Jennifer Wayne

Dr. Savio L-Y. Woo

## International Symposium on Ligaments and Tendons (ISL&T-XIV)

Time	Topics
7:00 AM	<b>Registration and Light Breakfast</b>
8:00 AM	<b>Welcome</b> Dr. Savio L-Y. Woo & Dr. Helen H. Lu
8:15 AM	<b>Thematic Keynote: ACL Surgery... Where are the Missing Gaps?</b> Dr. Kai-Ming Chan
8:30-9:40 AM	<b>Podium Session 1: Tissue Engineering</b> Moderators: Dr. James Goh & Dr. Chungeng Zhao
9:40-11:00 AM	<b>Podium Session 2: Entesis</b> Moderators: Dr. William Walsh & Dr. Johnna Temenoff
11:00-11:30 AM	<b>Break/ Poster Session I (even numbers)</b> Moderators: Dr. Kevin Hildebrand, Dr. Thay Lee, Dr. Nelly Andarawis-Puri & Dr. Alex Almarza
11:30AM-12:45 PM	<b>Podium Session 3: Biology &amp; Biomechanics</b> Dr. Albert Banes & Dr. Alice Huang
12:45 PM	<b>Group Photo, Lunch and Poster Viewing</b>
1:45-3:25 PM	<b>Podium Session 4: Tendinopathy</b> Moderators: Dr. Louis Soslowsky & Dr. David Corr
3:25-3:55 PM	<b>Break/ Poster Session II (odd numbers)</b> Moderators: Drs. Hildebrand, Lee, Andarawis-Puri & Almarza
3:55-4:15 PM	<b>Clinical Panel: Soft Tissue Fixation Strategies</b> Moderators: Dr. Scott Rodeo and Dr. Leesa Galatz
4:15-5:35 PM	<b>Podium Session 5: Rotator Cuff</b> Dr. Hazel Screen & Dr. Jason Shearn
5:35-6:05 PM	<b>Podium Session 6: Tissue Engineering and Stem Cells</b> Dr. Ronen Schweitzer & Dr. Matthew Fisher
6:05 PM	<b>Updates from Tendon/Ligament Meetings</b> Dr. Louis Soslowsky & Dr. Hazel Screen
6:10 PM	<b>Closing Remarks</b> Dr. Stavros Thomopoulos
6:45 PM	<b>Gala Dinner and Award Ceremony</b>